2023

Assessing the Economic Feasibility of Capturing and Utilizing Carbon Dioxide from Ethanol Production in South Dakota

Makiah Stukel
South Dakota State University, makiah.stukel@jacks.sdstate.edu

ASSESSING THE ECONOMIC FEASIBILITY OF CAPTURING AND UTILIZING CARBON DIOXIDE FROM ETHANOL PRODUCTION IN SOUTH DAKOTA

BY

MAKIAH STUKEL

A thesis submitted in partial fulfillment of the requirements for the

Master of Science

Major in Mechanical Engineering

South Dakota State University

2023

THESIS ACCEPTANCE PAGE
Makiah Stukel

This thesis is approved as a creditable and independent investigation by a candidate for the master's degree and is acceptable for meeting the thesis requirements for this degree. Acceptance of this does not imply that the conclusions reached by the candidate are necessarily the conclusions of the major department.

Todd Letcher
Advisor Date

Yucheng Liu
Department Head Date

Nicole Lounsbery, PhD
Director, Graduate School Date

To my parents, Liz and Jason, for their endless love and support.

Thank you for bringing so much positivity into this enervating adventure.

ACKNOWLEDGEMENTS

This work would not have been possible without the guidance of my thesis advisor, Michael Twedt. His immense knowledge and support inspired me to pursue and produce this research at the highest quality. In times where I doubted myself, his unwavering confidence in me and my work prompted me to keep going. I would like to also thank Dr. Todd Letcher, Dr. Zhong Hu, and Dr. Anne Fennell, for serving on my thesis committee and contributing to the improvement of this research. Thank you to South Dakota State University and the Department of Mechanical Engineering for providing me with such a rewarding educational experience and equipping me with the technological skillset needed to succeed. Thank you especially to Dr. Gregory Michna for being a large part of my graduate education and instilling in me the value of hard work in academic success. Next, I would like to thank Sameer Keshavan for letting me bug him with all my questions and volunteering his time to help me better this work. Lastly, I would like to thank my amazing support system for being there for me every step of the way. Without the continual encouragement from my family and friends, this seemingly never-ending process would have been unfathomable.

TABLE OF CONTENTS

ABBREVIATIONS viii

LIST OF FIGURES x

LIST OF TABLES xii

ABSTRACT xiv

1 INTRODUCTION 1

1.1 Background 1

1.2 The Carbon Cycle 4

1.3 Carbon Capture and Storage 8

1.4 Research Objectives 10

2 LITERATURE REVIEW 12

2.1 Climate Change and Global CO_2 Concentrations 12

2.1.1 The Carbon Cycle 12

2.1.2 Deforestation 18

2.2 The Greenhouse Effect 23

2.3 Corn Ethanol Production in SD 30

2.4 CO_2 Emissions in SD 35

2.4.1 CO_2 Emissions and Ethanol Fermentation 36

2.4.2 CO_2 Emissions from Energy Consumption in SD 39

2.5 Carbon Capture and Storage (CCS) 42

2.5.1 Historical Overview of CCS 43

2.5.2 CO_2 Capture at Ethanol Facilities 45

2.5.3 CO_2 Transportation 49

2.5.4 CO_2 Geological Storage 52

2.6 Enhanced Oil Recovery 55

2.6.1 Continuous CO_2 Injection 55

2.6.2 WAG Injection 57

2.6.3 Cyclic (Huff-n-Puff) Injection 59

2.7 Case Studies 61

2.7.1 CO_2-EOR in Nebraska and Kansas 61

2.7.2 Largescale CO_2-EOR in Midwest 62

3 METHODOLOGY 64

3.1 Modeling the Capture and Transportation System 64

3.1.1 CO_2 Capture 66

3.1.2 CO_2 Transportation 71

3.2 Storing CO_2 with EOR 79

3.2.1 CO_2 Storage Resource Estimation in Oil Reservoirs 79

3.2.2 Section 45Q Tax Credit 89

3.2.3 CO_2-EOR Performance and Economics 94

3.3 Sensitivity Analyses 100

3.3.1 Sensitivity of Oil Price 101

3.3.2 Sensitivity of Oil Recovery Production Rates (%OOIP) 102

4 RESULTS AND DISCUSSION 104

4.1 Base Case Scenario 104

4.1.1 Capture Results 104

4.1.2 Transportation Results 108

4.1.3 Storage Results 116

4.2 Sensitivity Analyses 121

4.2.1 Oil Price Sensitivity Results 121

4.2.2 Oil Recovery Rate Sensitivity Results 123

5 CONCLUSIONS AND FUTURE WORK 126

5.1 Conclusions 126

5.2 Future Work 127

6 APPENDIX 128

7 REFERENCES 139

ABBREVIATIONS

ARI	Advanced Resources International
bbl	barrels
Btu	British thermal units
bu	bushels
CapEx	capital expenses
CCS	carbon capture and storage
CH_4	methane
CO_2	carbon dioxide
DANR	Department of Agriculture and Natural Resources
DOE	US Department of Energy
EIA	US Energy Information Administration
EOR	enhanced oil recovery
EPA	US Environmental Protection Agency
GHG	greenhouse gas
GWP	global warming potential
HCPV	hydrocarbon pore volume
IEA	International Energy Agency

IPCC	Intergovernmental Panel on Climate Change
MMBUY	million bushels per year
MMGY	million gallons per year
MT	metric tons
$MtCO_2$	metric tons of CO_2
MTY	metric tons per year
NETL	National Energy Technology Laboratory
NPV	net present value
O&M	operating and maintenance
OOIP	original oil-in-place
OpEx	operating expenses
SD	South Dakota
US	United States
WAG	water alternating gas

LIST OF FIGURES

Figure 1. EIA's pie graph of the US primary energy consumption in 2020 [2] 2

Figure 2. A representation of the current warming rate by the IPCC [4] 4

Figure 3. A diagram of the carbon cycle illustrated by the National Oceanic and Atmospheric Administration (NOAA) [9] 6

Figure 4. World CO_2 emissions from fossil fuel combustion and global CO_2 concentrations (EIA) [26] 17

Figure 5. Global population and forest area, 1750-2020. 19

Figure 6. Global CO_2 generation and absorption, 1750-2020 22

Figure 7. Vibrational modes of a CO_2 molecule given by Olbrycht and others [37] 25

Figure 8. Global GHG emissions in 2019 by gas [15]. 28

Figure 9. Total energy consumed per capita in 2019 (EIA) [65] 39

Figure 10. Energy consumption by end-use sector in SD, 2019 (EIA) [66] 39

Figure 11. Phase diagram of CO_2 (Mohammadi, M. et al.) [84] 50

Figure 12. PNAS representation of current CO_2 pipeline locations [87]. 51

Figure 13. WAG injection process for CO_2-EOR from Carpenter and Koperna [95] 58

Figure 14. Stages of the cyclic injection method depicted by B. Jia et al. [100] 60

Figure 15. Small scale case study of a CO_2-EOR operation in Kansas and Nebraska 62

Figure 16. Large-scale case study of a CO_2-EOR operation in the Midwest 63

Figure 17. Overview of ethanol plants and storage facilities in SD 65

Figure 18. Location of ethanol plants in SD 66

Figure 19. Capture, compression, and dehydration operating expenses 70

Figure 20. CO_2 pipeline network 72

Figure 21. Location of Harding County EOR units taken from SD DANR [114] 81

Figure 22. Contour plot depicting $\boldsymbol{Eoil}$ as a function of reservoir depth and thickness .. 86

Figure 23. Pipeline segment investment cost per segment length 109

Figure 24. Pipeline segment investment cost per nominal diameter 110

Figure 25. Pipeline segment investment cost per number of booster pumps..... 111

Figure 26. Transport cost corresponding to segment CO_2 flow rate..... 114

Figure 27. CO_2-EOR project NPV with varying oil price 122

Figure 28. CO_2-EOR project NPV with varying oil recovery rates..... 125

LIST OF TABLES

Table 1. Atmospheric lifetime and 100-year GWP of selected GHGs [38] 27

Table 2. Crop production and value of production in SD, 2021 [47] 32

Table 3. Fuel ethanol and motor gasoline data for SD, 2020 34

Table 4. SD energy-related CO_2 emissions by sector, 2020 [71] 41

Table 5. United States CCS projects in operation and construction [80] 44

Table 6. Comparison of top CO_2 emitting facilities [82] 47

Table 7. Top CO_2 emitting facilities ranked from most to least cost-effective 48

Table 8. SD ethanol plant production capacity and CO_2 emissions 68

Table 9. Base case pipeline segment inputs for the NETL Transport Cost Model 74

Table 10. Base case optimized pipeline diameters 76

Table 11. Geological properties used to estimate $\boldsymbol{Eoil}$ from EOR [116] 84

Table 12. CO_2 storage resource estimate in SD at EOR units 88

Table 13. Key components of the Section 45Q Tax Credit [121][122] 91

Table 14. Tax credit value per $MtCO_2$ from 2017-2026 per Section 45Q [121] 92

Table 15. Inflation adjustment factor for calendar years beyond 2026 [123] 93

Table 16. Top two Harding County oil fields and key performance characteristics 95

Table 17. Equations for capital costs of CO_2-EOR operations 97

Table 18. Equations for O&M costs of CO_2-EOR operations 99

Table 19. Base case capture capital and O&M costs for each ethanol plant 105

Table 20. Comparison of base case capital and O&M costs of ethanol CO_2 capture 107

Table 21. Base case transportation capital and O&M costs by category 112

Table 22. Comparison of base case capital and O&M costs of CO_2 transportation 115

Table 23. CO_2-EOR costs in 2022 dollars 117

Table 24. Revenue generated from oil production and CO_2 storage 119

Table 25. Base case storage economics for CO_2-EOR 120

Table 26. Economic summary of EOR revenue and NPV with varying oil price 122

Table 27. Economic summary of a CO_2-EOR project for varying oil recovery rates 124

Table 28. SD ethanol plants annual production capacity and corn usage 128

Table 29. $\boldsymbol{Eoil}$ at varying HCPV values for six cases presented in Peck and others [116] 129

Table 30. $\boldsymbol{Eoil}$ as a function of reservoir depth and thickness 130

Table 31. CO_2 storage resource approximation data 130

Table 32. Individual pipeline segment transportation cost data 132

Table 33. All Harding County oil fields capital costs 133

Table 34. All Harding County oil fields O&M costs 135

Table 35. All Harding County oil fields produced revenue per year 137

ABSTRACT

ASSESSING THE ECONOMIC FEASIBILITY OF CAPTURING AND UTILIZING CARBON DIOXIDE FROM ETHANOL PRODUCTION IN SOUTH DAKOTA

MAKIAH STUKEL

2023

Since the Industrial Revolution, anthropogenic greenhouse gas (GHG) emissions have spiked dramatically, prompting discussions on climate change. Mitigating climate change requires significant reductions in global carbon dioxide (CO_2) emissions as CO_2 is the most abundant anthropogenic GHG. A process that assists in offsetting the exponential growth in CO_2 emissions is carbon capture and storage (CCS). Integrating carbon capture technology into the ethanol industry can provide an economically feasible way to achieve net reductions in CO_2 emissions. The proposed work investigates the economic viability of applying CCS technologies to the 16 ethanol facilities in South Dakota (SD) and quantifies the potential reduction in CO_2 emissions for the state.

A pipeline network is developed within the state, transporting the congregated CO_2 to the oil fields in Harding County, SD. Enhanced oil recovery (EOR) is examined as a storage option as this method provides additional revenue to the CCS operation and creates a more economically feasible option. Sensitivity analyses are performed to evaluate the impact of variations in performance parameters on the system. Results from this study show a positive net present value (NPV) for each CO_2-EOR scenario; hence, a CCS operation in SD can be economically viable when combined with the ethanol industry, and the financial benefits from EOR and tax credits are considered. Sensitivity

studies show NPV is highly sensitive to oil price and oil recovery rates. Additionally, the modeled CCS system can geologically store 50.44 million $MtCO_2$ in the Harding County oil fields. Thus, over the simulated storage period, 50.44 million $MtCO_2$ are put to beneficial use and prevented from entering the atmosphere.

1 INTRODUCTION

Climate change is a widely discussed topic in the world today, and much debate centralizes around ways to prevent global temperature rise. This work aims to demonstrate how the greenhouse gas (GHG) carbon dioxide (CO_2) can be captured from carbon-emitting industrial facilities to assist in mitigating climate change. The primary focus of this chapter is to highlight the current problem of excess CO_2 emissions into the atmosphere and introduce a solution.

1.1 Background

Fossil fuels – including petroleum, natural gas, and coal – account for the largest portion of energy production and consumption in the United States (US). Existing fossil-fueled power plants provided 61% of the US's generated electricity in 2020 [1]. These plants have provided reliable electricity for over the past century and will continue to power the economy in years to come. According to the US Energy Information Association (EIA), fossil fuels made up 79% of the total US energy consumption in 2020, which is the lowest recorded level since 1991 [2][3]. Figure 1 illustrates each energy sector's contribution to the total consumption for that year.

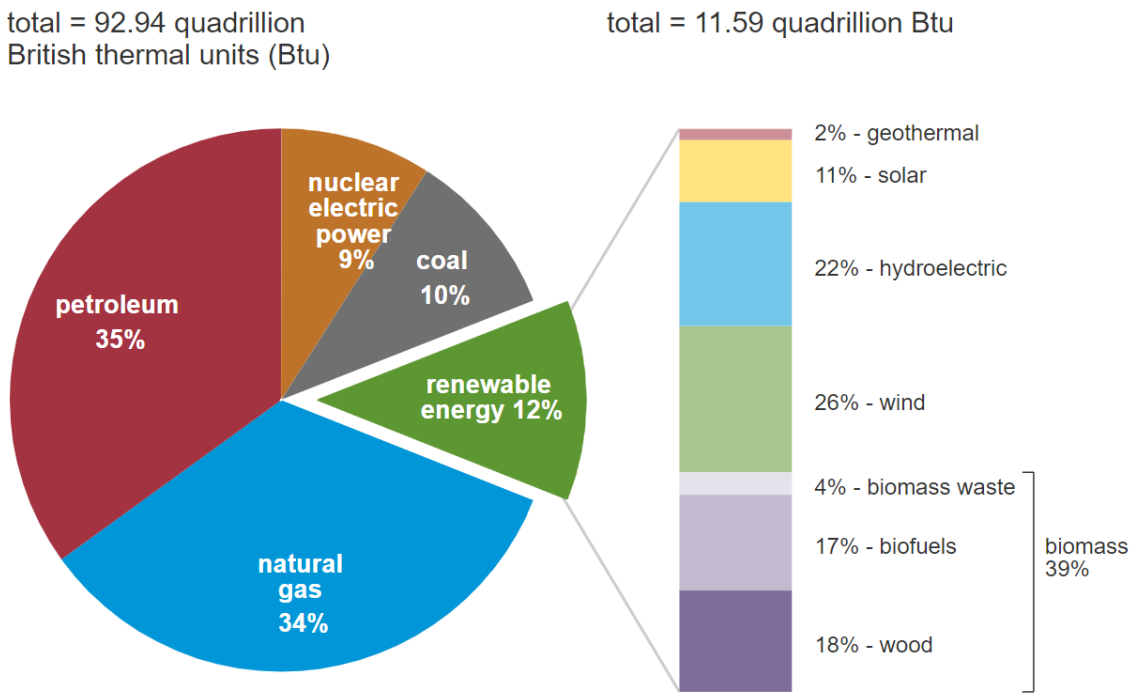

Figure 1. EIA's pie graph of the US primary energy consumption in 2020 [2]

Also shown in Figure 1 is that the percentage of renewable energy consumed surpassed that of coal. Despite growing shares of renewable energy consumption, it is evident that there is still a great dependence on fossil fuels to meet energy demands. There are multiple advantages to burning fossil fuels over using renewable energy that make switching over difficult. Some advantages include the ease with which these fuels can be found and produced, the reliability of these fuels, and the familiarity. Due to all these factors, it is not logical to cut these plants out completely, but rather introduce technologies that can limit GHG emissions.

The negative impact that GHGs have on the environment has been noticed globally. In December of 2015, the 21st Conference of the Parties was held in Paris to introduce an international agreement – the Paris Agreement. The legally binding treaty aims to promote a global response to the increasing threat of climate change by "*holding*

the increase in the global average temperature to well below 2°C above pre-industrial levels and pursuing efforts to limit the temperature increase to 1.5°C above pre-industrial levels." Pre-industrial levels have been noted by the Intergovernmental Panel on Climate Change (IPCC) to be between 1850 and 1900. Additionally, under this agreement the individual parties have agreed to cutting GHG emissions as a method to attain the "well below 2°C" goal [4].

At this conference, 195 out of 197 parties adopted the Paris Agreement thereby committing to the transition to a low-carbon economy. However, it was not until November 4th, 2016, that the agreement entered into force with the ratification of at least 55 parties that account for at least 55% of global GHG emissions. Currently, 193 of the parties have ratified the Paris Agreement and account for the majority of total global emissions [5]. To assist in the success of the Paris Agreement, the IPCC prepared a Special Report on both the impacts of achieving a 1.5°C global average temperature change and the pathways that would attain this enhanced goal. A depiction of the current warming rate following the lines of the Paris Agreement can be seen in Figure 2.

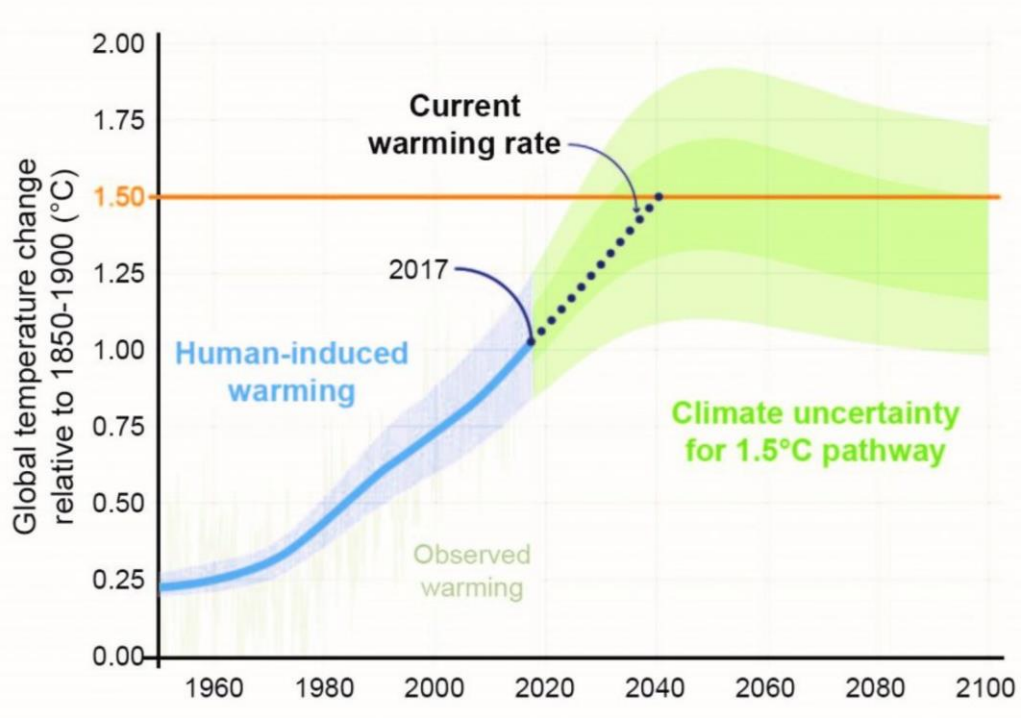

Figure 2. A representation of the current warming rate by the IPCC [4]

A short-term goal of the agreement is to reach global peaking of GHG emissions as soon as possible to achieve a climate neutral world by mid-century. Climate neutrality refers to the equal rate at which all GHGs are emitted to and removed from the atmosphere. As can be seen in Figure 2, global peaking of GHG emissions is not foreseen by the current warming rate. At the current rate, a 1.5°C change in global temperature will be around the year 2040, which is not hitting the mark of a climate neutral world by 2050. To understand how emitted CO_2 is currently regulated throughout the atmosphere, it is beneficial to review the carbon cycle.

1.2 The Carbon Cycle

Carbon is the backbone of life on Earth forming key molecules, such as proteins, DNA, carbohydrates, and fats, that are present in all living organisms. In the atmosphere, carbon primarily takes the form of carbon dioxide and is a key component in the

regulating of the earth's temperature [6]. Hydrocarbons, which are compounds of hydrogen and carbon, are also present in the atmosphere mainly in the form of methane (CH_4). Methane is produced through the decomposition of organic material and can enter the atmosphere through both natural processes and human activities. Other compounds known as halocarbons, carbon bonded to F, Cl, Br, or I, are also present in the atmosphere in miniscule concentrations [7]. These carbon compounds are constantly moving between reservoirs. A reservoir is any location in which carbon is stored, such as the atmosphere, soil, oceans, ocean sediment, rocks, and Earth's interior. This movement of carbon from reservoir to reservoir is known as the carbon cycle.

The carbon cycle represents nature's way of balancing the amount of carbon present in the atmosphere. Earth is a closed system, meaning the total amount of carbon present will never change. Thus, as carbon flows from one reservoir to another, the amount of carbon in a single reservoir can vary with time. Various pathways between reservoirs exist in the carbon cycle and can be seen in Figure 3. However, a large contributor to the flow of carbon between reservoirs is human activities such as fossil fuel emissions and deforestation, as these processes release large amounts of CO_2 very quickly and prevent CO_2 from being absorbed from the atmosphere [8].

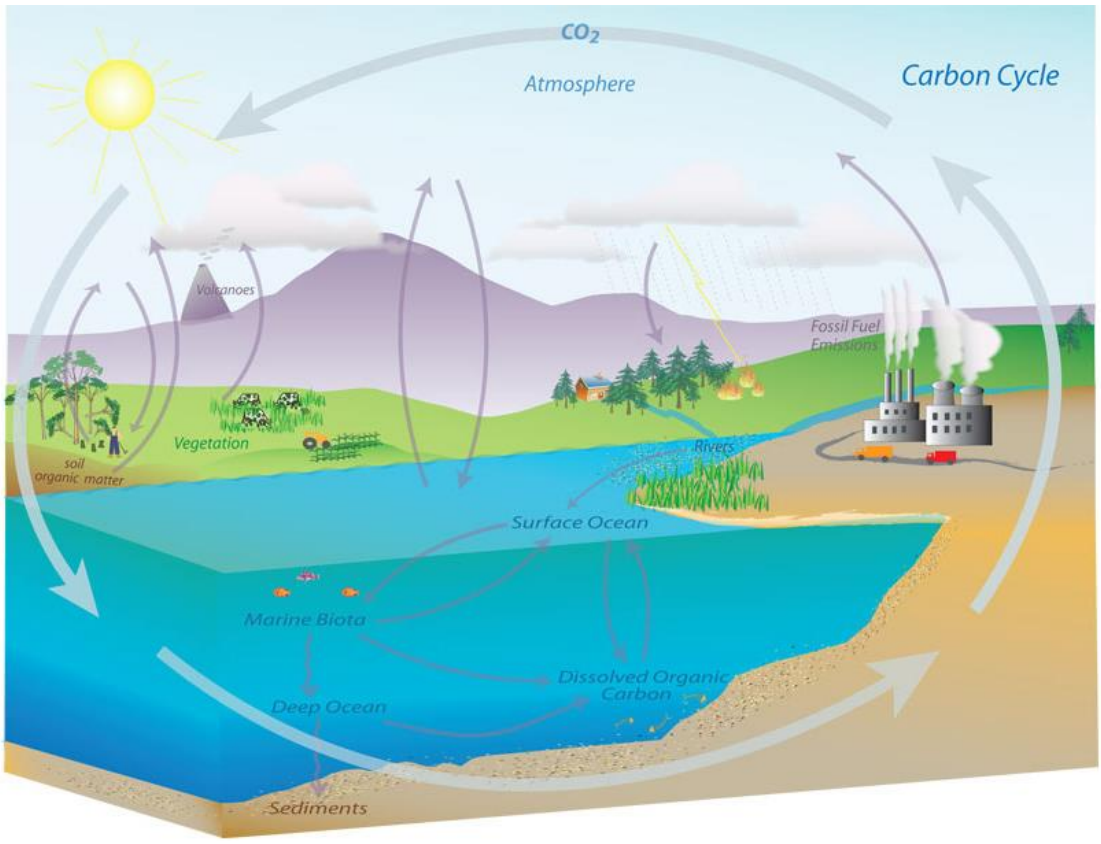

Figure 3. A diagram of the carbon cycle illustrated by the National Oceanic and Atmospheric Administration (NOAA) [9]

As shown in Figure 3, the flow of carbon can occur through a variety of sources and pathways. On land, carbon is introduced to the atmosphere through natural processes, such as photosynthesis, weathering, and respiration, and through industrial processes such as the burning fossil fuels. Carbon is also transferred from decaying organisms and from producers to consumers through the food chain. In the ocean, more carbon is able to be absorbed from the atmosphere than released, making the ocean a key influencer to the carbon cycle. Oceans continuously exchange carbon between the atmosphere and its waters through chemical processes, photosynthesis, and with the assistance of marine organisms [9]. All these sources and pathways of the carbon cycle will be explained in detail in Chapter 2, the Literature Review.

The carbon cycle is vital to understanding climate change. Carbon neutral, or net-zero, is a term often used when talking about limiting contributions to climate change. This term signifies a balance between the emissions of carbon and the amount removed or absorbed from the atmosphere [10]. Contrary to climate neutrality, carbon neutrality refers only to carbon emissions and therefore does not include all GHGs. Due to the rise in CO_2 emissions and the effects of the Paris Agreement, net-zero carbon emissions pledges are becoming increasingly popular in large corporations, such as Microsoft, Amazon, and Verizon [11]. Aiming for carbon neutrality ensures the carbon cycle can regulate the amount of carbon in the atmosphere and overall helps achieve global climate neutrality set out by the Paris Agreement.

The amount of carbon moved between reservoirs is largely affected by human activities. When fossil fuels are combusted, the greenhouse gas carbon dioxide is released. Additionally, land development and deforestation are leading to an increase in the amount of carbon released. This loss of vegetation consequentially results in a decrease of carbon dioxide able to be absorbed from the atmosphere. The carbon cycle does a suitable job at regulating the concentration of CO_2, but with such an excessive amount of CO_2 being released, it is hard to keep up. As previously mentioned, there is no change as to how much carbon is present in the system because Earth is a closed environment. Therefore, changes such as an increase in fossil fuel production and deforestation will result in higher concentration of carbon dioxide in the atmosphere and warmer temperatures [12].

1.3 Carbon Capture and Storage

As illustrated in the preceding sections, an internationally recognized issue exists in the form of a steady increase in global temperatures due to increasing amounts of GHG emissions. In a 2022 GHG inventory report, the US Environmental Protection Agency (EPA) estimated that CO_2 accounts for 79% of overall GHG emissions (11% methane, 7% nitrogen dioxide, 3% fluorinated gases). Additionally, since the Industrial Revolution, global CO_2 concentrations in the atmosphere have increased nearly 48%, predominately due to the burning of fossil fuels. The significant increase in CO_2 concentrations can also be attributed to deforestation. Deforestation is considered one of the largest global contributors of anthropogenic, or human-generated, carbon emissions to the atmosphere [13]. This notable 48% increase in CO_2 concentrations poses a threat to the terms and pledges of the Paris Agreement. Thus, researchers started searching for strategies that could significantly lower the amount of GHG emissions being released into the atmosphere.

Because CO_2 accounts for the majority of GHG emissions, an emphasis has been on substantially reducing CO_2 emissions to limit warming to the terms of the Paris Agreement. Currently, more anthropogenic CO_2 is remaining in the atmosphere due to changes in land and ocean carbon sinks, where a carbon sink represents any natural or artificial environment that absorbs more carbon than it emits to the atmosphere [14]. In the pre-industrial era, CO_2 absorption through these carbon sinks were able to balance out CO_2 emissions to the atmosphere, resulting in similar CO_2 concentration amounts throughout the years. However, the natural CO_2 absorption rate is decreasing, making other mitigation strategies necessary to keep up with increasing emissions. All major

energy sectors – energy supply, transport, building, industry, and agriculture, forestry and other land use – are required to develop mitigation pathways that limit warming to at least 2°C. As detailed by the IPCC in its 2022 Mitigation of Climate Change Report, a process known as carbon capture and storage (CCS) is a modelled pathway that is able to achieve this warming limit [15].

CCS is the process of capturing CO_2 from fossil-fueled or industrial plants, transporting this CO_2 by ship or pipeline, and either permanently storing the CO_2 underground or utilizing its potential in a range of applications. The existing global CCS infrastructure has an annual capture capacity of more than 40 $MtCO_2$ which is equivalent to over 4,501 gallons of gasoline consumed, or over 44,256 lbs of coal burned [16][17]. Additional CCS facilities are underway, and the CCS infrastructure is expanding due to stronger financial incentives and climate targets (1.5 to 2°C warming). The International Energy Agency (IEA), a professional agency that helps shape the worlds energy policies towards sustainability states that "*CC[U]S technologies will play an important role in meeting net zero targets, including as one of few solutions to tackle emissions from heavy industry and to remove carbon from the atmosphere* [18]." Likewise, it is evident that CCS has significant potential in achieving the goals set out in the Paris Agreement and limiting CO_2 emissions from stationary sources globally. However, prompt action is needed to ensure the impact occurs before temperatures rise and the expense of combating climate change increases.

There are several challenges that limit the implementation of CCS facilities in the US. The capital-intensive investment into the capture plant, transport pipelines, and storage resources is a major challenge that limits the number of investments to date.

Similarly, with CCS technology still in large-scale development, there is a high perceived risk associated with making an initial investment. Furthermore, a considerable amount of skepticism exists amidst the public when it comes to full deployment of CCS. Most public concerns emerge from the transportation and storage of CO_2 as many assume if CO_2 is stored in the gaseous state, leakage must occur, and it could be catastrophic. However, CO_2 is not flammable or toxic and at a depth greater than 1 km (0.6 mi), a leakage to the atmosphere is infinitesimal [19]. Despite these challenges, CCS is gaining momentum as developing CCS projects demonstrate that the right combination of capture technology, pipeline routes, and storage options can lead to a net positive financial investment.

1.4 Research Objectives

To achieve the goals of the Paris Agreement, each state needs to establish strategies that allow for the reduction of GHG emissions. Because it is not logical to cut out fossil-fueled energy sources completely, a more viable solution would be to deploy technologies that can reduce carbon emissions from existing fossil-fueled energy sources. Thus, the transition towards renewable energy sources can be alleviated.

The implementation of CCS systems has proven to be successful in reducing carbon emissions from power generation and industrial processes. However, because fossil-fueled power plants release significantly more CO_2 into the atmosphere, smaller industrial facilities are often overlooked as a solution to reduce CO_2 emissions. There is limited research that exists for applying CCS to industrial processes, let alone to bioenergy sources such as corn ethanol plants. Corn ethanol is noted to be a great source

of CO_2 emissions due to its high purity; capturing this CO_2 would result in lower capture costs and more feasible implementation than installing separation units at power plants.

Because large-scale CCS deployment comes at high associated costs and limited financial incentives, not a lot of experimentation is done to iterate and improve these systems. Applying CCS to existing ethanol plants would offer a less expensive route to CCS deployment until it is practical to use in more difficult capture sources like power plants. The Midwest offers a cost-effective carbon capture option as this area is comprised of numerous ethanol facilities. Likewise, the goals of this work are to (1) evaluate the opportunity to reduce CO_2 emissions through capturing and utilizing ethanol-based CO_2 in South Dakota (SD), and (2) develop an economically feasible CCS model in SD by incorporating financial incentives. By developing a CCS model within the state, the impact of capture, transport, and storage parameters on the profitability of the system can then be understood.

2 LITERATURE REVIEW

This chapter covers underlying principles related to the deployment of CCS technologies to reduce CO_2 emissions and the added benefits of applying CCS to the ethanol industry. The regulation and imbalance of CO_2 emissions are discussed as well as the influence of CO_2 on Earth's climate. Additionally, the importance the ethanol industry in SD is detailed, and the state's CO_2 emissions are examined. Then, the CCS process is described with a focus on ethanol production as a source of CO_2 capture. Enhanced oil recovery (EOR) rationale is also presented as added benefits can be applied to the system through additional oil production, enhancing the overall economic feasibility of the CCS operation. Finally, details from published CO_2-EOR case studies are provided to gain insight into expected outcomes of varying CCS projects.

2.1 Climate Change and Global CO_2 Concentrations

A variety of factors influence the concentration of carbon dioxide in the atmosphere. Volcanic eruptions, wildfires, and the burning of fossil fuels are significant events that release vast amounts of carbon into the atmosphere. As mentioned in Chapter 1, the movement of carbon through Earth's environment is known as the carbon cycle. Since the carbon cycle maintains a balance of all Earth's carbon, a ripple effect occurs between the reservoirs. So, when carbon is removed from one reservoir, it is then added to another. The sources and pathways present in the carbon cycle will now be explained.

2.1.1 The Carbon Cycle

The carbon cycle can be grouped into two interrelated subcycles: the biological carbon cycle and the biogeochemical carbon cycle. Described first, the biological carbon

cycle refers to the exchanges of carbon among living organisms. Autotrophs – plants, algae, phytoplankton (ocean organisms), and some types of bacteria – are able to make their own food using carbon compounds present in the environment. Most autotrophs absorb CO_2 through a process called photosynthesis to make their own food. During this process, the self-feeders utilize energy from the sun and combine CO_2 from the atmosphere and water from the soil to form oxygen and glucose, a carbohydrate. The carbon-based compound is stored and used to make the substance cellulose, which is needed by the plant in order to grow. The oxygen is released by the plant to the atmosphere. For marine autotrophs, CO_2 from the atmosphere is dissolved in water to produce bicarbonate ions (HCO_3^-). Then marine photosynthesis can convert these bicarbonate ions into organic molecules [20].

Aside from autotrophs, heterotrophs are another essential part to the biological carbon cycle. Heterotrophs, also referred to as consumers, rely on autotrophs for energy. Energy is produced from the ingested biomass through a process known as cellular respiration. Cellular respiration takes place in the mitochondria of cells in all living organisms. During this process, organisms use oxygen produced by autotrophs to break down glucose into CO_2 and water. Released energy in the form of adenosine triphosphate, or ATP, is also produced and is then used for all other processes within the cells. To recognize the continual exchange between autotrophs and heterotrophs in the two processes described, photosynthesis and cellular respiration, the chemical equations are presented in Equation 1 and 2 [21].

$$Photosynthesis: \quad Energy + CO_2 + H_2O \rightarrow C_6H_{12}O_6 + 6O_2 \tag{1}$$

$$Cellular\ Respiration: \quad C_6H_{12}O_6 + 6O_2 \rightarrow CO_2 + H_2O + Energy \tag{2}$$

As can be seen from Equation 1 and 2, there is a link between the two processes that constantly occur in the carbon cycle. Photosynthesis requires CO_2 and water, which are the by-products of cellular respiration. Similarly, the products of photosynthesis are glucose and oxygen, which are the reactants for cellular respiration. The difference in equations is only in the energy absorbed and released, sunlight versus ATP. More oxygen is released by autotrophs through photosynthesis than is taken in and converted through cellular respiration, which permits more to be utilized by cellular respiration in heterotrophs. Because of this linked relationship, it can be noted that the global rates of both processes can have a considerable impact on the amount of CO_2 present in the atmosphere [21].

The other subcycle to discuss is the biogeochemical carbon cycle. This subcycle represents long-term carbon cycling via geological processes. Reservoirs including the atmosphere, oceans, ocean sediment, soil, rocks, and Earth's interior are able to store carbon for long periods of time. As mentioned in Chapter 1, the ocean plays a vital role in the carbon cycle by taking up a significant amount of CO_2 from the atmosphere. In the ocean, atmospheric CO_2 dissolves in water and reacts with water molecules to form carbonic acid (H_2CO_3). This reaction can also occur in the opposite direction in which carbonic acid can form water and CO_2. Carbonic acid easily separates and releases hydrogen ions (H^+) and produces bicarbonate ions (HCO_3^-). The described oceanic reactions can be seen in Equation 3 [22].

$$CO_2 + H_2O \leftrightarrow H_2CO_3 \leftrightarrow H^+ + HCO_3^- \quad (3)$$

Bicarbonate ions can also readily separate into carbonate (CO_3^{2-}) and hydrogen ions. Carbonate ions combine with calcium ions (Ca^{2+}) that are present in seawater to

form calcium carbonate ($CaCO_3$), which is utilized by marine organisms to build shells and skeletons [23]. When these organisms die, they settle on the ocean floor, and over long periods of time, the calcium carbonate gradually forms limestone [22]. Moreover, the four forms of carbon that exist in the oceans – dissolved CO_2, carbonic acid, bicarbonate ions, and carbonate ions – have previously been in balanced proportions. However, the ocean is taking in more CO_2 due to an increase in CO_2 concentrations in the atmosphere. This leads also to a rise in the proportion of dissolved CO_2 at the ocean's surface creating an increasing amount of carbonic acid which lowers the pH of the ocean causing the waters to be more acidic. An increasing amount of carbonic acid also lowers the proportion of carbonate that is able to be utilized by marine organisms for their shells and skeletons [23]. Before the Industrial Revolution, around 1750, the pH of the ocean was noted to be about 8.2. Currently, the pH of the ocean is about 8.1, which may not seem like much of a decrease; however, the pH scale is logarithmic, so a 0.1 change in pH units corresponds to about a 30% increase in acidity [12]. Thus, rising CO_2 levels in the atmosphere are causing concern not only for terrestrial organisms, but also for the state of the planet's oceans.

In the biogeochemical subcycle, carbon is also stored in the soil on land as a result of both organism decomposition and weathering of rock and minerals. Over long periods of time, the decomposition of dead organisms generates fossil fuel products like coal, oil, and natural gas. Because fossil fuels take millions of years to form, the rate at which they are used greatly exceeds the rate of geological formation, making them a non-renewable resource. When fossil fuels are burned, CO_2 is released into the atmosphere. Another pathway carbon takes to enter the atmosphere from land is through the eruption of

volcanoes. Volcanoes occur around converging plate boundaries and when one plate descends under another a process called subduction occurs. During this process, the carbon sediments on the ocean floor are carried with the descending plate and experience great pressure and temperature. CO_2 is formed and released to the atmosphere when the volcano erupts [20].

Although a variety of events play a part in the movement of carbon between reservoirs, major shifts occur largely due to human activities. Since the Industrial Revolution (roughly 1750-1850), human activities have significantly affected the global carbon cycle. These human activities have increased the abundance of GHGs, specifically CO_2, in the atmosphere and are largely responsible for the noticeable rise in global temperature [24]. In the Industrial Era, the amount of CO_2 in the atmosphere increased by about 35% [25]. This is contributed mainly by the burning of fossil fuels and deforestation. In 2009, about 8.4 billion tons of carbon were released into the atmosphere by humans burning fossil fuels [12]. Figure 4 depicts the rise in anthropogenic CO_2 emissions and atmospheric concentrations of CO_2 worldwide [26].

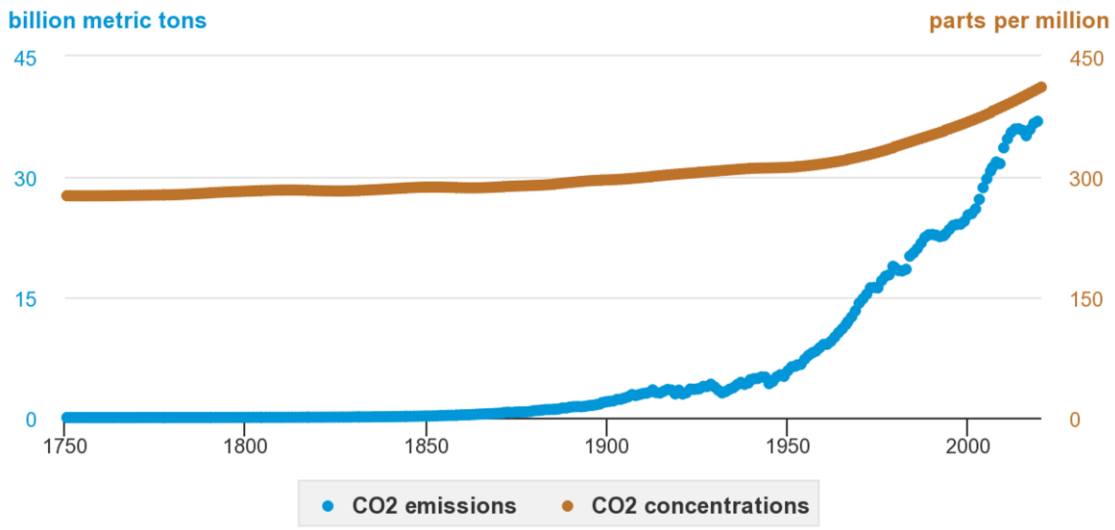

Figure 4. World CO_2 emissions from fossil fuel combustion and global CO_2 concentrations (EIA) [26]

From the trends shown in Figure 4, it is evident that both CO_2 emissions and concentrations have increased since the start of the Industrial Revolution. In 1750, the concentration of CO_2 in the atmosphere was around 277 parts per million (ppm). Leading up to this point, most CO_2 emissions were a result of fires and land conversion and were small enough to be regulated by the carbon cycle. It can be seen in Figure 4 that CO_2 emissions began noticeably increasing around 1850, or just after the Industrial Revolution. In 1850, the concentration of CO_2 in the atmosphere was around 287 ppm, which is about a 4% increase since 1750. Around the year 1950, the impact of excessive amounts of carbon dioxide emissions on the overall CO_2 concentrations can be observed, as the amount of CO_2 concentrations also starts to noticeably increase. The CO_2 concentration in 1950 was about 312 ppm, which is now approximately a 13% increase since the start of the Industrial Revolution. By the end of 2020, the global average amount of CO_2 concentration in the atmosphere was about 412 ppm, a 49% increase since the start of the Industrial Era [26].

2.1.2 Deforestation

While a large contributor to the increase in atmospheric CO_2 concentration is the burning of fossil fuels due to industrialization, it is important to recognize that another major contributor exists – deforestation. Similar to the ocean, forests are able to store large amounts of carbon and thus play a key role in maintaining a balance of carbon throughout the carbon cycle. The trees of forests absorb CO_2 from the atmosphere and store it in their fibers, helping to offset increasing CO_2 emissions. Research reports that a mature tree, or one that is close to its full height and size, can take in over 48 lbs of CO_2 from the atmosphere in one year. Additionally, one tree is able to provide as much as four people with one day's worth of oxygen [27].

Forests absorb approximately 33% of the CO_2 that is released from burning fossil fuels. However, the land sector in all accounts for about 25% of global GHG emissions, which is the second largest source after the energy sector. Of the 25% GHG emissions, half is due to deforestation and forest degradation [28]. Between the years of 1990 and 2020, over one billion acres of forests have been lost through deforestation globally [29]. This amount of deforestation alone significantly reduces the amount of CO_2 able to be absorbed from the atmosphere. One cause of the significant increase in deforestation is the rapid rise in global population. An increasing global population leads to the expansion of urban areas and the conversion of land to make that happen. Figure 5 shows the change in both global population and global forest area from start of the Industrial Revolution to 2020.

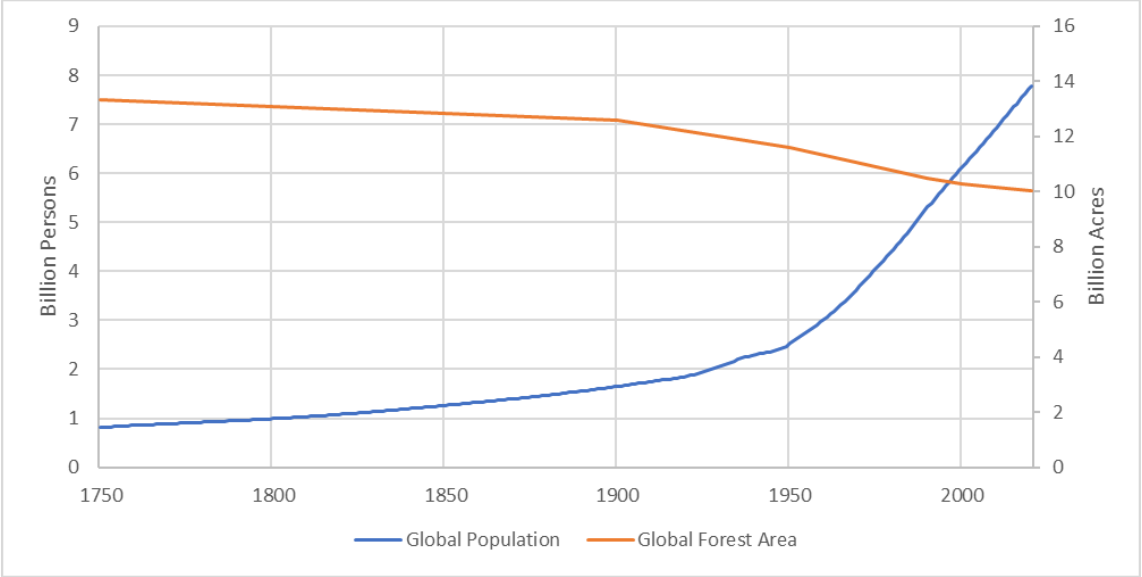

Figure 5. Global population and forest area, 1750-2020.

From Figure 5, a trend can be identified between the two data sets. Around the year 1900, the amount of global forest area starts to noticeably decrease, and contrastingly, the global population starts to noticeably increase. In 1750, the global population was approximately 814 million people [30]. However, as of 2020, the population had dramatically increased to about 7.8 billion people [31]. To be expected, as population increases, land that includes forests and other vegetation is converted over time to meet the demand for new services. In terms of CO_2 emissions, a rapidly increasing global population would release increasing levels of CO_2 to the atmosphere through respiration. Although respiration emission values would not be as drastic as burning fossil fuels or clearing lands, research has shown it is significant and should be included in calculations [32].

In terms of forest area, in 1750, the total global forest area was around 13.3 billion acres [33]. Having declined since the start of the Industrial Revolution, the total global forest area is now 10 billion acres [29]. Thus, between 1750 and 2020, the total global

forest area experienced nearly a 25% reduction. As forests represent a major carbon sink, any reduction in forest area can consequentially influence the regulating effects of the carbon cycle. Likewise, the act of achieving carbon neutrality in response to the goals of the Paris Agreement is further hindered by the elimination of natural resources that can absorb carbon – primarily in the form of CO_2 – from the atmosphere. It is therefore important to investigate how the carbon cycle manages current trends in CO_2 emissions with the reduction in global forest area. Using the global CO_2 emissions data from Figure 4 along with publicly available data regarding deforestation, the amount of carbon sequestered by global forests can be estimated; furthermore, the corresponding loss of vegetation and its diminishing effects to the carbon cycle can be emphasized.

Much research was analyzed to determine global CO_2 absorption rates since the start of the Industrial Revolution. Pre-1950 data comes from an online database documenting global forest area dating back 10,000 years before the present in which forest area accounted for nearly 57% of global land area (nearly 15 billion acres) [33]. Data beyond 1950 were taken from the most recent forest resources assessment published by the Food and Agriculture Organization of the United Nations (FAO). According to the FAO, the global forest area in 2020 accounts for about 31% of total land area (10 billion acres), an overall significant reduction in the absorption capacity of forests. The EPA reports the conversion factor to estimate the amount of carbon sequestered by one acre of forest in one year to be 0.84 MT CO_2 per acre per year [17]. This conversion estimation can be seen by Equation 4.

$$\frac{0.23\ metric\ ton\ C}{\frac{acre}{yr}} * \frac{44\ units\ CO_2}{12\ units\ C} = \frac{0.84\ metric\ ton\ CO_2}{\frac{acre}{yr}} \quad (4)$$

One caveat to implementing this conversion is that it uses the characteristics of forests in the US. So, a level of uncertainty results when estimating absorption levels of forests globally. However, an article by the Congressional Research Service categorizes forests according to biome type – tropical, boreal, and temperate – and then analyzes the corresponding amount of carbon able to be stored in each. Forest biomes are grouped according to similar geological location and climate due to the varying amount of carbon stored in different areas. In total, the cumulative amount of carbon stored equated to 861 billion MT. This yields to a global average value of 0.22 MT of carbon per acre per year, a comparable value to the one reported by the EPA (0.23 MtC/acre/year) [34]. Because of the resulting similarity, the EPA conversion is accepted (0.84 $MtCO_2$/acre/year). Applying the EPA conversion to the collected global forest area data, global CO_2 absorption estimates can then be plotted with global CO_2 emissions. Figure 6 displays these data sets between 1750 and 2020.

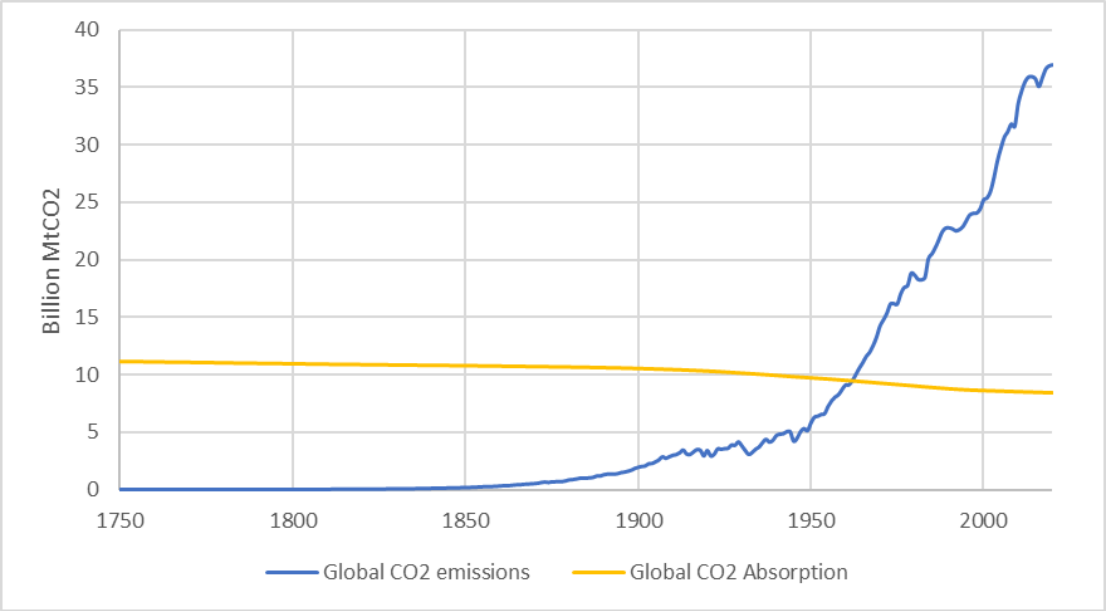

Figure 6. Global CO_2 generation and absorption, 1750-2020

During the period 1750-2020, the amount of CO_2 able to be absorbed globally from the atmosphere by forests decreased from 11.2 to 8.4 billion MT, nearly 3 billion MT. In comparison, global CO_2 emissions rose from 0.01 to 37 billion MT during that same period. As displayed in Figure 6, around year 1960, global CO_2 emissions began to exceed the amount of CO_2 absorbed from the atmosphere by the world's forests. After this time, the carbon cycle's ability to manage the amount of carbon in the atmosphere was hindered due to the increasing disparity between global CO_2 emissions and absorption. By year 2020, an accumulated 28.6 billion MT of CO_2 was unable to be regulated through the biological carbon cycle. To counteract this blatant imbalance in the carbon cycle, the excess 28.6 billion MT of CO_2 would require the establishment of 34 billion acres of forest, roughly 4 times the current global forest area. Hence, achieving carbon neutrality is unattainable when focusing solely on accelerating the development of forest ecosystems around the world. Although reversing deforestation is an invaluable

component in combating climate change, alternative carbon sequestering methods are needed to reach carbon neutrality due to the rapid increase in CO_2 emissions.

To summarize, the amount of CO_2 in the atmosphere has increased at an alarming rate since the Industrial Era. There are a variety of sources and pathways in which carbon flows that release CO_2 to the air. Earth is a closed system, so the amount of carbon present in the environment never changes. Land and ocean sinks are able to absorb large amounts of CO_2 from the atmosphere, but more CO_2 is remaining in the atmosphere than is ideal for upcoming years. It is important that CO_2 is present in the atmosphere because it helps regulate Earth's temperature. However, excess amounts of CO_2 in the atmosphere lead to more heat being trapped and an overall increase in global temperatures. To fully understand the extent of excess CO_2 in the atmosphere, the greenhouse effect will be examined.

2.2 The Greenhouse Effect

Earth is made livable because of a natural process referred to as the greenhouse effect. The greenhouse effect warms Earth's surface through the presence of atmospheric heat-trapping gases known as GHGs and their ability to absorb and emit infrared radiation. Additionally, the main greenhouse gases include water vapor (H_2O), CO_2, CH_4, nitrous oxide (N_2O), ozone (O_3), and fluorinated gases. During this natural phenomenon, the solar radiation emitted from the sun gets absorbed by Earth's surface, and when cooled, infrared radiation is emitted back from Earth's surface. Of the re-emitted infrared radiation, a portion passes through the atmosphere while the remainder is absorbed by GHGs. The energy from the infrared radiation causes the GHG molecules to vibrate and then re-emit this energy outwards where it can return to Earth in the form of heat or

escape to space. In absence of the greenhouse effect, Earth's average surface temperature, which is currently 14°C, would be about -19°C [35].

A key indicator of an atmospheric gas's impact on Earth's climate is how well it can absorb infrared radiation. To absorb infrared radiation, a molecule must experience a change in its dipole moment during vibration. By definition, a dipole moment occurs when there is a difference in electronegativity within a molecule. Furthermore, homonuclear diatomic molecules, such as nitrogen and oxygen, consist of two identical atoms that equally share electrons and thus the vibrations within the molecules exhibit no change in electronegativity. Consequentially, no dipole moment is present which means these molecules cannot absorb infrared radiation. Though nonpolar molecules are geometrically symmetric and have no net dipole moment, some have different modes of vibration that induce change in their overall dipole moments [36]. The number of vibrational modes possible for a molecule is defined by its degrees of freedom. For nonlinear molecules, the number of vibrational modes is equal to $(3N - 6)$, and for linear molecules, the number of vibrational modes is equal to $(3N - 5)$, where N represents the total number of atoms in these equations. Looking at CO_2, which is a nonpolar, linear molecule, a total of three atoms are present yielding a total of four vibrational modes possible [37]. These different modes are shown in Figure 7.

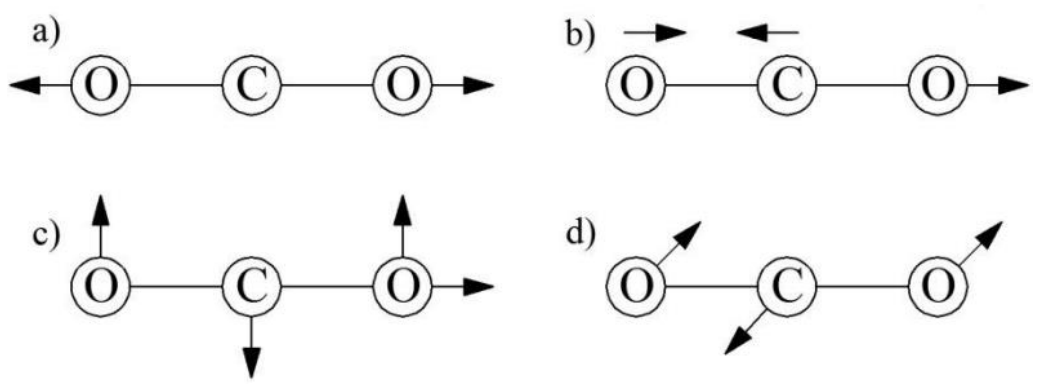

Figure 7. Vibrational modes of a CO_2 molecule given by Olbrycht and others [37]

Two vibrational modes that can occur within any molecule are stretching and bending. The heat-trapping ability of CO_2 is a result of the different types of vibration that occur within the molecule in response to passing infrared radiation. Symmetrical stretching, shown in Figure 7 (a), represents the synchronous stretching and contracting motions of the two bonds in a CO_2 molecule. No infrared energy is absorbed from this type of vibration as the dipole moment is not changed. On the other hand, infrared radiation is absorbed by a CO_2 molecule from an asymmetrical stretch, shown in Figure 7 (b). During this vibration, the two bonds stretch and contract in opposition, creating a change in the dipole moment from the unequal sharing of electrons. Another vibrational mode of CO_2 that is infrared active is bending, and this motion occurs when the angle between two bonds changes, resulting in fluctuating dipole moments. Figure 7 (c) and (d) depict this vibration within a CO_2 molecule in-plane and out-of-plane, respectively [37]. It can be noted that the number of vibrational modes vary based on the complexity of a molecule; so, the more vibrational modes that exist within a molecule, the increased likelihood it has to interact with traveling infrared waves. Ultimately, molecular compounds in the atmosphere consisting of three or more atoms, or two different typed atoms, will yield a vibrational mode that can absorb and re-emit infrared radiation. For

this reason, the major constituents of Earth's atmosphere – nitrogen (78%) and oxygen (21%) – have no heat-trapping capabilities, and hence, the atmosphere must rely on properties of GHGs to keep the planet at sustainable temperatures.

In addition to absorption and radiative capabilities, the overall potency of a gas's greenhouse effect is also characterized by its duration spent in the atmosphere before being naturally removed. This is often referred to as the atmospheric lifetime of a gas. Incorporating both the atmospheric lifetime and radiative efficiency of a gas, the global warming potential (GWP) can be found, and the strength of each GHG can be measured relative to CO_2. GWP compares the radiative force of a GHG over a specific time period (i.e. 100 years) to the radiative force of CO_2 (weight equivalent). A high GWP signifies that, during the same period, a gas warms Earth's surface more than an equivalent amount of CO_2 would. Similarly, a long atmospheric lifetime may increasingly contribute to warmer temperatures due to the inability of a gas to leave the atmosphere as quickly as one with a shorter lifetime. The atmospheric lifetime and GWP reported in the 2021 Sixth Assessment Report by the IPCC are displayed in Table 1.

Table 1. Atmospheric lifetime and 100-year GWP of selected GHGs [38]

GHG	Atmospheric Lifetime (years)	100-year GWP
H_2O* [39]	< 1	-10^{-3} to 5×10^{-4}
CO_2	100**	1
CH_4	11.8	28
N_2O	109.0	265
Fluorinated gases***	Ranges from weeks to thousands of years	Varies – highest is sulfur hexafluoride at 25,200

*Values are not formally quantified in literature. Sherwood et al establishes H_2O has no single lifetime and is short (< 1 year) over oceans and negligible over land area [39].
**CO_2 has no set atmospheric lifetime value as the gas transfers through the atmosphere at different rates. Some is absorbed quickly, while some stays for thousands of years.
***Numerous types exist creating a wide range of lifetime and 100-year GWP values.

Recognizable in Table 1, CH_4 and N_2O have prominently larger GWP values than CO_2. This means that molecules of CH_4 and N_2O are remarkably more effective at altering the amount of heat present in the atmosphere than is CO_2. However, CO_2 is immensely more prevalent in the atmosphere than both CH_4 and N_2O, and its overall abundancy is what makes the gas so imperative to Earth's climate system. Comparably, water vapor (H_2O) has the smallest GWP value of the selected gases and is less effective in increasing surface temperatures. However, water vapor is the most abundant GHG in the atmosphere and one of the best absorbers of infrared energy, so despite its small lifetime and GWP value, it is still the largest contributor to the Earth's greenhouse effect [40]. In contrast to other GHGs, water vapor is condensable and can thus change form from a gas to a liquid and vise-versa depending on the temperature of the atmosphere. A rise in global temperature causes more water vapor to enter the atmosphere through evaporation. Nonetheless, an increase in GHG emissions allows the absorption of more

infrared radiation and thus the entrapment of more heat, which subsequently results in a rise in global temperature. Ultimately, increasing atmospheric concentrations of water vapor result indirectly from the increasing emissions of other heat-trapping gases [41]. Moreover, also shown in Table 1 are fluorinated gases, and while some of these gas molecules do not have much of a warming impact, the industrial and manufacturing processes from which they result have increased significantly since pre-industrial times. To gain more insight into how human activity has impacted the individual levels of GHGs in the atmosphere, an EIA study regarding the magnitude of these emissions is examined.

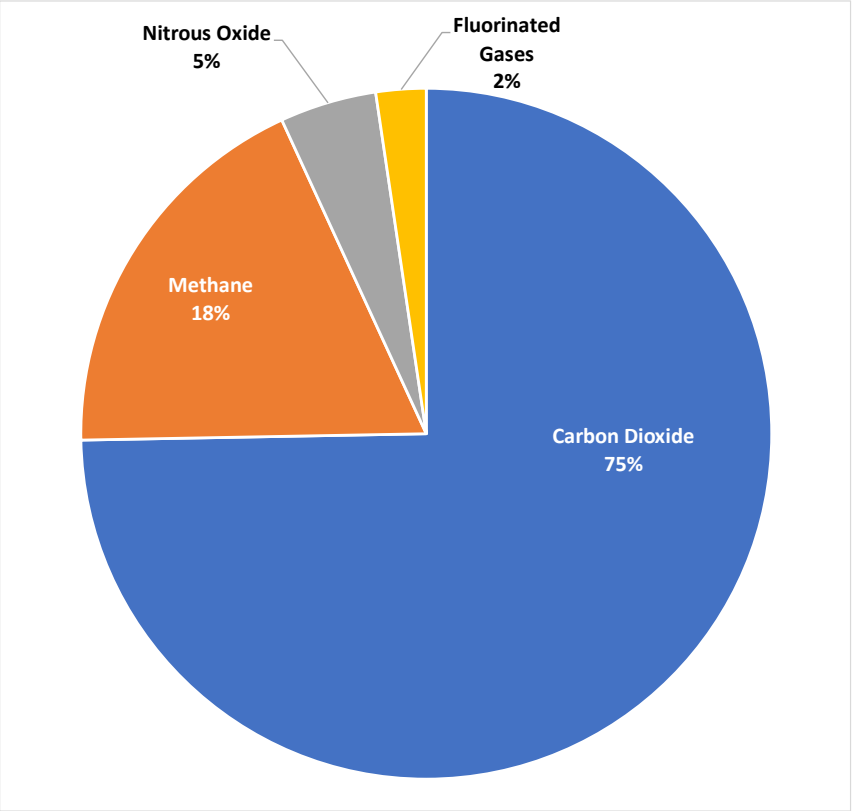

Figure 8. Global GHG emissions in 2019 by gas [15].

Figure 8 depicts the GHGs that were emitted directly from human activities in 2019. Most recent data from the 2022 IPCC report regarding the mitigation of climate

change was used in order to analyze the extent to which each gas is released. As seen in Figure 8, in 2019, 75% of all global GHG emissions were from CO_2. The primary source of these CO_2 emissions is fossil fuel usage, while another major source is from industrial processes. Of the 75% total CO_2 emissions, fossil fuel and industrial processes accounted for 64%. Similarly, as described in the carbon cycle process, CO_2 can also be largely released through land changes, and that is where the other 11% of global CO_2 emissions comes from [15].

Methane (CH_4) is the second most GHG emitted by human activities, accounting for 18% of the 2019 global GHG emissions [15]. A significant contributor to global methane emissions is the energy sector in which the major sources are natural gas and oil systems. Natural gas is composed primarily of CH_4. Additionally, CH_4 emissions can result from the processes involved with oil and gas production, such as the refinement, transportation, and storage of these products. Increasing levels of fossil fuel production generally results in CH_4 representing a larger share of global GHG emissions [42]. Another key source of CH_4 emissions is the agriculture sector. Most emissions from this sector result from the digestion processes of livestock, or otherwise known as enteric fermentation. The third largest source of anthropogenic CH_4 emissions is the waste sector in which most emissions are generated in landfills. Solid waste is sent to landfills from commercial and residential areas where it decomposes and releases significant amounts of CH_4 [13].

The remaining GHGs that constitute the total emissions from human activities are nitrous oxide (N_2O) and fluorinated gases. N_2O accounted for 5% of the global GHG emissions from human activities in 2019 [15]. Various human activities can yield

increased emissions of N_2O, but the primary source of anthropogenic N_2O emissions is the agriculture sector – particularly soil management activities. Nitrogen-based fertilizers used to stimulate plant growth can produce and emit N_2O through the remnants of nitrogen not absorbed by the plant. Other sources of N_2O emissions include fuel combustion and wastewater management [13]. Continuing on, the remaining 2% of the total GHG emissions in 2019 includes fluorinated gases [15]. Fluorinated gases can be categorized in four ways: hydrofluorocarbons (HFCs), perfluorocarbons (PFCs), sulfur hexafluoride (SF_6), and nitrogen trifluoride (NF_3). As previously noted, no natural sources can directly emit these gases, meaning they are essentially produced solely from human activities. Predominantly, fluorinated gases are emitted through refrigerant use, for example, in air conditioning systems. Similarly, emissions also result from aluminum production and semiconductor manufacturing in the industrial sector [13].

Because CO_2 accounts for the vast percentage of GHGs in the atmosphere, the gas has a large influence on and is a key regulator of global temperatures. A study by the NOAA has shown that there has been a 0.08°C change in global temperatures per decade since 1880; however, the average warming rate since 1981 has been 0.18°C per decade, which is more than double the previous rate [43]. It can be concluded that without additional efforts to decrease GHG emissions, CO_2 especially, the change in global temperature would keep increasing at concerning rate.

2.3 Corn Ethanol Production in SD

Ethanol is an alternative fuel that is domestically produced using corn as a feedstock. Promotion for the switch to corn ethanol began in the 1970s when oil embargoes were in effect and oil prices began to spike. This posed a great threat as the

US heavily relied on imported oil, so the need for an alternative fuel source was imperative. Because corn ethanol is derived from a readily available renewable resource, the use of fuel ethanol was reintroduced. Since then, fiscal incentives and environmental standards requiring cleaner-burning fuels have increased the usage and production of ethanol [44].

Two processes exist to produce corn ethanol: dry milling and wet milling. The dry milling process's main product is ethanol, whereas wet milling separates parts of the corn kernel to produce ethanol as well as corn starch and corn syrup to be used for both food and industrial uses [45]. The focus of this work is on dry mill facilities as they produce over 90% of today's grain ethanol [46]. At dry mill ethanol plants, corn is ground into a flour and fermented into ethanol. During this fermentation process, distiller grains and carbon dioxide are released as by-products. Details regarding the ethanol fermentation process and its corresponding CO_2 emissions are discussed in the following section.

Finding ways to utilize the abundance of crops is imperative for SD as agriculture is the number one industry in the state. Table 2 shows different crops in the state listed from most to least produced for the year 2021. The table also shows the corresponding value of production for each crop in US dollars. As can be seen in the table, corn is the top-ranking crop in the state and has notable potential to bring revenue to the state [47]. Using corn to produce biofuels, and other by-products, can ultimately expand economic opportunities by boosting its demand and promoting energy independence.

Table 2. Crop production and value of production in SD, 2021 [47]

Crop	**Production (MMBU*)**	**Value of Production ($)**
Corn	739.8	4,142.9 million
Soybean	215.6	2,781.2 million
Wheat	44.5	349.3 million
Sunflower	34.1 – 25.6	261.6 million
Oats	3.8	17.1 million

*MMBU = million bushels

Table 2 provides a segue into the vast importance of corn ethanol production in SD. Currently, SD consists of 16 dry mill ethanol plants that are primarily located on the eastern side of the state. Corn is used as furnish feedstock for the state's ethanol industry at all 16 plants. With SD being one of the top ten corn producers in the US, utilizing this crop to produce ethanol gives the state an economic advantage [48]. When producing ethanol from corn, each bushel of corn generates roughly 2.7 gallons of ethanol [49]. Additionally, the combined ethanol production capacity of the state's plants is estimated to be approximately 1,300 MMGY (million gallons per year). This yields a cumulative 480 MMBUY (million bushels per year) able to be processed by the 16 ethanol plants. Data used to generate this cumulative value is displayed in the Appendix. Correspondingly, approximately 65% of the total 740 MMBU of corn produced in SD (Table 2) is used to make ethanol. Thus, the agriculture industry, and more specifically corn production, is proven to be an essential part of the state's economy. Information regarding each ethanol plant, such as production capacities and location, will be analyzed in the Methodology chapter.

Ethanol production in SD has vastly increased since the establishment of the first ethanol plant in 1988 in Scotland, SD. A majority of the ethanol industry's expansion in SD took place around year 2000. Starting in 2000, 12 of the state's 16 currently operational ethanol plants were built between 2000 and 2010. This rapid expansion also occurred in numerous Midwest states where corn is of great abundance, such as Iowa and Nebraska [50]. Based on data from the Renewable Fuels Association (RFA), the state's existing ethanol production capacity in 2000 was approximately 44 MMGY, or slightly over 1 MMbbl per year, where MMbbl is million oil barrels (volume equivalent) of ethanol. By 2010, the existing ethanol production capacity in SD had increased to 1016 MMGY, which is just over 24 MMbbl per year [51]. During this 10-year period, the total ethanol production capacity in the state experienced over a 20-fold increase. As of January 1, 2022, the RFA reports the current ethanol production capacity at about 1300 MMGY, or 30.8 MMbbl per year, which is nearly a 30-fold increase since the year 2000 [52]. Therefore, the substantial increase in production capacity indicates the vital contributions ethanol has on SD's economy.

With increasing ethanol production capacity rates, the total amount of ethanol produced by SD has also increased significantly over time. Dating back to the 1960s, the EIA reports production data for each state up until year 2020. At the beginning of the expansion of ethanol production, few ethanol plants were established, and low production values were reported. In 2000, SD produced about 0.4 MMbbl of ethanol and accounted for 1% of total US ethanol production. After state-wide development of the industry, the production values rose dramatically. Notably, in 2006, the state produced over 13 MMbbl of ethanol, more than 30 times the amount in 2000, and accounted for over 11% of US

ethanol production. Moreover, current data from the EIA documents the state produced approximately 27.7 MMbbl of ethanol in 2020, ranking SD the fourth largest ethanol producer in the nation and accounting for 7.4% of total US ethanol production [53]. Because fuel ethanol is primarily exported and blended into motor gasoline, it is beneficial to see how these fuels compare in terms of production and consumption data.

Table 3. Fuel ethanol and motor gasoline data for SD, 2020

	Production (MMbbl)	**Consumption (MMbbl)**
Fuel Ethanol	27.7 [53]	1.1 [54]
Motor Gasoline (Excl Ethanol)		9.9 [55]

*MMbbl = millions of barrels

Table 3 documents fuel ethanol and motor gasoline (excluding ethanol) production and consumption data for SD in 2020. As can be seen in the table, roughly 1.1 MMbbl of the 27.7 MMbbl of ethanol produced in 2020 were consumed in the state [53][54]. This equates to about a 3% utilization rate of SD's own ethanol production, further indicating the critical role SD plays in providing fuel ethanol to other states. Also shown in Table 3, SD consumed 9.9 MMbbl of motor gasoline (excluding ethanol) in 2020. Motor gasoline excluding fuel ethanol was reported instead of including fuel ethanol to avoid double counting fuel ethanol values. It can be noted that the state's total amount of motor gasoline including ethanol produced in 2020 is 10.7 MMbbl [55]. Nonetheless, SD produces over 2.5 times more fuel ethanol than it consumes motor gasoline, creating a great opportunity for the state to capitalize on the benefits of the ethanol industry.

The data from Table 3 demonstrates the importance of corn ethanol in the state of SD in terms of providing an economic advantage. SD produces over twice as much ethanol energy as the state consumes gas energy. Because the only source of oil in SD is in the northwestern corner of the state, a lot of it needs to be purchased from outside states creating a reliance on this product. Fuel ethanol allows the state to be independent and market this product to others. However, some challenges do exist with ethanol producing facilities. Producing ethanol by fermentation results in a pure stream of CO_2 that gets emitted to the atmosphere [44]. Unlike other fossil-fueled powered plants, it is not mixed with any other gases. This can be seen as a challenge to the terms of the Paris Agreement as the goal is to limit all GHG emissions to near zero. However, this characteristic also proves advantageous as it could lead to easy capture of CO_2 when looking into capture technology.

2.4 CO_2 Emissions in SD

Due to industrialization's effects on the atmosphere, the US has a moral obligation to both spread awareness to recent CO_2 emission trends and, in total, reduce CO_2 emissions to assist in the mitigation of climate change. Establishing the overall carbon dioxide emissions in SD will paint a picture of how much the state affects the warming of the planet. Population and demographic data have an impact on total CO_2 emissions of a state. As of 2021, the average CO_2 emissions per capita in the US is 14 MT [56]. Because the population of SD is significantly less than other states, 895,376 people as of 2021, the state is expected to release significantly less CO_2 than larger states, such as Texas or California [57].

An important factor in a state's total CO_2 emissions is the amount of energy consumed. Recent studies provide evidence that a relationship between energy consumption, national output, and CO_2 emissions exists [58][59]. This relationship refers to the link between a region's increasing economic growth and its similar increasing effects on economic consumption and CO_2 emissions. Generally, as a state experiences population and economic growth, there is often a significant increase in energy consumption and CO_2 emissions. As SD rapidly expands to promote economic growth, the state's corresponding energy consumption and CO_2 emissions must be emphasized. Ethanol production provides a major economic benefit to the state and therefore could significantly contribute to increasing amounts of CO_2 emissions. Because of this, it is pivotal to understand how the state's CO_2 emissions are affected by the ethanol production process.

2.4.1 CO_2 Emissions and Ethanol Fermentation

When ethanol is produced, it goes through a fermentation process. During ethanol production, the fermentation step occurs after the corn has been grinded, cooked, and cooled, and before the mixture undergoes distillation. At the start of fermentation, the corn mixture includes original components of the corn kernel – proteins, fiber, water, and oil – as well as glucose. The glucose present in the mixture is a result from the introduction of an enzyme which assists in breaking down the starch present in the step before fermentation. It is not until the glucose gets broken down that ethanol is produced. To initiate the decomposition of glucose, yeast is added to the corn mixture during the fermentation step. Once yeast is added, the glucose is then converted into ethanol and

CO_2, completing the fermentation process [61]. The chemical reaction for ethanol fermentation is presented by Equation 5.

$$\underset{Glucose}{C_6H_{12}O_6} \xrightarrow{Yeast} \underset{Ethanol}{2C_2H_5OH} + \underset{Carbon\ Dioxide}{2CO_2} \quad (5)$$

The CO_2 generated during the fermentation process gets released back into the atmosphere, if not captured. Corn production to make more ethanol then can re-absorb the released CO_2, impacting the net carbon balance described in the carbon cycle. Equation 5 shows that 2 moles of ethanol and 2 moles of CO_2 result from the chemical reaction. Additionally, the defined molecular weights of ethanol and CO_2 are 46.07 and 44.01 g/mol, respectively. This slight difference in molecular weight subsequently yields an exceptionally high purity stream of CO_2. It is this fact that distinguishes ethanol plants from power plants as power plants are known to produce low purity CO_2 streams with several impurities. Therefore, ethanol plants are being increasingly studied as the fermentation process proves to reduce the cost of capture in CCS projects.

From Equation 5, it is evident that by-products CO_2 and ethanol are released in equal parts; therefore, during fermentation, producing one pound of ethanol emits approximately one pound of CO_2 [49]. Theoretically, one gallon of ethanol produced releases 6.29 lbs of CO_2 during fermentation. A detailed calculation for deriving this value is shown in the Appendix. Using this conversion, the total barrels of ethanol produced (Table 3) can be translated into overall CO_2 emissions produced in SD from fermentation. In total, 3.32 million $MtCO_2$ were released during the production of 27.7 MMbbl of ethanol in 2020. The individual ethanol plants in SD and their corresponding

CO_2 emissions from the fermentation process will be examined more closely in the Methodology chapter.

It is important to distinguish the total amount of CO_2 emissions from both ethanol combustion and fermentation. To determine the amount of CO_2 emissions resulting from combustion, a conversion factor found using certain properties of fuel ethanol is needed. The documented gross heat content and carbon coefficient of fuel ethanol is 3.539 MMBtu/bbl and 68.44 $kgCO_2$/MMBtu, respectively. Using these properties, the conversion factor is found to be 0.24 $MtCO_2$/bbl (metric tons of CO_2 per barrel of ethanol) [62][63]. Subsequently, the total amount of CO_2 emitted from the 1.1 MMbbl of fuel ethanol consumed (Table 3) in the state equates to 0.27 million MT. Looking at both fermentation and combustion CO_2 emissions, the entirety of the state's ethanol production and its impact to the environment can be examined.

Collectively, the CO_2 emissions from ethanol fermentation and combustion is 3.59 million MT. In terms of nonrenewable resources, motor gasoline (excluding fuel ethanol) has a heat content and carbon coefficient of 5.222 MMBtu/bbl and 70.22 $kgCO_2$/MMBtu, respectively [63][64]. Looking at Table 3, the consumed 9.9 MMbbl of motor gasoline (excluding fuel ethanol) results in 3.64 million $MtCO_2$ released to the atmosphere by the state of SD. Therefore, the total CO_2 emission data from ethanol fermentation and combustion are nearly equivalent to the motor gasoline consumption emissions in the state. So, although ethanol production provides a significant economic benefit to the state, the resulting CO_2 emissions must not be overlooked.

2.4.2 CO_2 Emissions from Energy Consumption in SD

When analyzing energy consumption information, a key aspect for SD is the population. Variations between states frequently reflect population size, so comparing states' energy consumption per person is often relevant. The total energy consumption per capita for SD in 2019 was 453 million Btu, ranking the state 9th in the nation [65]. Figure 9 illustrates how each state compares in relation to energy consumption per capita. Along the same lines, Figure 10 indicates the percentage of energy consumption in each sector.

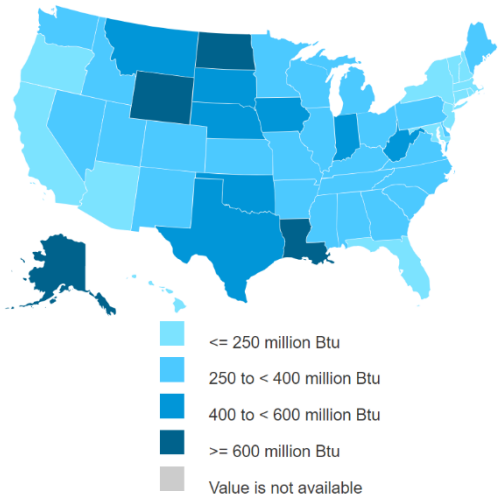

Figure 9. Total energy consumed per capita in 2019 (EIA) [65]

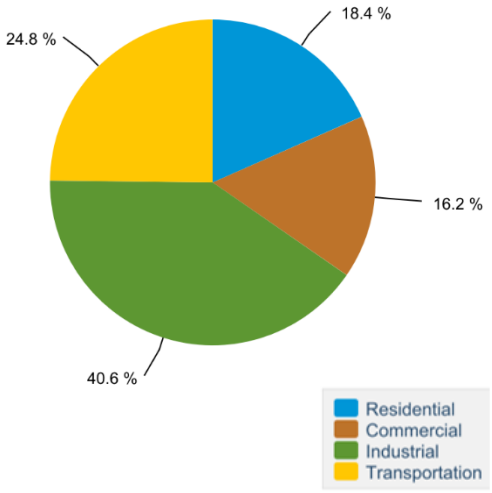

Figure 10. Energy consumption by end-use sector in SD, 2019 (EIA) [66]

From Figure 9, it can be noted that SD consumes one of the largest amounts of energy per capita. This can be attributed to the various energy-intensive industries that exist in the state. Also, from Figure 10, it is depicted that the transportation sector makes up a significant portion of consumption in the state. In 2019, SD ranked 9th in the nation in transportation consumption per capita [67]. This is largely due to the spread-out, small towns making it difficult for the residents to complete daily activities without vehicle

transportation. In terms of emissions, a typical vehicle emits roughly 4.6 MT, or 10,141 lbs of CO_2 a year [68]. In comparison, CO_2 emissions for energy use in a typical household are about 8 MT, or 17,505 lbs of CO_2 equivalent [17]. Based on this data, significantly more CO_2 is emitted considering there are commonly multiple cars to household. Because transportation is a necessity in most areas, it is difficult for state residents to substantially lessen vehicle use to avoid these CO_2 emissions. Though compensation can be applied to other sectors.

As previously mentioned, large amounts of energy consumption yield large amounts of CO_2 emissions. In 2020, SD released 14.9 million $MtCO_2$ into the atmosphere, ranking the state 45^{th} in the nation [69]. When looking at CO_2 emissions per capita, the state ranked 21^{st} with 17.7 $MtCO_2$ emitted per person [70]. Similar to the energy consumption results, most of SD's CO_2 emissions come from the transportation and industrial sector [71]. Table 4 details the energy-related CO_2 emissions by sector in SD as of 2020. It can be noted that energy-related CO_2 corresponds to emissions that result from the combustion of fossil fuels.

Table 4. SD energy-related CO_2 emissions by sector, 2020 [71]

Sector	**Million $MtCO_2$**	**Shares (%)**
Transportation	6.6	44.3
Industrial	4.1	27.6
Electrical Power	2.3	15.3
Residential	1.1	7.1
Commercial	0.9	5.9
Total*	**14.9***	**100***

*Totals off due to rounding for simplification

From Table 4, it is clear that the transportation and industrial sectors contribute the most to SD's effect on climate change, making up over 70% of the state's total emissions. To reduce the amount of CO_2 emissions in the state, making a change in one of these sectors will exhibit the best results. Although the transportation sector generally makes up a larger portion of CO_2 emissions, in SD, the industrial sector shows significant potential to reduce CO_2 emissions widely due to ready access to renewable resources, such as biomass. As stated in the above section, biomass is used in the fuel ethanol production process. Taking advantage of incorporating renewable resources in place of fossil fuels can have a significant impact on the state's overall CO_2 emissions.

Because overall energy consumption is related to the amount of CO_2 emissions, SD must act in these sectors as it is one of the top ten energy consumers in the nation. To satisfy terms of the Paris Agreement, even fossil-fueled plants will need to reduce their total GHG emissions to near zero. This will require extensive planning in existing plants and an elimination of any pending facility constructions in the future. Aside from fading

out fossil-fuel usage, capturing the carbon dioxide from CO_2 emitting facilities through a process called carbon capture and storage (CCS) has shown great promise to energy leaders. In SD, ethanol facilities would make a primary candidate due to the high purity stream of CO_2 that is emitted; however, limited research exists into the economic feasibility of implementing these systems at ethanol refineries.

2.5 Carbon Capture and Storage (CCS)

Finding practical strategies to minimize CO_2 emissions is a popular issue today. Due to the rapid rise in global temperatures, countries have banded together in hopes of lowering GHG emissions and thereby mitigating climate change. Unfortunately, because of the current reliance on fossil fuels to provide energy, completely eliminating fossil fuel usage is not an option. A process that allows for a transition away from fossil fuels while reducing CO_2 emissions is carbon capture and storage (CCS). However, CCS technology is still in its early stages of development and additional research is needed to address various challenges before it can be widely deployed.

The CCS process involves separating CO_2 from other gases emitted by power plants and industrial facilities. The CO_2 is then transported from the facility and stored, keeping the gas from entering the atmosphere. This technology captures up to 90% of released CO_2 from the combustion of fossil fuels and is viewed as the most feasible way to decarbonize the industrial sector [73]. While CCS still allows for a continued use of fossil fuels, the technology has the potential to reach negative emissions of CO_2 and should not be ignored [74].

Current debate on CCS mainly centralizes around coal-fired and gas-fired plants [75][76]. This is largely because these plants release significantly more carbon dioxide than industrial facilities. A lack of literature exists on the industrial application of CCS technology, specifically at ethanol facilities [74][77]. The United Nations Industrial Development Organization (UNIDO) stated in a synthesis report that *"[the industrial] area has so far not been in the focus of discussions"* regarding CCS applications. More research into deployment at industrial sites, particularly in applying CCS to biomass processes, is needed to unlock the full potential of CCS, according to the report [78].

2.5.1 Historical Overview of CCS

The idea of capturing CO_2 has been around for many decades. Dating back to the 1920s, CO_2 capture technology was utilized in natural gas reservoirs to separate CO_2 from methane gas [79]. During this time, the primary focus was on extracting CO_2 from a marketable product rather than preventing large amounts from entering the atmosphere. Prevention ideologies and CO_2 mitigation efforts did not come around until the 1970s; however, even after the establishment of the first commercial-scale CCS project in 1972, it was not until decades later that CCS deployment reached the US ethanol industry. To gain an understanding of CCS development in the US, a summary of the established and planned projects is presented. For each project, Table 5 summarizes the year of operation, the industry involved with carbon capture, and the method used to store supplied CO_2.

Table 5. United States CCS projects in operation and construction [80]

Project Name	Operational	Industry	Storage Type
Operating Projects			
Val Verde Natural Gas Plant	1972	Natural Gas Processing	EOR
Enid Fertilizer	1982	Fertilizer Production	EOR
Shute Creek Gas Processing Plant	1986	Natural Gas Processing	EOR
Great Plains Synfuel Plant and Weyburn-Midale Project	2000	Synthetic Natural Gas	EOR
Core-Energy CO_2-EOR	2003	Natural Gas Processing	EOR
Arkalon CO_2 Compression Facility	2009	Ethanol Production	EOR
Century Plant	2010	Natural Gas Processing	EOR
Bonanza BioEnergy CCUS EOR	2012	Ethanol Production	EOR
Air Products Steam Methane Reformer	2013	Hydrogen Production	EOR
Coffeyville Gasification Plant	2013	Fertilizer Production	EOR
Lost Cabin Gas Plant	2013	Natural Gas Processing	EOR
PCS Nitrogen	2013	Fertilizer Production	EOR
Illinois Industrial Carbon Capture and Storage	2017	Ethanol Production	Geological
In Construction			
The ZEROS Project	2023	Power Generation	EOR
Louisiana Clean Energy Complex	2025-2026	Various	Geological

Depicted in the table, only three operational CCS projects involving ethanol facilities exist in the US currently. The first commercial-scale CCS operation in the ethanol industry occurred at an ethanol plant in Kansas in 2009. Following this project, the second became operational three years later, also in Kansas. Both projects involved supplying the captured CO_2 to oilfields for EOR. Additionally, it wasn't until five years later, in 2017, that the third ethanol related CCS project would be established in Illinois. In contrast to the first two projects, this project stores captured CO_2 in an underground formation without EOR. Overall, it should be noted that all three CCS projects involving carbon capture from ethanol facilities occur in the Midwest, making this area favorable towards successful commercial-scale CCS deployment. However, publicly available data regarding CCS deployment in the ethanol industry is scarce, which is a major impediment to the widespread development of this application.

2.5.2 CO_2 Capture at Ethanol Facilities

Carbon capturing from ethanol plants is now the most preferred source of CO_2 in the US [49]. Previously, the most preferred source was from anhydrous ammonia plants, but now the number of plants in operation are limited. Power plants, along with coal-fired and natural gas combined-cycle plants, emit dilute streams of CO_2 making them not the best option for capture technology as separation (capture) costs would be high. Because low capture costs are critical for increasing the development of CCS systems, industries with high purity streams should be looked at to pave the way for increasing CCS maturity.

Unlike many other CO_2 emitting industries, capturing CO_2 from ethanol plants requires no separation of exhaust gases making the process fairly simple and cost-

effective. Since a nearly pure stream of CO_2 is released during the fermentation process, the only CCS retrofit needed is additional dehydration and compression processing units [49]. Dehydration is of the CO_2 is essential as any water vapor left in the gas will corrode the pipeline over time. After the dehydration process occurs, then the captured CO_2 is compressed to standard pipeline pressure. These added units can be implemented at reasonable low costs using existing technologies, such as glycol dehydration, and centrifugal or reciprocating compressors and pumps [81]. The main driving point for implementing a CCS system at ethanol facilities is that the typical large capture cost is avoided due to the high purity stream of CO_2. A 2017 study determined how the process conditions in various industries affected the overall capture cost of CO_2 and the results are displayed in Table 6.

Table 6. Comparison of top CO_2 emitting facilities [82]

Stationary Source	**CO_2 Concentration (%)**	**% US emissions**	**Cost ($/Mt$CO_2$)**
Natural Gas	3-5	24.8	75-100
Petroleum	3-8	7.9	58-100
Coal	10-15	29.8	41-51
Refineries	3-20	1.0	35-100
Ethylene production	7-12	0.3	46-62
Cement production	14-33	1.2	26-42
Iron and steel production	20-27	1.0	31-35
Ethylene oxide production	30, 98-100	0.02	14-28
Hydrogen production	30-45, 98-100	0.8	14-28
Ammonia Processing	98-100	0.4	14
Natural gas processing	96-99	0.3	14
Ethanol (fermentation)	98-99	0.7	14

The above table outlines the top CO_2 emitting industrial facilities and compares the CO_2 concentrations, percent of the US emissions, and the overall cost of CO_2 of each source. From this data, it is noted that the main fossil fuel sources – natural gas, petroleum, and coal – have the lowest CO_2 concentration and some of the highest CO_2 cost of all stationary sources in the table. A clear trend is that increasing CO_2 concentration leads to decreasing overall capture cost. Therefore, the most cost-effective options for CO_2 capture include ammonia and natural gas processing, along with ethylene oxide, hydrogen, and ethanol production [82]. Table 7 depicts the stationary sources of

CO_2 in order from most to least cost-effective, and correspondingly from highest to lowest CO_2 concentration.

Table 7. Top CO_2 emitting facilities ranked from most to least cost-effective

Stationary Source	**CO_2 Concentration (%)**	**Cost ($/Mt$CO_2$)**
Ethanol (fermentation)	98-99	14
Natural gas processing	96-99	14
Ammonia Processing	98-100	14
Hydrogen production	30-45, 98-100	14-28
Ethylene oxide production	30, 98-100	14-28
Iron and steel production	20-27	31-35
Cement production	14-33	26-42
Ethylene production	7-12	46-62
Refineries	3-20	35-100
Coal	10-15	41-51
Petroleum	3-8	58-100
Natural Gas	3-5	75-100

As previously mentioned, low capture costs are an important factor in the success of CCS technology. The higher the purity is of a CO_2 stream, the less energy required to separate the CO_2 molecules from a stationary source. At fossil-fueled plants, CO_2 is emitted in very large amounts as can be seen from the percent of US shares column in Table 6, but a large deterrent is the high cost of capture for the systems that would have to be installed. In SD, ethanol plants are a main source of energy production, and

correspondingly contribute to the state's overall CO_2 emissions, making them prime locations for CCS technology.

While high purity streams emit high concentrations of CO_2, the percentage of US CO_2 emissions is not nearly as high as sources with dilute streams. Looking at Table 6, the CO_2 emissions from ethanol fermentation account for 0.7% of total US emissions. When compared to the amount of CO_2 emitted by fossil-fueled facilities, this percentage seems relatively small, which is often an opponent of applying CCS technology at low-emitting CO_2 sources. This is one reason as to why limited research on CCS applications at ethanol facilities exists, as it is easy to underestimate the value of industrial CO_2 capture. However, as the use of fossil fuels declines in the coming decades, CO_2 emissions from high-purity, renewable facilities will rise, accounting for a larger share of US emissions and paving the path for an increase in CCS deployment.

2.5.3 CO_2 Transportation

Once CO_2 has been through the capture stage, it is then transported to a geological storage site. The acquired CO_2 can be transported in three different states: liquid, solid, and gas, and by three different methods: ships, tanks, and pipelines. Because of pressure drops and temperatures changes that are associated with topographic variations, CO_2 is most efficiently transported as a supercritical or dense fluid. This assures that two-phase flow is avoided. Currently, the primary method for large-scale transport is via pipelines. Pipelines are the main source of captured CO_2 and become economically feasible when large quantities of CO_2 are continuously moved over long distances [83].

A critical design concern for transporting collected CO_2 is the accompanying phase behavior. As stated, transportation of CO_2 is most efficient in dense or supercritical phases. CO_2 pipeline operating pressures and temperatures generally range from 10 to 15 MPa and 15 to 30 °C, respectively. From Figure 11, the phase diagram of CO_2 shows the critical point at a pressure of 7.3 MPa and a temperature of 304.1 K, or 30.95 °C [84].

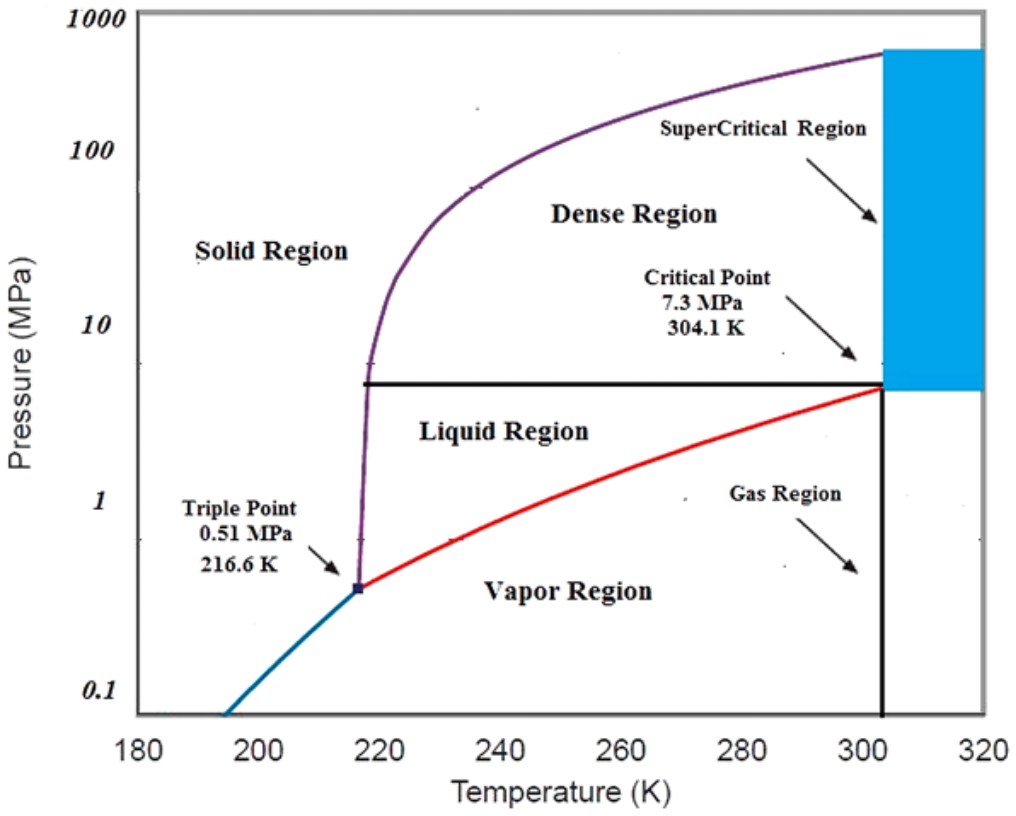

Figure 11. Phase diagram of CO_2 (Mohammadi, M. et al.) [84]

The phase diagram shown above depicts the amount of compression needed for CO_2 transport to achieve a supercritical or dense phase flow. CO_2 is shown to exist in a supercritical phase at pressures above 7.3 MPa and temperatures above 30.95 °C. Correspondingly, the dense region exists at higher pressures and lower temperatures than the critical point [84]. At temperatures lower than the critical temperature, density increases, and pressure losses decrease. Because of this, research has shown that it may

be more cost-effective to transport CO_2 under these conditions in the dense phase [83][85]. When the density of CO_2 is increased, CO_2 is able to flow at high volumes allowing for more efficient transport.

Transportation through pipelines has become standard practice when connecting various sources of CO_2. As of 2021, there are approximately 5,000 miles of CO_2 pipelines active across the US. Of these pipelines, the primary delivery site is oil fields where the CO_2 is used for enhanced oil recovery (EOR) [86]. Most pipelines that transport CO_2 are in states outside of the Midwest. A recent study in the *Proceedings of the National Academy of Sciences of the USA* (PNAS) journal investigated future growth of CCS systems through expanding the transport infrastructure in the US. The location of current CO_2 pipelines is shown in Figure 12.

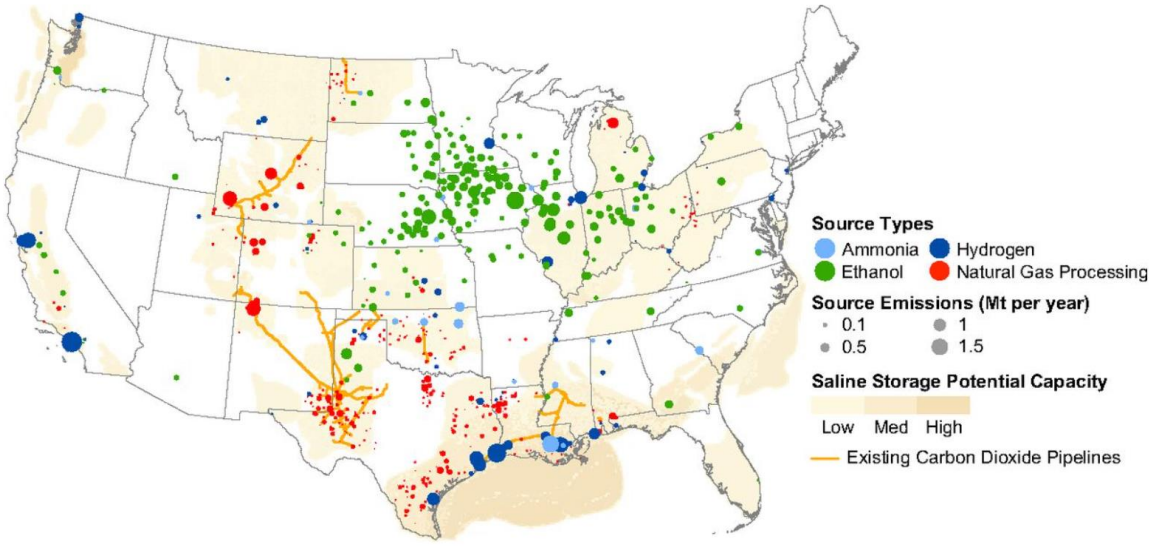

Figure 12. PNAS representation of current CO_2 pipeline locations [87].

Figure 12 also shows the size and location of CO_2 emitting sources with a low cost of capture. As described in the previous subsection, sources that release highly concentrated streams of CO_2 are associated with a low capture cost. Furthermore, there

are noticeably no existing CO_2 pipelines in the Midwest. Therefore, as stated by the Regional Carbon Capture Deployment Initiative and the Great Plains Institute, *"there is immediate economic potential for geographically concentrated, low-cost industrial sources in the Midwest (e.g., ethanol facilities) to aggregate their* CO_2 *supply"* and then deliver the CO_2 to storage locations such as oil fields to increase economic potential [88].

2.5.4 CO_2 Geological Storage

The final step in the CCS process is geological storage of CO_2. This step is significant as it ensures that CO_2 is not released into the atmosphere. Common types of geological formations considered for CO_2 injection are deep saline aquifers, unmineable coal beds, and depleted oil and gas reservoirs. While storing CO_2 deep in the ocean and in deep-sea sediments are also options, CCS technology is not widely applied in these areas due to the negative effects it may have on the marine environment [89].

Saline aquifers are presented as an important option when considering CO_2 storage locations. One benefit to this geological formation is that these sites are widely distributed across the country, which leads to vast amounts of storage capacity. As a result, these sites are more likely to be positioned close to stationary sources of CO_2 and could potentially lower transportation costs. However, there has been slow progress into the advancement of long-term storage at these sites, resulting in a delay of CCS projects in saline aquifers. A known and frequent issue of storing CO_2 in saline aquifers is leakage of CO_2 due to notable pressure build up and migration of CO_2 away from the injection site. Also, saline aquifers do not provide any financial benefits to offset the known high cost of CCS systems [89]. The combined lack of knowledge and no commercial value create an interest in utilizing geological sites that fill this gap.

Unmineable coal beds, also referred to as coal seams, utilize CO_2 to extract gases such as methane in a process known as enhanced coal bed methane recovery (ECBM). Coal beds that are unmineable include those that are too thin, too deep, and do not have enough structural stability to support mining. Gases, the most common one being methane, are found in the existing voids of coal seams where the gases are structurally bonded (adsorbed) to the coal [86]. Correspondingly, the IPCC has documented that coal has a higher affinity for CO_2 than it does for gases like methane that exist in its seams. Therefore, injecting CO_2 into a coal bed allows the trapped methane to be desorbed and recovered. The CO_2 is then able to adsorb in the vacant pores of the coal bed and remain there without being released. ECBM provides a financial incentive for storing CO_2 as the extracted methane can be sold to market for domestic and industrial uses and can assist in offsetting the cost of injection [90]. While ECBM incentivizes the sequestration of CO_2, it is hard to ignore the major issues associated with this method of CO_2 storage. Studies on CO_2 storage in unmineable coal beds have shown that storage capacity, coal permeability, and technology readiness are all key issues that still need to be addressed before CCS technology is implemented at these sites [75][86][91][92]. As of 2021, there are no active ECBM projects making this storage option unconventional for CCS applications [92].

Like saline aquifers, the technologies for CO_2 injection are mature for storage in depleted gas and oil fields. Injecting CO_2 into depleted oil or gas reservoirs implies permanent sequestration of the CO_2. Existing infrastructure already exists at various depleted reservoirs and this equipment would require minimal modifications to be repurposed for CO_2 storage, which serves as an advantage to this storage option [89].

Moreover, the injected CO_2 has no detrimental effect on depleted fields as the fields previously contained hydrocarbons that make up oil and gas. If any hydrocarbons are left after the field is depleted and the field is used for storing CO_2, extra barrels of oil or gas can be produced which would provide an economic incentive for storing CO_2 [90]. As previously mentioned, pressure build up is a frequent issue seen when injecting CO_2 in deep saline formations, with depleted reservoirs, the final pressure has proven to not be above the initial reservoir pressure. Common challenges associated with depleted reservoirs are wellbore integrity, repeated pressure cycling, and reusing infrastructure. At depleted oil or gas fields, the number of wells can range from one to potentially hundreds of wells causing concern for the integrity of the well. Also, there is little documentation regarding the continuous cycling of pressure over long periods of time making it difficult to gauge the overall storage capacity of a field and often time additional equipment is needed resulting in higher operating costs [93].

One of the main concerns when selecting a CO_2 storage method is cost-effectiveness. As discussed, a high cost is associated with implementing CCS technology, so financial incentives play a vital role in the success of these systems. Research has shown that in the coming years utilizing CO_2 to recover additional barrels of oil show the most promise economically [87][94]. The process of injecting CO_2 into oil reservoirs to extract residual oil is known as carbon dioxide-enhanced oil recovery (CO_2-EOR). Enhanced oil recovery (EOR) when paired with carbon capture at ethanol refineries could be a favorable solution to climate mitigation.

2.6 Enhanced Oil Recovery

Enhanced oil recovery (EOR) presents a low-cost option to store CO_2 underground permanently. Unlike other options such as saline aquifers and deep-sea storage, EOR provides a financial incentive for CCS applications. Currently, 90% of captured CO_2 from these anthropogenic sources is used for EOR [87]. Every ton of this CO_2 utilized for EOR results in a net emissions (CO_2e) reduction of 63%, as found in an analysis performed by the IEA [94]. The captured CO_2 from emission sources can be sold to the oil industry for use in active or depleted fields to recover stagnant oil. EOR is an attractive option due to the benefits it provides to the seller and buyer of CO_2. On one hand, the profit that is made by selling the captured CO_2 offsets the high initial costs of CCS systems, which enhances the feasibility of CCS implementation. On the other hand, there is an increase in oil recovery from utilizing CO_2, which allows the oil industry to also make a profit by producing additional barrels of oil. Researchers from Advanced Resources International, a research and development firm that emphasizes on EOR and CCS, states in a document standard *"[w]hile there are still many economic and technical hurdles to overcome…the possibility that the* CO_2*-EOR industry could spur the onset of large-scale commercial storage operations is the most likely pathway for the generation of a CCS industry [95]."* Typically, the injection of CO_2 for EOR is performed using three methods: continuous CO_2 injection, water alternating gas (WAG) injection, or cyclic injection [89].

2.6.1 Continuous CO_2 Injection

Continuous CO_2 injection is utilized in reservoirs that are both highly permeable and thin allowing the CO_2 to distribute throughout the reservoir without the additional

injection of water slugs [95]. In general, reservoir permeability ranges from 0.001 mD to 0.1 mD, where the unit mD represents millidarcy [96]. Additionally, a reservoir is considered thin if its net pay thickness is less than 100 ft. Net pay thickness refers only to the productive zones within the entire reservoir thickness that produce oil and gas, and non-productive rock intervals are not considered because they provide no economic value [97]. Unlike permeability data, the net pay thickness of a reservoir is often not given and must be derived from well log data to obtain an approximate value.

Thin and highly permeable properties are ideal for this method as a frequent issue in EOR operations known as gravity override does not affect the amount of oil recovered in these types of reservoirs. Gravity override occurs due to density differences between the native reservoir fluids and the injected CO_2. Consequentially, CO_2 being the less dense fluid flows over top of the other reservoir fluids and leaves a fraction of oil still in place at the bottom of the formation. Thus, if thick reservoirs were to undergo the continuous CO_2 injection process, low oil recoveries would result from significant amounts of oil being bypassed due to the gravity override phenomena [98].

Continuous CO_2 injection is not as common as WAG or cyclic injection practices, but it is becoming increasingly popular as GHG reduction becomes the primary focus for EOR projects. Historically, the main concern of CO_2-EOR operations was the amount of CO_2 purchased; therefore, minimal amounts of CO_2 were used to recover additional barrels of oil – hindering the implementation of continuous injection processes. However, the future of EOR operations now looks to maximize the potential value of sequestered CO_2 per the Section 45Q Tax Credit, which will be discussed in the next chapter. Now,

larger CO_2 volumes will likely be used paving the way for continuous CO_2 injection methods [99].

2.6.2 WAG Injection

Currently, WAG injection is the most widely deployed process for CO_2-EOR because of its ability to decrease the mobility ratio between the injecting fluid and the oil and reducing the amount of CO_2 that is purchased for EOR [100]. Most CO_2-EOR studies expect that CO_2 injection begins around the end of water flood activities. Thus, WAG picks up where the water flooding stops and injects a large slug of CO_2 to initiate the movement of residual oil. The injected slug of CO_2 is then followed by a water slug to further disseminate the succeeding CO_2 injection into less porous zones, allowing better contact to residual oil. The laid-out process for WAG injection is shown in Figure 13 below [95].

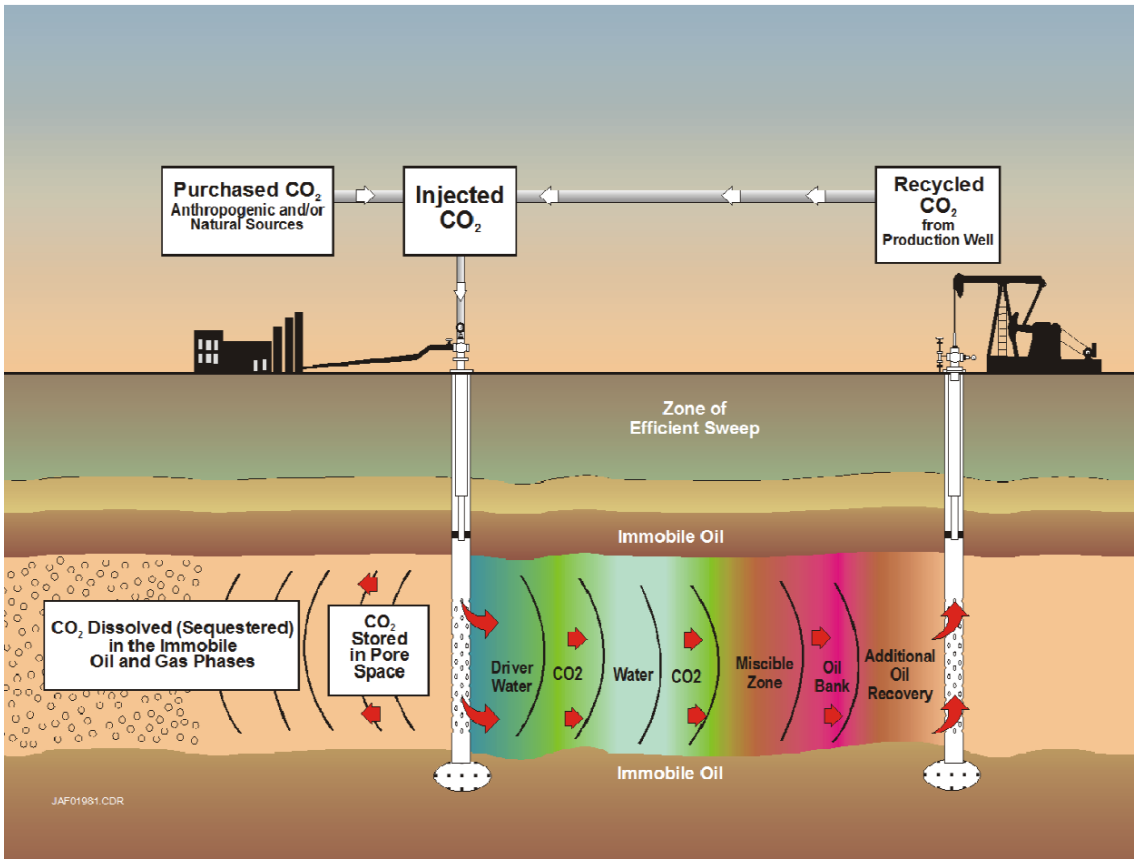

Figure 13. WAG injection process for CO_2-EOR from Carpenter and Koperna [95]

A drawback of this method is that the large density differences between the water, oil, and CO_2 can cause an issue called gas override in areas distant from the injection site. Gas override occurs when the injected gas starts to flow upward and the water and oil flow downward. Early gas breakthrough is a subsequent issue that can occur especially in reservoirs with large vertical heterogeneity and highly permeable channels [100]. This event references the abrupt increase of gas flow due to the steady increase of gas injection pressure to a critical value [101]. To address this problem, researchers have been proposing the three-stage cyclic injection method, which is often referred to as the huff-n-puff process.

2.6.3 Cyclic (Huff-n-Puff) Injection

Injecting CO_2 via the huff-n-puff method consists of three stages: huff, soak, and puff. During the huff stage – Step 1 and 2 below – CO_2 is injected and rapidly flows through the existing fractures in the reservoir. The CO_2 then permeates into the rock due to an existing concentration gradient. As can be seen in Figure 14 below, which illustrates this huff-n-puff process, CO_2 carries residual oil into the rock which causes a decrease in overall oil production; however, the CO_2 can also push oil out of the rock which would cause an increase in production. The soak stage – Step 3 – involves "shutting in" the well to allow the CO_2 and oil sufficient time to interact, reducing the viscosity of the oil. Finally, the puff stage – Step 4 – occurs when the pressure has reached equilibrium. The residual can now move through the fractures and be recovered from the same well [100].

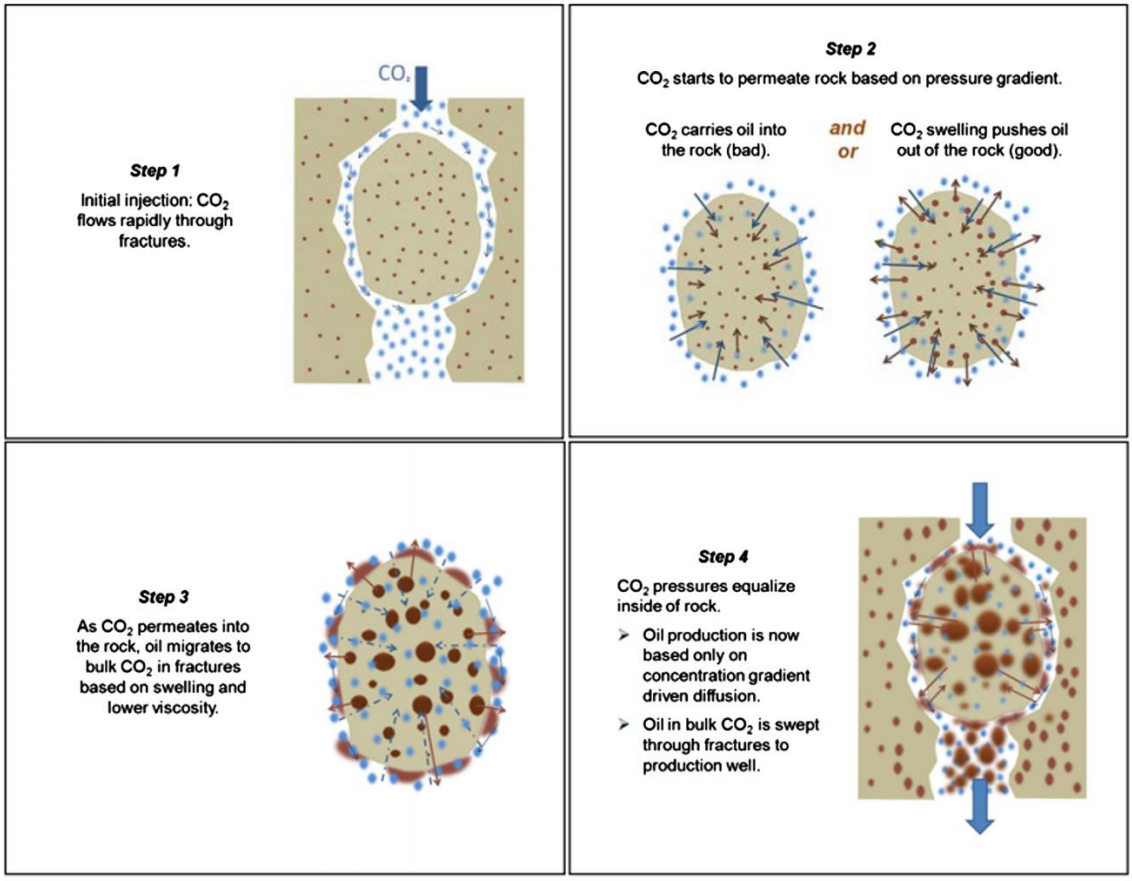

Figure 14. Stages of the cyclic injection method depicted by B. Jia et al. [100]

In contrast to the previous methods, the cyclic process utilizes only one well for both injecting CO_2 and extracting residual oil. Due to this simplicity and low CO_2 consumption, this method of injection for EOR is associated with a relatively low cost and is utilized to improve oil recovery in ultra-low permeable reservoirs [102]. Though cyclic injection has shown potential for atypical reservoirs, few field projects exist making the public data from these projects scarce [103]. In order to successfully deploy this method, the reservoirs first need to meet certain requirements and second, more publications need to be made available in order to make this process feasible and maximize oil recovery.

2.7 Case Studies

As publicly available research regarding CCS operations at ethanol facilities is limited, estimating the economic feasibility of future projects proves to be challenging. Studies that investigate capturing and utilizing CO_2 from the ethanol industry are introduced here in relation to economic feasibility. Key findings from the detailed studies in this section will be compared against the findings of this work to assess the overall accuracy. A whitepaper published in 2017 by the State CO_2-EOR Deployment Workgroup analyzes the economic opportunity of the ethanol industry through modeling two CO_2-EOR scenarios at different scales. The two scenarios will now be discussed.

2.7.1 CO_2-EOR in Nebraska and Kansas

The smaller scaled CO_2-EOR scenario involves collecting CO_2 from 15 ethanol plants located in Nebraska and Kansas, and then transporting CO_2 to oil fields in Kansas. During the capture process, the combined ethanol capacity of 1,575 million gallons per year (MMGY) from ethanol plants provide 4.3 million MT of capturable CO_2 per year. This captured CO_2 is transported via a pipeline network consisting of 737 miles in total. After performing a cost analysis on the modeled system, the capital and operating and maintenance (O&M) costs were determined individually for the capture and transportation process. The total capital cost associated with carbon capture, compression, and dehydration resulted in $364 million. O&M capture costs were estimated to be about $37 million per year. Similarly, the total capital cost associated with pipeline transport was estimated to be $642 million, and the O&M costs were estimated to be $16 million per year for CO_2 transport. Figure 15 illustrates the model used for this case study.

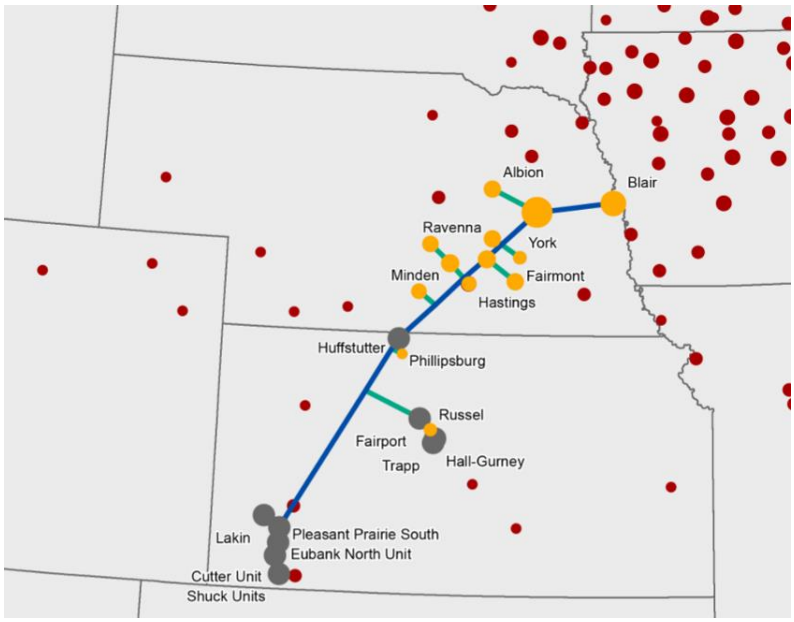

Figure 15. Small scale case study of a CO_2-EOR operation in Kansas and Nebraska

2.7.2 Largescale CO_2-EOR in Midwest

The other scenario analyzed by the State CO_2-EOR Deployment Work Group was a large-scale CCS network involving numerous ethanol facilities in the Midwest. In this scenario, 34 ethanol plants that produce 9.85 million $MtCO_2$ are connected via 1,546 miles total of pipeline. A large-scale model was developed to capitalize on the economic benefits available through capturing and utilizing CO_2 from ethanol facilities. With the modeled CCS system, the related capture and transportation costs were evidently higher than the small scale scenario. Total capture capital costs were estimated to be $809 million, and total capture O&M costs were estimated to be $85 million per year. On the other hand, total capital transportation costs were found to be $1,857 million, and total transportation O&M costs were found to be $47 million annually. Figure 16 illustrates the large-scale CCS system in the Midwest.

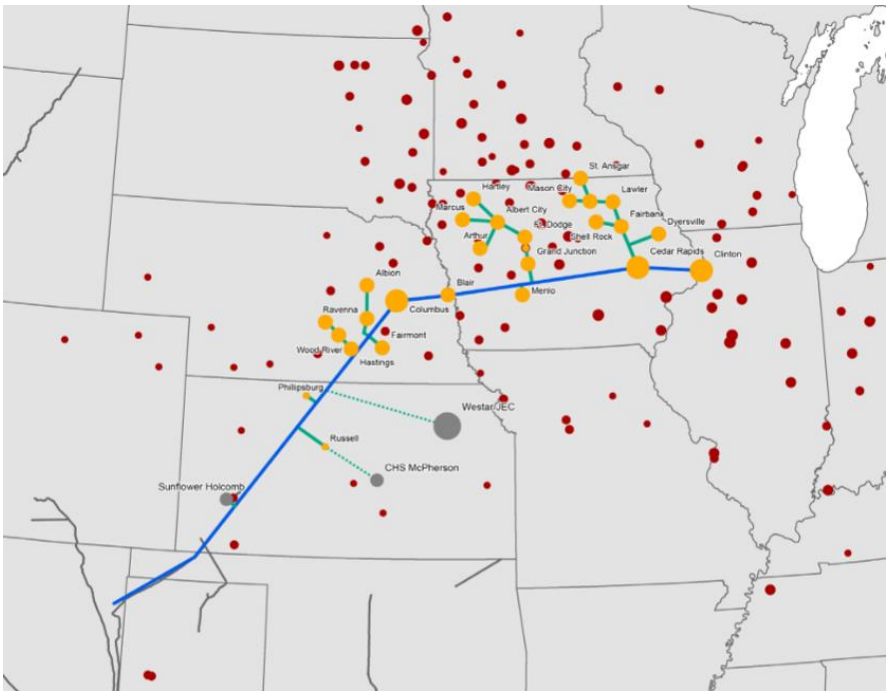

Figure 16. Large-scale case study of a CO_2-EOR operation in the Midwest

The results from this whitepaper establish theoretical cost results that are accepted estimates. Therefore, these costs of capture and transportation will be used to compare and validate the results found in this study. There are a lot of outside factors that could contribute to the overall costs of a capture and transportation system, but what will be highlighted for comparison are the capture quantity and the pipeline length. Now, the methodology used to model and analyze the CCS system presented in this study will be discussed.

3 METHODOLOGY

As CCS technology is being recognized as a way to reduce GHG and assist in reaching net-zero carbon emissions by 2050, few large-scale projects have been deployed due to significantly high costs of implementation. Despite the great number of high-purity CO_2 sources in the Midwest, large-scale CCS projects have yet to gain traction. SD consists of numerous ethanol plants concentrated on the same side of the state, and thus is a prime contender to assist in the reduction of CO_2 emissions using CCS technology at these facilities. The decision to install a CCS system at any facility is largely determined by the expected costs and benefits of the selected system. Therefore, the goal of this thesis is to determine if implementing a CCS system at dry mill ethanol facilities in SD is economically feasible and to analyze the systems overall effect on GHG emissions of these facilities. By analyzing the costs of CO_2 capture and transport at ethanol facilities, the economic feasibility can be assessed. To provide economic benefits to the state and create a more viable option, EOR methods will be analyzed using the existing oil fields in the state. The impact of varying cost influential factors such as oil price and oil recovery rates will also be examined.

3.1 Modeling the Capture and Transportation System

The analysis to determine the feasibility of capturing CO_2 from high purity sources involves highlighting the effect of different parameters to the overall system. First, a base case scenario is established capturing CO_2 from each ethanol plant in SD and transporting this CO_2 via pipeline to existing storage facilities in the state – oil fields and saline formations. Because of the financial benefits provided through geological storage with EOR, the oil fields in Harding County will be the main point of focus. The National

Energy Technology Laboratory's (NETL) CO_2 Transport Cost Model will be used to calculate capital and operating costs of this pipeline. Whereas capture, compression, and dehydration cost estimates will be derived using data from publicized DOE-funded projects as a lack of publicly available data from ethanol plants exists. For modeling and analyzing purposes in this study, the project's operational period is 20 years with a 2-year construction period. Figure 17 illustrates the location of ethanol plants along with the location of storage facilities in SD.

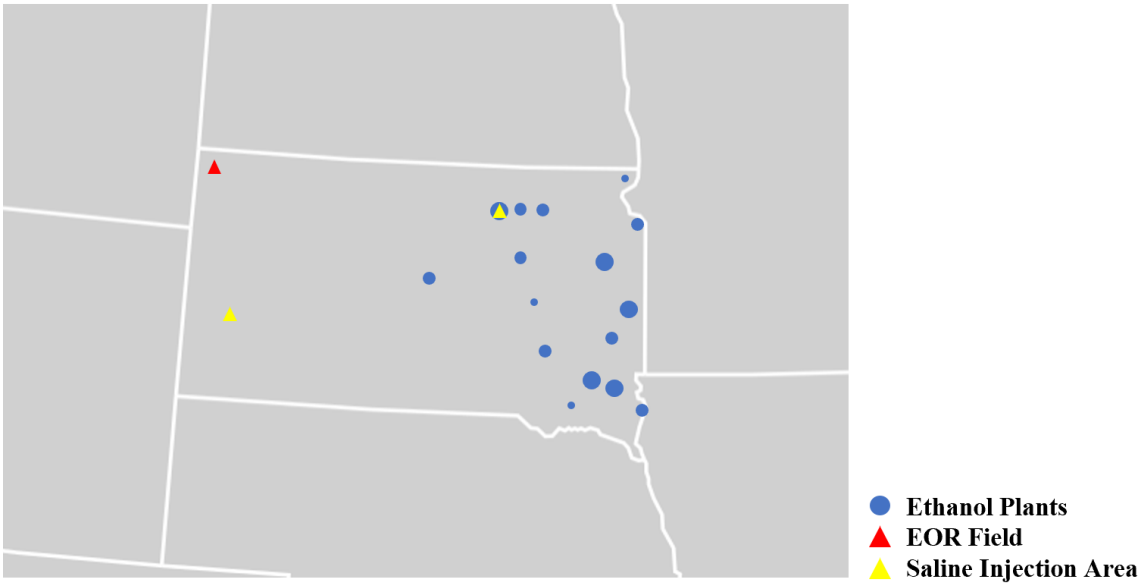

Figure 17. Overview of ethanol plants and storage facilities in SD

It is seen in Figure 17 that potential storage formations and capture sites are on opposite sides of the state, which will result in a large pipeline network. With such a long pipeline, large volumes of CO_2 are needed to ensure financial feasibility. The size of each blue circle indicates the amount of ethanol production from that plant and will be discussed in the following subsection. To estimate storage costs, the federal 45Q tax credit benefits will be taken into account. The saline formations shown in Figure 17

(yellow triangles) pose an alternative storage option for the captured and transported CO_2 volumes. The modeling methodology for the capture, transportation, and storage processes will now be discussed.

3.1.1 CO_2 Capture

The base case CCS system involves installing capture technology at all 16 ethanol plants in SD. Therefore, an analysis of these plants is necessary to determine the total amount of CO_2 emitted from ethanol fermentation and thus the CO_2 capture capacity of each plant. The capture capacity will represent the average annual amount of CO_2 transported throughout the pipeline and similarly, and the amount that needs to be stored. As previously noted, ethanol plants in SD are mainly clustered on the eastern side of the state. Figure 18 depicts the location of all 16 ethanol plants in SD.

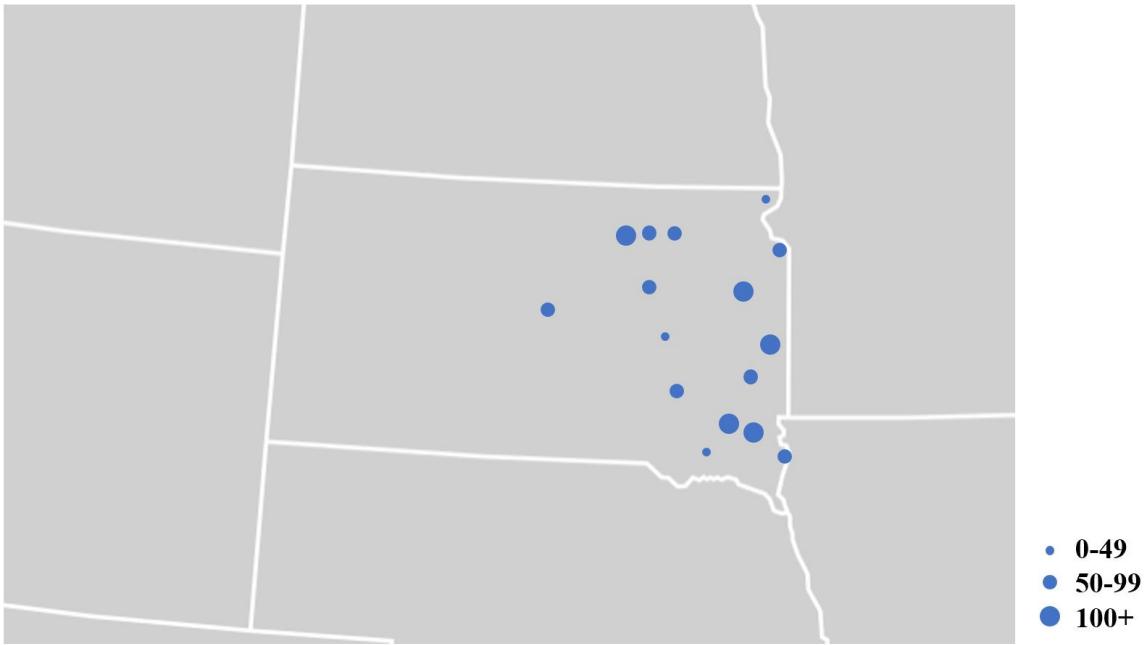

Figure 18. Location of ethanol plants in SD

Also represented in Figure 18 is the production capacity of the plants. The size of each circle corresponds to the nameplate capacity of ethanol production, which ranges from 12 to 150 million gallons per year (MMGY). Notably, all but three operating plants have the capacity to produce over 50 MMGY, making SD a primary state for ethanol production. The largest producing ethanol facilities in the state are located in Marion, Aurora, Mina, and Watertown. Ethanol production capacities for each of the 16 ethanol plants in SD are listed in Table 8.

Table 8. SD ethanol plant production capacity and CO_2 emissions

Ethanol Plant	**Location**	**Ethanol Capacity (MMGY) [104]**	**CO_2 Emissions (Million MTY)**
NuGen Energy	Marion	150	0.45
Valero Renewable Fuels	Aurora	140	0.42
Glacial Lakes Energy	Mina	140	0.42
Glacial Lakes Energy	Watertown	130	0.39
POET Biorefining	Chancellor	110	0.33
Dakota Ethanol	Wentworth	90	0.27
Ringneck Energy	Onida	80	0.24
POET Biorefining	Big Stone	79	0.24
POET Biorefining	Mitchell	68	0.20
Redfield Energy	Redfield	60	0.18
POET Biorefining	Hudson	56	0.17
POET Biorefining	Groton	53	0.16
Glacial Lakes Energy	Aberdeen	50	0.15
Glacial Lakes Energy	Huron	40	0.12
Red River Energy	Rosholt	35	0.11
POET Biorefining	Scotland	12	0.04
Total		**1,293**	**3.89**

Along with ethanol capacity, the corresponding CO_2 emissions from the ethanol fermentation process is listed for each plant in million metric tons per year (million MTY). Research has documented that one gallon of ethanol produced yields 6.624 lbs of

CO_2 [105]. Pounds of CO_2 was then converted to MT using a weight equivalent (4.536×10^{-4} MT per one lb). From Table 8, it is shown that SD has a total ethanol production capacity of 1,293 MMGY while also emitting a total of 3.89 million MTY of CO_2 from ethanol fermentation.

Because data from fermenters in an ethanol plant is not widely available to the public, it is more challenging to estimate capital and operating expenses associated with CO_2 capture, compression, and dehydration. As discussed in the Literature Review, there are currently only three operating CCS systems utilizing CO_2 from ethanol plants. For the three systems, CO_2 is delivered via pipeline for and two are stored in EOR fields and the other in saline formations. Although data such as capture capacity and pipeline routes is available to the public, information regarding capital and operating costs of the three projects is not. To monetize these expenses for a CCS project in SD, estimates from three publicly available reports funded by the Department of Energy (DOE) and Great Plains Institute (GPI) are used [106][107][108]. Data regarding the capital expenditures (CapEx) and the corresponding ethanol plant size were plotted to establish the line of best fit. A linear correlation was found between these variables and the equation for CapEx of CO_2 capture, compression, and dehydration can be seen in Equation 6 [108].

$$CapEx\ (\$Million) = 0.15 * Plant\ Size\ [(MMGY)] + 9 \quad (6)$$

Operating expenses (OpEx) for capture technology at ethanol plants represent a small portion of the overall capture costs. Similar to the capital costs approach, data was taken from the three available sets of data to determine an equation that can estimate the operation and maintenance cost of CO_2 capture, compression, and dehydration. The CO_2 capture amount in million MTY was plotted against the total OpEx for each system. Once

the data was plotted, a linear regression was found to be the best fit for the data and the OpEx equation was established. Figure 19 illustrates the relationship between these data sets, and the equation used to estimate the OpEx for different scenarios presented in this study is presented in Equation 7.

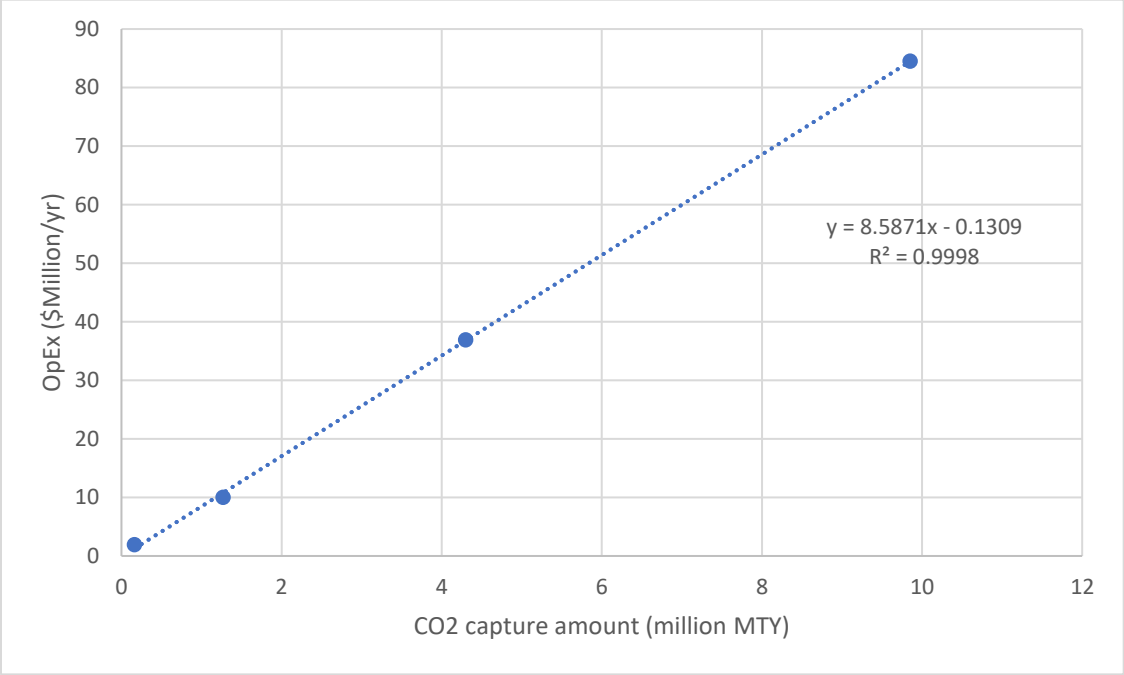

Figure 19. Capture, compression, and dehydration operating expenses

$$OpEx\left(\frac{\$Million}{year}\right) = 8.59 * Captured\ CO_2\ [(million\ MTY)] - 0.13 \qquad (7)$$

After establishing equations for both capital and operating costs pertaining to CO_2 capture, compression, and dehydration, the total costs of the carbon capture process at SD's ethanol facilities can be determined. The results section will discuss the estimated cost results in detail, and conclusions can be made regarding the overall feasibility of capturing CO_2 from ethanol plants in SD. As detailed in Section 2.5.2 of the Literature Review, ethanol plants are now a preferred source of CO_2 capture due to lower capture costs than fossil fuel-fired power plants. Therefore, to pose a financially feasible option

for SD, results must show the reduced costs of capturing CO_2 from ethanol facilities can still provide revenue to the state. Methodology will now be discussed for the transportation of CO_2 via pipeline.

3.1.2 CO_2 Transportation

In the base case scenario, the CO_2 is transported from the ethanol plants to oil fields in the northwestern corner of the state. This pipeline consists of a primary trunk line starting in Hudson, SD, running through Onida, SD, and ending at the Harding County oil fields where EOR processes will be initiated. Feeder lines then connect the remainder of the ethanol plants outside the primary trunk line. This route was selected as it minimized the total pipeline length required to reach all ethanol plants in the state. Along with storage in the Harding County oil fields, the pipeline network also passes through a saline injection site providing an alternative storage option in case any additional storage is needed. Figure 20 illustrates the described pipeline route.

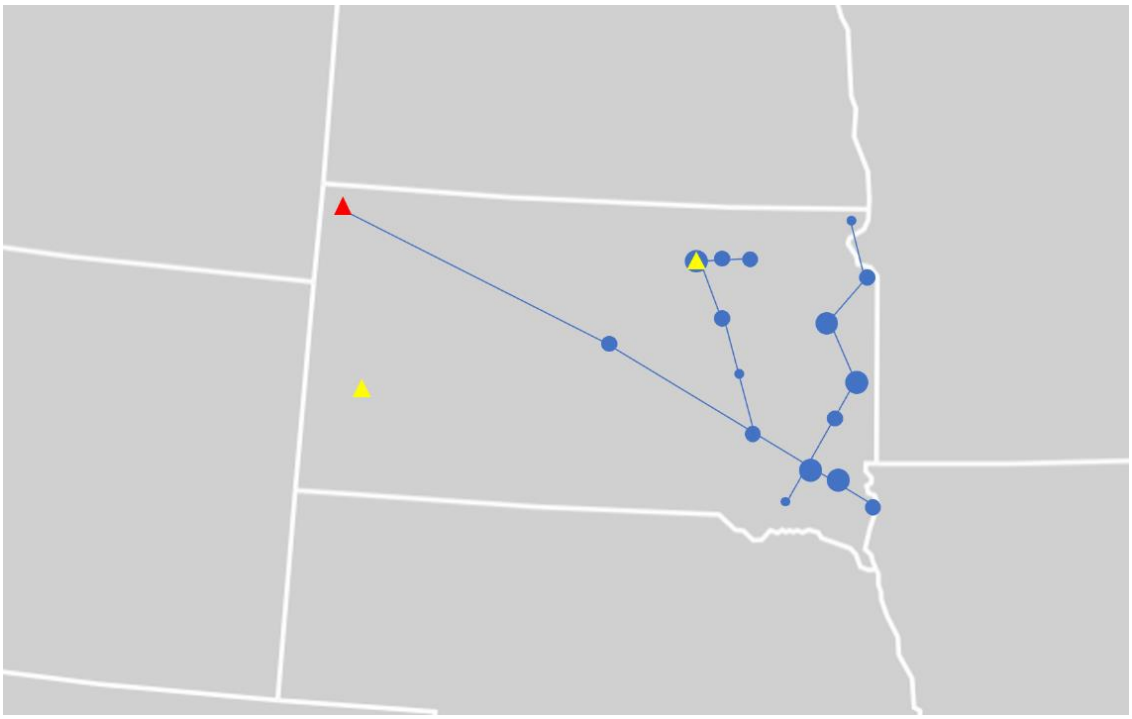

Figure 20. CO_2 pipeline network

To estimate capital and operational costs of transporting CO_2 via the depicted pipeline, the NETL Transport Cost Model is used [109]. The NETL Transport Cost Model has been used in multiple research projects, including those funded by the DOE, to efficiently evaluate transportation costs for numerous pipeline networks [106][107][110]. This mathematical transportation cost model consists of both a financial and engineering module. With the financial module, cash flows of revenues and costs are outputted over the span of the project and various financial inputs are required such as the percent equity, interest rate on debt, and escalation rate to the project's start year. To generate these cash flows, the financial module is dependent on cost data which is evaluated by the engineering module. In this study, only the engineering module is used because the costs of transporting CO_2 are separate from the costs of capture and storage.

The engineering module estimates total transportation capital and operating and maintenance (O&M) costs from an array of user-inputs. Inputs to the module include pipeline length, number of booster pumps, annual CO_2 flow rate, capacity factor, input and output pressures, and elevation change. Based on these inputs, the module then can size the pipeline by determining the minimum inner pipe diameter and the corresponding smallest nominal diameter of the pipe. Calculations for the total number of booster pumps required throughout the pipeline are also included. Furthermore, the overall cost per MT of transported CO_2 can be determined from the given input parameters and the resulting costs of the system. This variable represents the cost required to transport CO_2 throughout the pipeline and comparing this over various transportation systems can yield the most efficient pipeline network.

One drawback of the NETL Transport Cost Model its inability to analyze more than one pipeline segment. Because different flow rates exist in between each capture facility, the pipeline must be broken up and analyzed in separate segments to obtain overall cost estimates. A straight-line distance between ethanol plants was used to determine segment lengths. Given the actual pipeline route will not be a straight line through capture sites, a multiplication factor of 1.2 was applied to the pipeline mileage to account for any additional routing needed [110]. Inputs used in the NETL Transport Cost Model for each segments in the pipeline network are displayed in Table 9.

Table 9. Base case pipeline segment inputs for the NETL Transport Cost Model

Segment	Length (x1.2) (mi)	Number of Pumps	Annual CO_2 (Million MTY)	Input Pressure (psig)	Outlet Pressure (psig)	Elevation Change (ft)
1	38	1	0.17	2,200	1,600	100
2	17	1	0.50	2,200	1,600	50
3	52	1	2.42	2,200	1,600	-50
4	146	4	3.65	2,200	1,600	500
5	216	8	3.89	2,200	1,600	1000
6	36	1	0.04	2,200	1,600	0
7	50	1	0.11	2,200	1,600	50
8	50	1	0.35	2,200	1,600	500
9	56	2	0.74	2,200	1,600	-100
10	29	1	1.16	2,200	1,600	50
11	50	1	1.43	2,200	1,600	-200
12	23	1	0.16	2,200	1,600	0
13	16	1	0.31	2,200	1,600	50
14	48	2	0.73	2,200	1,600	-50
15	46	1	0.91	2,200	1,600	0
16	55	1	1.03	2,200	1,600	0

It is important to note key assumptions used with this cost model. First, the assumed duration of operation for the project is 20 years, which has been established as the default for the cost model per research into typical CCS lifetimes [111]. The

transportation cost model uses a base year of 2011 for its cost estimates but allows for escalation to $2022. For the purpose of this study, 2022 is taken as the project's start year to avoid excess extrapolation. Also, booster pumps are spread out evenly along each pipeline segment with no booster pump at the very end of each pipeline. The booster pumps are assumed to keep inlet and outlet pressures the same throughout the pipeline increasing the outlet pressure to the inlet pressure of the following booster pump. For the pipeline network, the inlet pressure is assumed to be 2,200 psig, and the pressure drop is set to not exceed 800 psig for each pipeline segment; therefore, the assumed outlet pressure at the end of each segment is 1,600 psig. The capacity factor is set at 85%, which is the default for the cost model. The maximum CO_2 flow rate throughout the pipeline is found by dividing the annual average flow rate of CO_2 by this assumed capacity factor. Thus, for the base case scenario, the maximum CO_2 flow rate through the pipeline is 4.58 million MTY. Ultimately, the values described and listed in Table 9 are used to find the minimum inner diameter and the nominal diameter of each pipeline segment. The sized pipeline diameters for the base case scenario are listed in Table 10.

Table 10. Base case optimized pipeline diameters

Segment	Minimum Inner Diameter for Pipe (in)	Pipeline Nominal Diameter (in)
1	3.37	4
2	4.33	6
3	9.77	10
4	11.91	12
5	11.77	12
6	1.91	4
7	3.00	4
8	4.82	6
9	5.83	6
10	6.62	8
11	7.88	8
12	2.96	4
13	3.55	4
14	5.63	6
15	6.58	8
16	7.16	8

The number of booster pumps in combination with the nominal pipeline diameter that result in the lowest cost of the pipeline can be determined by the cost model. Because the model does not recognize the system is being analyzed in separate segments, a booster pump was manually added to the system if the cost model returned a value of 0.

This ensures the CO_2 pressure is maintained throughout the pipeline. Additionally, the cost model ultimately can determine the booster pump and nominal diameter combination that yields the lowest break-even CO_2 price for the system. An increasing number of booster pumps ultimately increases the cost of the system; however, when combining and increasing amount of booster pumps and a smaller pipe diameter, the overall cost of the system can be reduced. Table 10 shows the optimized minimum inner diameter and nominal diameter for the pipeline segments per the amount of booster pumps required. After the number of booster pumps and nominal diameter of the pipeline have been determined, the overall transportation expenses of the pipeline network can be evaluated.

Capital costs developed by the transportation cost model are placed into various categories. These categories include the costs of materials, labor, right-of-way (ROW) and damages, control systems, CO_2 surge tanks, booster pumps, and miscellaneous costs. The material category accounts for pipeline material, coating, and corrosion protection expenses. Labor distinctly covers all labor costs needed to produce the pipeline. Additionally, the ROW and damages category includes obtaining ROWs from property owners and damages that may result. On the equipment side of the capital cost categories, pipeline control systems cover the monitoring and supervision of the pipeline. CO_2 surge tank equipment is needed to address pressure changes and monitor CO_2 flow rates in the pipeline. Similarly, booster pump installation is needed throughout the pipeline to maintain ideal CO_2 pressure. Lastly, miscellaneous costs generally cover any additional non-production related expenses and fees such as surveying, supervision, engineering, contingencies, and taxes.

For this study, contingency costs are not included in total transportation capital cost estimates. This is primarily because the models used for comparison and validation also do not report contingency capital costs. However, as previously noted, some contingencies are incorporated in miscellaneous capital costs. When the engineering-based analysis within the NETL Transport Cost Model is performed, the distribution between the capital cost categories can be examined. Total transportation costs (capital and O&M) will be discussed in detail in the results chapter.

Like the categorization of transportation capital costs, O&M costs are separated into three subparts: pipeline O&M, equipment and pump O&M, and pump electricity requirements. Annual pipeline O&M costs are evaluated using a fixed cost per mile of the pipeline. The NETL cost model determines this value to be $8,477/mi-yr using supplemental data regarding transportation and storage costs. Likewise, annual equipment and pump O&M expenses are computed taking 4% (cost model default per NETL professional judgement) of the total combined CO_2 surge tank, control system, and pump capital costs. Electricity costs are estimated using the cost of electricity from the base year (2011), which was $68.20/MWh. The base year is used to avoid double scaling as the total costs are escalated from the base year to the project start year (2022) by the cost model when displaying the end results. Total O&M costs for the 20-year project are evaluated for each segment and then summed to obtain a total value for the project.

3.2 Storing CO_2 with EOR

3.2.1 CO_2 Storage Resource Estimation in Oil Reservoirs

Two geological storage sites in SD – oil reservoirs and saline aquifers – are prime candidates to permanently store CO_2 using CCS techniques. In addition to geological storage in oil reservoirs, a process that both produces oil and stores CO_2 underground is EOR. EOR is particularly attractive in early development stages of CCS because, as discussed in the Literature Review, the value of additional oil offsets high initial CCS costs. If SD is able to store its captured CO_2 in EOR units within the state, the added revenue of oil could be what makes CCS technology financially feasible. Therefore, a key characteristic of CCS feasibility is the amount of available carbon storage space within a storage site. A methodology was established by the DOE to assess CO_2 storage resource potential and provide high-quality assessments of prospective storage formations. Using the DOE methodology, CO_2 storage resource estimates are made to determine the potential geological storage within the state, as well as the ability of CCS technologies to assist in reducing CO_2 emissions.

There are two types of CO_2 storage estimates referenced in the DOE methodology: CO_2 storage resource estimates and CO_2 storage capacity estimates. A detailed analysis is provided solely for CO_2 resource estimates due to its ability to be administered globally. The CO_2 resource estimate represents a formation's fraction of pore volume available for CO_2 storage which will be filled by CO_2 injected through completed wellbores. For resource estimates, only certain physical considerations are needed to define the available portion of the formation. Moreover, the CO_2 storage capacity estimate requires knowledge of current economic and regulatory considerations

of the storage site, such as the number and type of wells drilled and well spacing requirements. These site-specific assessments yield a significantly higher-level analysis than already global scale CO_2 storage resource estimates [113].

In oil reservoirs, the DOE methodology estimates the CO_2 storage resource using a volumetric approach. A widely accepted assumption of this methodology is that the total volume of oil produced will be replaced by an equivalent volume of CO_2; although, an even exchange between oil and CO_2 does not always exist. When accessible, production-based CO_2 resource estimates are preferred over volumetric-based analyses as production data details valuable information regarding the quality of the formation. Nonetheless, production data from all reservoirs in question is not always readily available. This study uses various accessible geological parameters of the oil fields in Harding County to determine the total CO_2 storage resource estimate in the state. Specifically, for the base case, utilizing the existing EOR units in Harding County. The SD Department of Agriculture and Natural Resources (DANR) has a publicly available interactive map, which allows each EOR unit in the state to be displayed. For reference, the location of the EOR units in Harding County, SD, are shown in Figure 21.

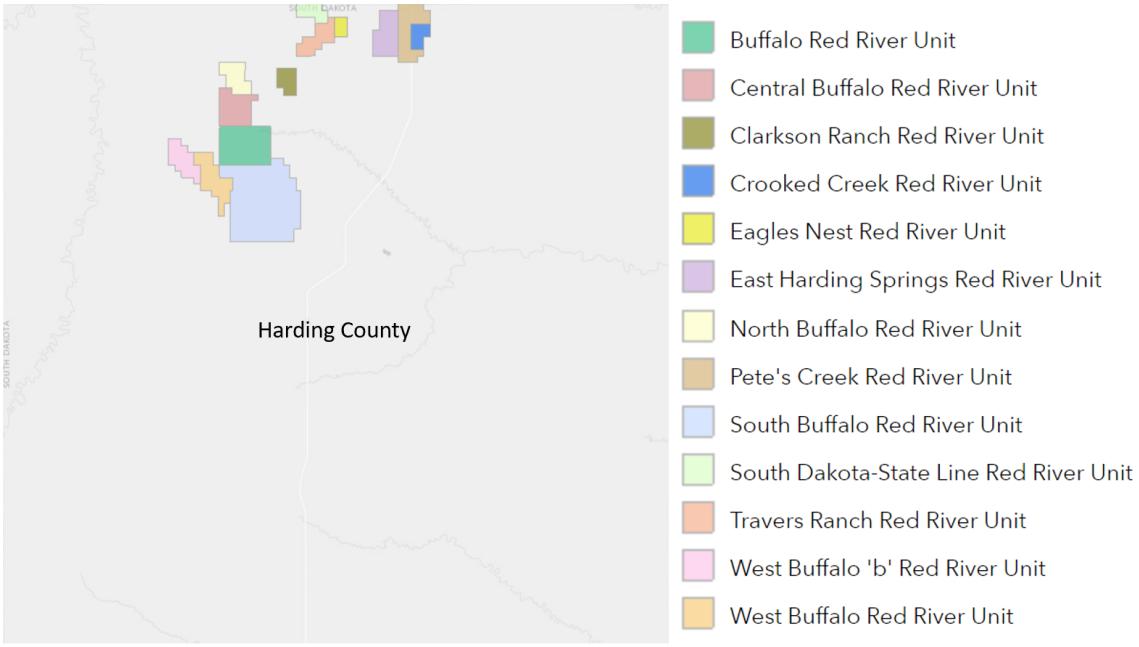

Figure 21. Location of Harding County EOR units taken from SD DANR [114]

In addition to the EOR units in Harding County, three more exist in Fall River County – Alum Creek, Igloo, and Indian Creek Red River Unit – in the lower left corner of the state. Because the Fall River units are smaller than the majority of those in Harding County and are a significant distance away from the selected pipeline route, the three EOR units are not going to be considered in the CCS scenarios. Nevertheless, the volumetric approach is used for the selected EOR units to estimate the total CO_2 storage resource available. Equation 8 shows the volumetric equation in its general form for oil reservoir estimates that is published in the DOE methodology. It can be noted that this equation can also be used for gas reservoirs by replacing E_{oil} with E_{gas} and B_o with B_{gas} [113].

$$G_{CO_2} = A\ h_n\ f_e\ (1 - S_{wi}) \left(\frac{1}{B_o}\right)\ \rho_{co_2}\ E_{oil} \quad (8)$$

Where, G_{CO_2} = Mass estimate of oil reservoir CO_2 storage resource (MT)

A = Reservoir area (acres)

h_n = Net thickness (ft)

f_e = Average effective porosity (%)

S_{wi} = Initial water saturation in reservoir (%)

B_o = Oil formation volume factor at reservoir conditions (reservoir barrel [RB]/stock tank barrel [STB])

ρ_{co_2} = CO_2 density (metric ton [MT]/thousand standard cubic feet [Mscf])

E_{oil} = CO_2 storage efficiency factor (Mscf/STB)

The volumetric-based estimate also incorporates the standard industry method to determine the original oil-in-place (OOIP) (or OGIP for gas reservoirs). Per the standard industry method, the OOIP is a product of $A,\ h_n,\ f_e,\ (1 - S_{wi})$, and $\left(\frac{1}{B_o}\right)$ [113]. In calculating OOIP and ultimately G_{CO_2}, the oil formation volume factor, B_o, represents the ratio between the volume of oil at high reservoir conditions (RB) to that at the surface (STB). Additionally, this value typically ranges from 1.1 to 1.3, which means the oil produced at the surface loses some volume due to the storage of gases in the reservoir [115]. To obtain OOIP in STB, a conversion factor of 7,758 bbl/acre-ft is used. Once the OOIP is determined for the state's oil fields, the CO_2 storage resource estimate (in MT) can be found by identifying the density of CO_2 at standard conditions and the storage

efficiency factor (E_{oil}). While the density of CO_2 at standard temperature (21°C) and pressure (14.7 psi) corresponds to the common industry conversion of 1 MT per 19.25 Mscf, or 0.052 MT/Mscf, E_{oil} can be derived from local CO_2-EOR experience or reservoir simulations [116]. Since CO_2 has yet to be utilized in EOR techniques for the proposed EOR units (Figure 21), no local CO_2-EOR data is available; therefore, E_{oil} is derived from existing reservoir simulation results.

For EOR operations, the factor E_{oil} is the product of the incremental oil recovery factor (RF) and the CO_2 net utilization factor (UF_{net}). RF is defined as the cumulative volume of oil recovered over the OOIP, and it is expressed in units of %OOIP. Likewise, UF_{net} represents the volume of purchased CO_2 used to produce one barrel of oil and is measured in Mscf/bbl. It should be noted that the calculation only refers to the amount of CO_2 purchased and does not include recycled CO_2 from the EOR units. Both of these components are frequently documented in CO_2-EOR projects; therefore, Equation 9 yields a more practical estimation for CO_2 storage resource in EOR fields [116].

$$G_{CO_2} = OOIP * RF * UF_{net} * \rho_{co_2} \quad (9)$$

In Equation 9, it should be noted that variables RF and UF_{net} vary with time and the factors that define these terms such as cumulative oil production, CO_2 injection, and CO_2 storage are thus examined at a selected point in time. This point in time is ultimately linked with the cumulative hydrocarbon pore volume, or HCPV, injected. HCPV is a dimensionless variable defined as the total volume of pore space in a reservoir that is taken up by hydrocarbons. Additionally, both CO_2 and water injection data are expressed in terms of HCPV, where 100% HCPV (1.0 HCPV) is the equivalent of the OOIP.

Throughout the duration of the reservoir's life, more than 1.0 HCPV may be injected into as a result of poor sweep efficiency and a significant portion of oil still in place. Literature reports a typical threshold value of 3.0 HCPV, although it is realized that some fields may inject more or less than this set amount [116].

As mentioned above, reservoir simulations are used to determine the storage efficiency factor. Storage efficiency factors are largely dependent on the geological properties of oil reservoirs. Because of this, simulation results from six case studies analyzed by Peck and others are used to establish a correlation between oil reservoirs and E_{oil}. The six case studies were chosen out of 12 total case studies because they most closely matched the lithology (carbonate reservoirs) of the EOR units in SD, which are primarily dolomite. The various geological properties of each case, along with average values for the actual EOR fields in SD, are shown in Table 11.

Table 11. Geological properties used to estimate E_{oil} from EOR [116]

Case	Depth (ft)	Thickness (ft)	Temperature (°F)	Pressure (psi)
1	4,000	25	120	1,730
2	4,000	66	120	1,730
3	4,000	209	120	1,730
4	8,000	25	180	3,465
5	8,000	66	180	3,465
6	8,000	209	180	3,465
Actual [117]	8,500	14	210	3,600

Continuous injection was the EOR method used for the simulated cases. Although WAG injection was also documented in Peck and others, the EOR units in Harding County are favorable towards continuous injection due to the reservoirs being thin and highly permeable. Also, continuous injection allows more CO_2 to be stored and kept from entering the atmosphere. As will be discussed in the Section 45Q Tax Credit section, the more CO_2 stored, the greater the tax credit value will be and the more economically feasible the CCS project becomes.

Peck and others also summarized RF and UF_{net} values and subsequently derived E_{oil} for all simulated cases. For this study, E_{oil} values are evaluated using 3.0 HCPV as the end-of-life value for the EOR units in Harding County. The estimated values of E_{oil} for the selected six cases are tabulated in the Appendix. Ultimately, it is revealed that E_{oil} is strongly influenced by reservoir thickness, depth, and lithology [116]. Because the selected cases are all of the same lithology (carbonate reservoirs), E_{oil} can be plotted as a function of reservoir thickness and depth to obtain a more accurate prediction for the EOR units in Harding County. That being said, Figure 22 illustrates the effect that reservoir thickness and depth have on overall E_{oil} estimates. The data used to compose this contour plot can be found in the Appendix.

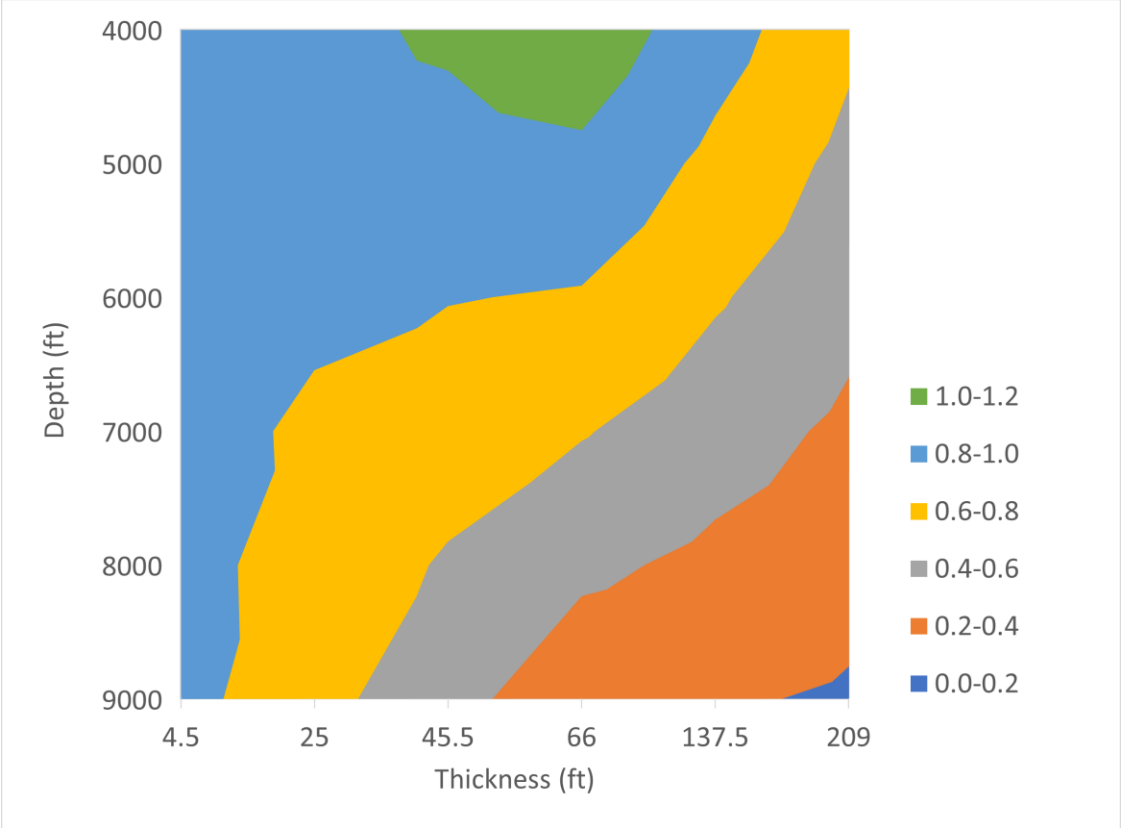

Figure 22. Contour plot depicting E_{oil} as a function of reservoir depth and thickness

From Figure 22, it can be established that thinner reservoirs will generally yield higher storage efficiency values. This is largely attributed to the reduced risk of gravity override within thin reservoirs. Because the reservoirs are thinner, more pore spaces can be contacted by the injected CO_2, increasing the amount of stored CO_2. Regarding depth, it can be seen that E_{oil} values predominantly decrease as reservoir depth increases. The primary cause for this inverse relationship is greater bottomhole pressure differences between injection and production wells. In oilfields, bottomhole pressure is equivalent to the sum of all the pressures acting on the bottom of the drilled hole. Correspondingly, increasing depths yield a higher bottomhole pressure at the injection well, which leads to a larger difference from the bottomhole pressure at the production well. Ultimately, the increased pressure difference directs the injected CO_2 from the injection well to the

production well in a more defined path. Therefore, a smaller volume of pore space is reached, and less CO_2 is geologically stored resulting in lower E_{oil} values [116]. As illustrated by the contour plot, the EOR units in Harding County with an average thickness and depth of 14 and 8,500 ft, respectively, are expected to have an estimated E_{oil} value of 78%.

After defining the variables that make up Equation 8 and ultimately Equation 9, the CO_2 storage resource can be estimated for the Harding County EOR fields. The total area in acres was determined using documented board orders for each EOR unit made accessible by the SD DANR [118]. An average thickness of 14 ft is taken from an early study on selected Red River Units in Harding County, which reports the average thickness interval to be 14 ± 4 ft in the "B" zone of these fields. Using the same study, the average volume factor is found to be 1.17 RB/STB [117]. In terms of oil production, the Red River Formation contains four productive rock layers labeled zones "A" through "D." These zones are aligned vertically with zone "A" at the top of the formation and zone "D" at the bottom. Out of the four zones, the "B" zone is the primary source of oil production; thus, the "B" zone is the focus for this study [119]. The average effective porosity of zone "B" is estimated to be 20% for the Red River units and the average initial water saturation fraction is estimated to be 58% for all units [118]. Table 12 displays the discussed variables and the overall CO_2 storage resource estimate for EOR units in Harding County.

Table 12. CO_2 storage resource estimate in SD at EOR units

Variable	**Value**	**Unit**
Area	59,867	acres
Average thickness	14	ft
Average effective porosity	20	%
Average water saturation fraction	58	%
Average volume factor	1.17	RB/STB
CO_2 density at STP	0.052	MT/Mscf
E_{oil}	78	%
Total EOR storage	**17.71**	**million MT**

The selected EOR units in SD provide an estimated CO_2 storage resource of 17.71 million MT. Assuming all 3.89 million MtCO_2 is purchased by oil operators over the course of the project, over four and a half years of total CO_2 storage is available. Because the CCS operation is modeled throughout 20 years, there will not be enough storage resource in the state's established EOR units alone to support the annual supply of CO_2. Even if EOR were to be completely utilized over those four years and delivered to an alternate storage site throughout the remaining duration of the project, the benefits received would likely not be suitable to offset the initial costs of the system. Therefore, additional oil fields must be considered.

For this study, all Harding County oil fields (including the EOR units) are assumed to be suitable for continuous CO_2 injection. Average data from the EOR units (Table 12) are applied to the 14 additional oil fields in Harding County. The area of each

additional oil field is measured using the SD DANR oil and map database. Because some EOR units are located within the boundaries of other oil fields, a net OOIP value was taken to determine the CO_2 storage resource in the additional oil fields separate from the EOR units. The CO_2 storage resource in the additional oil fields is estimated to be 46.44 million MT. Combining all oil producing areas in Harding County yields a total CO_2 storage resource of 64.15 million MT. Data used to produce these results can be found in the Appendix.

The combined CO_2 storage resource allows for over 16 years of storage in the Harding County oil fields, assuming all the CO_2 captured is stored. This means that in order to supply CO_2 for EOR over the total course of the project, alternative storage methods would still need to be considered. However, for the purpose of this study, the storage costs and benefits will be modeled over a 16-year period to determine if the CCS system is financially feasible within those 16 years of EOR operation. Since additional oil production and federal tax credits would be received for the majority of the project's lifetime, an opportunity exists for SD to capitalize on these economic benefits while significantly reducing its industrial CO_2 emissions.

3.2.2 Section 45Q Tax Credit

As mentioned previously, the initial cost for implementing CCS technology will be exceedingly high. To combat high initial costs and provide an incentive for capturing CO_2 emissions before they reach the atmosphere, the Section 45Q Tax Credit was introduced. Qualified carbon oxide (CO) per the tax credit is any carbon oxide that would have entered the atmosphere but is instead captured by qualifying equipment. Previously, the Section 45Q Tax Credit referenced specifically CO_2 emissions; however, the tax

credit was expanded by the Bipartisan Budget Act of 2018 (BBA) on February 9, 2018, to include all CO emissions, along with various other changes, which will be described below [121]. For the purposes of this study, CO_2 emissions will be the center of focus, as those emissions will be captured from the ethanol plants in SD.

Specific criteria need to be met to secure the credit amount allotted for the captured CO_2 at the selected ethanol facilities. Because of the BBA, tax credits can be obtained from a wider range of facilities – including SD ethanol facilities. The original tax credit did not account for facilities capturing less than 500,000 $MtCO_2$ per year, which likely contributed to the delay in widespread development of CCS technology. Another significant expansion to the tax credit is the adjusted claim period. Once limited to the first 75 million $MtCO_2$ captured and sequestered by all projects, the tax credit is now applicable for each metric ton captured and sequestered throughout a 12-year period. Table 13 documents the credit amount and other significant features of the revised 45Q tax credit.

Table 13. Key components of the Section 45Q Tax Credit [121][122]

	In Service Before 2/9/2018	**In Service on or After 2/9/2018**
Geologically Sequestered CO_2 (per $MtCO_2$*)	$20	$37.85
Geologically Sequestered with EOR (per $MtCO_2$*)	$10	$25.15
Other Qualified Use (per $MtCO_2$*)	None	$25.15
Claim Period	Limited to the first 75 million tons captured and sequestered	12-year period once in service
Qualifying Facilities	Capture carbon after 10/3/2008	Begin construction before 1/1/2026
Annual Capture Requirements	Capture at least 500,000 MT	***Power plants:*** Capture at least 500,000 MT ***Facilities emitting 500,000 MT per year or less:*** Capture at least 25,000 MT ***DAC and other capture facilities:*** Capture at least 100,000 MT
Eligibility to Claim Credit	Person who captures and ensures the disposal of CO_2	Owner of capture equipment and who ensures the disposal of CO_2

*CO_2 used for simplification – credit can be claimed for all COs (BBA)

Based on the requirements presented in Table 13, it is seen that the ethanol plants in SD will qualify for the Section 45Q Tax Credit if construction begins before 2026. These plants emit less than 500,000 $MtCO_2$ a year, with the largest amount of emissions being 450,000 $MtCO_2$ (Table 8). However, the tax credit is only awarded for successfully captured, injected, and geologically stored CO_2. It is not able to be claimed if the CO_2 enters the atmosphere. Storing this CO_2 in saline formations within the state would yield a credit value of $37.85 per MT in 2022. Moreover, when utilizing EOR to sequester

CO_2, a credit value of $25.15 per MT is applied, as of 2022. The applicable dollar value per $MtCO_2$ from 2017 until 2026 as per the tax credit is shown in Table 14.

Table 14. Tax credit value per $MtCO_2$ from 2017-2026 per Section 45Q [121]

Year	Geological Storage ($ per $MtCO_2$)	Geological Storage with EOR ($ per $MtCO_2$)
2017	22.66	12.83
2018	25.70	15.29
2019	28.74	17.76
2020	31.77	20.22
2021	34.81	22.68
2022	37.85	25.15
2023	40.89	27.61
2024	43.92	30.07
2025	46.96	32.54
2026	50	35

For geological storage of CO_2 – such as in saline formations – there is a linear increase in credit amount up to $50 per MT in the year 2026. After 2026, inflation adjustment factors are considered to determine an applicable dollar amount. On the other hand, the cost per MT of geologically storing CO_2 with EOR linearly increases to $35 in 2026. Similarly, inflation rates are applied thereafter [121]. This study takes the starting year of the CCS project to be 2022 (year 1); hence, for a 12-year operational period, inflation adjustment factors will need to be applied through year 2033 to establish the

total amount of tax credit received for the project. The inflation adjustment factors established by the Internal Revenue Service (IRS) are presented in Table 15 [123].

Table 15. Inflation adjustment factor for calendar years beyond 2026 [123]

Year	Inflation adjustment factor
2026	1
2027	1.0363
2028	1.0708
2029	1.0992
2030	1.1160
2031	1.1485
2032	1.1720
2033	1.1999

Utilizing saline formations and/or enhanced oil recovery units in the state, the economic viability of a CCS project is notably enhanced by the presence of the 45Q tax credit. Currently, 3.89 million $MtCO_2$ can be captured per year from all 16 ethanol plants in SD (base case scenario). Solely storing the captured CO_2 geologically with EOR would result in nearly $98 million claimable tax credits in 2022, which would only increase per the credit values shown in Table 14. It should be noted that per Table 13, tax credits can only be claimed for the first 12 years of service for any operation. Furthermore, EOR would also generate other revenue streams by producing additional barrels of oil, making this option more financially appealing. Alternatively, if all CO_2 was to be stored in saline formations within the state, just over $147 million in tax credit value could be claimed

from the CCS project per year, for the first 12 years of operation. All tax credits go to the owner of the capture equipment (Table 13); however, the owner can also make an election to transfer the credits to the EOR or storage operator. For this study, different scenarios are evaluated to gauge the overall economic viability CCS in the ethanol industry. Overall, the financial benefits provided by the 45Q tax credit will help relieve high initial costs for establishing the CCS system which will increase the opportunity for SD to reduce its CO_2 emissions and assist in combating climate change.

3.2.3 CO_2-EOR Performance and Economics

Because EOR further enhances the economic feasibility of CCS operations by providing additional revenue streams, this study highlights the use of CO_2 for incremental oil production in SD's oil fields. Ideally, the performance of a CO_2-EOR project would be evaluated using reservoir modeling software (ECLIPSE, GEM/STARS, TOUGH2, etc.) to take into account site-specific reservoir properties. Inputs of site-characteristics and oil properties in specific areas allow performance-based models to predict the cumulative amount of oil produced per the overall amount of CO_2 injected and stored. However, due to the lack of publicly available performance data for CO_2-EOR projects, empirical models and semi-analytical models are often used in replace of reservoir simulations. For this study, the incremental oil recovery from CO_2 injection is obtained using the average percentage of OOIP projected for EOR projects. This approach is accepted because limited reservoir characteristics are given for Harding County fields, and a comparison of performance data between oil fields should be avoided as results will vary based on site characteristics [124]. The top two producing wells in Harding County are examined to show individual contributions to the entirety of the CO_2-EOR project. A

summary of the factors used to evaluate CO_2-EOR performance of the oil fields in scope of this study is presented in Table 16.

Table 16. Top two Harding County oil fields and key performance characteristics

	South Buffalo Red River	**Buffalo Red River**	**All Oil Fields (Total)**
Area (Thousand acres)	21	8	**262**
OOIP (Million STB)	114	54	**1,576**
CO_2 injection rate (Million MT/yr)	0.38	0.21	**3.89**
Oil recovered* (MMbbl)	11	5	**158**

*Assuming average 10% OOIP recovered (base case)

As previously described, publicly available data provided by the SD DANR was used to determine the area of each oil field in Harding County. Similarly, the CO_2 storage resource methodology detailed in the previous chapter was used to estimate OOIP for each oil field. The individual amounts were summed for the total OOIP to be referenced as one value in the analysis. CO_2 injection rate data for the EOR units were determined using each units corresponding production data found in the SD DANR's oil and gas database. The percentage of a unit's contribution to overall oil production then established the overall CO_2 rate that would be supplied to the fields. This allowed the establishment of up-to-date oil production quantities (current as of May 2022) [125]. For the additional oil fields, CO_2 injection amounts are based on a field's percentage of total productive area. Moreover, as a result of secondary recovery having reported production amounts of 20-40% OOIP, it is assumed that an average 30% of the OOIP will have been recovered prior to initiating CO_2-EOR methods in the Harding County oil fields. Likewise, EOR efforts with large amounts of injected and stored CO_2 are reported to

yield approximately 13% of additionally recovered OOIP [94]. To avoid over estimating oil production potential, an additional oil recovery of 10% OOIP is assumed for this study's CO_2-EOR operation. Though, this value will be varied and assessed through a sensitivity study.

To further analyze the option of geologically storing CO_2 with EOR, the costs and incomes pertaining to CO_2-EOR projects must be considered. Typical economic parameters associated with CO_2-EOR projects include capital costs, operating and maintenance costs, and the price of oil ($/bbl). Averaging the EIA's US crude oil first purchase price data over the last year (Aug 2021 – July 2022), an average oil price of $90/bbl is established [126]. Various methodologies exist that estimate the economics of CO_2-EOR, however uncertainties arise due to varying reservoir properties and conditions of oil fields in different regions. In terms of establishing the costs of the CO_2-EOR system, this study primarily uses a cost model prepared by Advanced Resources International (ARI) which focuses on oil fields in the Williston Basin and further highlights specific properties of the oil fields in SD [127]. An additional study from Dahowski et al is used in conjunction with the ARI cost model to further asses the costs of CO_2-EOR operations [128].

CO_2-EOR capital costs are highly influenced by the amount of infrastructure needed to support CO_2 injection at new and/or existing oil wells. A typical assumption for CO_2-EOR projects is that the process involves existing wells, and no new infrastructure needs to be added. This assumption is widely accepted because drilling new wells substantially increases overall costs of CO_2-EOR projects, and thus sways operators to modify existing wells when designing these operations [129]. However,

because the additional oil fields in Harding County are not set up for EOR operations as of currently, these fields may need new additional wells and will require more costs to retrofit. Thus, the costs associated with well drilling and completion are considered in this cost model. Capital costs also include costs of converting production wells into CO_2 injection wells, reworking existing injection and production wells prior to CO_2 flooding, and installing a CO_2 recycling plant to capture and reinject CO_2 produced with recovered oil. The costs associated with distributing CO_2 across the oil fields with smaller pipelines are not included in this study due to the proximity of the oil fields in Harding County and the minor contribution of this distance to the entire pipeline network (Figure 20). A summary of the equations developed by the two cost models are shown in Table 17.

Table 17. Equations for capital costs of CO_2-EOR operations

Cost Parameter ($)	**Equation**
Well drilling and completion cost	$C_{well} = 1{,}000{,}000 * 0.1271e^{0.0008d} + 530.7$ (10)
Conversion cost	$C_{convert} = 13{,}555 + 5.16 * d$ (11)
Well rework cost	$C_{rework} = 14.38 * d$ (12)
CO_2 recycling plant investment	$C_{recycle} = 23.66 * Q$ (13)

In Equations 10 – 12, d is the reservoir depth in feet, and in Equation 13, Q is the annual flow rate of CO_2 injected in MT. Methodology from ARI cost model is used to evaluate conversion and reworking costs. Both estimates relate the capital cost to the depth of the reservoir. As per Section 3.2, the average well depth of the reservoirs in Harding County is 8,500 ft. Costs are expressed in 2004 US dollars. Moreover, methodology from Dahowski et al is used to estimate well drilling and completion and

CO_2 recycling plant costs. Well drilling and completion costs are represented on a per-well basis; therefore, the number of new wells to the oil fields is taken into account. For this study, five new wells are considered. The CO_2 that breaks through to production wells is purified and combined with the new, purchased CO_2 from the pipeline before getting reinjected into the oil field. Additionally, the flow rate used in Equation 13 corresponds to the maximum annual CO_2 flow rate in the recycling plant at each field [128]. For this study, the maximum flow rate of each field corresponds to the distributed CO_2 flow rate in each oil field. It should be noted that further study is needed regarding the overall on-site properties of the Harding County oil fields. This study involves making fair assumptions regarding certain physical aspects of the oil fields, with the primary focus being on the financial benefits of additional oil production and received tax credits.

Like the presented capital costs, operating and maintenance (O&M) costs can be grouped into different categories. In estimating the annual O&M costs, the ARI cost model considers surface and subsurface well maintenance (including periodic workovers); recycling CO_2; and liquid lifting, transporting, and re-injecting due to the incremental production of liquid (oil and water). Annual CO_2 recycling O&M costs are assumed to be 16% of the total CO_2 recycling plant investment (capital) cost based on a CO_2 storage cost analysis presented by Dahowski et al [128]. On top of these factors, additional general and administrative costs of 20% are added to well maintenance and lifting costs to account for efforts that have not been represented directly by both cost models [127]. The individual capital and O&M costs for each of the Harding County oil

fields are then totaled to estimate the overall cost of the CO_2-EOR project. Table 18 presents a summary of the equations and factors used to determine these O&M costs.

Table 18. Equations for O&M costs of CO_2-EOR operations

Cost Parameter	**Equation**
Annual O&M cost (including workovers)	$O\&M_{well} = 31{,}381 + 6.46 * d$ (14)
CO_2 recycling O&M cost	$O\&M_{recycle} = 0.16 * C_{recycle}$ (15)
Lifting cost	$\$0.25\ per\ barrel\ of\ oil$
General and administrative cost	$20\%\ of\ O\&M_{well}\ and\ lifting\ costs$

In Equation 14, d represents reservoir depth, and O&M costs for CO_2 recycling operations in Equation 15 reference the initial investment cost, $C_{recycle}$. Once both capital and O&M costs for CO_2 storage for EOR have been established, the revenues generated by the system can be included in the evaluation of the results. Economic benefits of CO_2-EOR projects come from additional oil production and the Section 45Q Tax Credit. Annual revenue from additional oil production of each oil field is determined by multiplying the average annual oil production of each unit by the average price of oil ($90/bbl – base case). The total amount for the combined system is the sum of each unit's annual revenue. Annual revenue from the 45Q tax credit is determined using the allotted tax credit value (Table 14) and the inflation adjustment factors for years beyond 2026 (Table 15). The credit value for each year ($/Mt$CO_2$) is then multiplied by the annual amount of CO_2 stored at each oil field (MT/yr) and summed over the first 12 years of the project. For this analysis, received tax credits are treated directly as revenues even though tax credits represent dollar-for-dollar amounts rather than direct subsidies. Also, it is

assumed that all captured and transported CO_2 is effectively stored and eligible to be claimed per the tax credit requirements.

The overall viability of CCS is augmented by the economic benefits provided to a system. Likewise, the performance of CO_2-EOR operations significantly impacts the value of these benefits. As SD consists of oil wells suitable for EOR operations, a great financial opportunity is available for the state to utilize CO_2 for additional oil production. Along with the enhancement of the state's energy production, millions of MT of CO_2 could be stored, increasing the state's contribution to global climate change mitigation efforts.

3.3 Sensitivity Analyses

Now that the base case scenario has been defined, a best-case scenario can be established by varying different parameters of the CCS system. The ideal scenario is one that is the most economically feasible and still yields a significant reduction in CO_2 emissions for the state of SD. To assess and quantify the influence of different parameters on the CCS system, sensitivity analyses are performed. In this study, the parameters that will be modified are the oil price and oil recovery rates from CO_2-EOR operations. These project variables are selected because they notably characterize the system but are hard to accurately quantify. For example, when CCS is paired with EOR, a determining factor in the economic benefits provided to the CO_2-EOR operation is the price of oil. Lower oil prices generate less revenue from the additional oil production of EOR techniques; however, the average price of oil is difficult to estimate as it can fluctuate over time, largely impacting the entire oil industry. Lastly, the amount of oil recovered likely plays a large role in the economic benefits of a CO_2-EOR system as more recovered oil provides

increasing amounts of revenue through oil production; although, it is difficult to estimate the amount of recoverable oil from EOR operations due to the wide approximation of reservoir properties.

3.3.1 Sensitivity of Oil Price

Oil price plays an important role in the total revenue produced for EOR operations. Annual data published by the EIA show significant fluctuations in US crude oil prices [126]. Because of this, the price of oil is varied to investigate its overall effect on the state's CO_2 storage capability. Scenario A uses a $30/bbl oil price and Scenario B uses a $120/bbl oil price (base case model remains $90/bbl). As described in Section 3.2.3, the capital and O&M storage costs are determined for each EOR in Harding County and then totaled to obtain overall storage costs for the CCS project. In the case of changing solely the price of oil and keeping all other storage factors the same, the variable experiencing noticeable change is the revenue generated from oil production. Consequentially, variation in total revenues of the system will affect the net present value (NPV) of each scenario; therefore, the NPV of each scenario is measured.

The NPV is a key indicator of the financial viability of a project. Additionally, a NPV that returns a value greater than zero indicates the project will generate an overall profit, whereas a negative NPV indicates the project is expected to yield an overall loss in profits. For this sensitivity analysis, the NPV will be calculated from the oil operator's perspective and therefore only involves cash flows regarding EOR costs and revenues. Equation 16 depicts this calculation.

$$NPV_{Total} = -CAPEX_{Total} + \sum_{t=0}^{16} \frac{REV_{Total,t} - OPEX_{Total,t}}{(1+i)^t} \quad (16)$$

As seen in Equation 16, the total CCS system is combined to evaluate the profitability the generated revenues have on the expenses of the entire operation. Thus, in this equation, it is assumed that revenues from sequestering CO_2, per the 45Q tax credit, and producing additional barrels of oil are not transferred between operators and the benefits are applied to the entire system. Moreover, the evaluation of EOR expenses and revenues for the additional scenarios uses the same methodology as in the base case (Section 3.2.3). For this study, a discount rate of 10% over the CO_2 storage resource availability lifespan of 16 years.

3.3.2 Sensitivity of Oil Recovery Production Rates (%OOIP)

Recovery rates of an oil field's OOIP can also determine how successful a CO_2-EOR operation is in providing benefits for geological storage of CO_2. Because it is not known how much of the OOIP will be produced in Harding County, a low and high case are analyzed. The low case uses a 5% OOIP recovery rate and the high case uses a 15% OOIP recovery rate. The results of the sensitivity analysis will determine the overall effects of varying recovery rates on the different costs and revenues provided to the system.

The CO_2-EOR variables investigated include capital and operational costs, EOR oil production, and EOR revenues. Using the same procedures as described for the base case and for the last sensitivity analysis, the overall expenses of the system (capital and O&M) are determined. Because the oil recovery rate is varied, the total amount of oil

produced is different for each scenario. Hence, a 5% OOIP recovery rate notably yields a total production amount that is 5% of an oil field's OOIP. The same goes for the analyzed 10% and 15% OOIP recovery rates. Furthermore, the revenue generated from additional oil production is established on an annual basis incorporating the constant oil price of $90/bbl for each scenario in this analysis. Similarly, the revenue generated through 45Q tax credits is determined for each operating year of the project based on the tax credit value and the amount of CO_2 stored for each year. It is assumed in each scenario that all CO_2 captured is stored.

As a note, successful oil fields would exhibit higher OOIP recovery rates due to increasing amounts of production and revenues. However, the overall lack of information regarding site-specific oil field properties makes it difficult to accurately assess the economic feasibility of future EOR operations. For this study, the evaluation of the NPV will represent how profitable a scenario is and ultimately determine the opportunity for SD to sequester large amounts of CO_2 while still generating revenue to the system.

4 RESULTS AND DISCUSSION

The goals of this work focused on modeling various CCS networks to determine if SD is a viable choice for adopting this technology, while subsequentially analyzing the state's overall impact on global climate change mitigation efforts. A base case was presented that highlights initial characteristics of the CCS system. Through a combination of sensitivity analyses, the economic feasibility of utilizing ethanol captured CO_2 for EOR in SD can be assessed. Because of the lack of publicly available data regarding ethanol-based CO_2-EOR operations, it is important to vary different parameters that can influence the model's overall success. The results found in this study can provide insight into largescale deployment of CCS technology and identify the magnitude in which SD can contribute to global CO_2 emissions reductions.

4.1 Base Case Scenario

4.1.1 Capture Results

The base case scenario captured CO_2 from all 16 ethanol plants in SD in order to prevent the maximum amount of CO_2 from entering the atmosphere and capitalize on additional financial benefits. As previously detailed, a large component of the overall costs of CCS systems is the cost of capture. For this study, the evaluation of capture related costs from ethanol fermentation accounted for CO_2 capture, compression, and dehydration. The equations detailed in Section 3.1.1 were used to establish capital and O&M costs of capture. Table 19 lists the costs associated with each ethanol plant in SD.

Table 19. Base case capture capital and O&M costs for each ethanol plant

Ethanol Plant	Location	Ethanol Capacity (MMGY)	Capital Cost ($Million)	Operating Cost ($Million/yr)
NuGen Energy	Marion	150	31.50	3.74
Valero Renewable Fuels	Aurora	140	30.00	3.48
Glacial Lakes Energy	Mina	140	30.00	3.48
Glacial Lakes Energy	Watertown	130	28.50	3.22
POET Biorefining	Chancellor	110	25.50	2.71
Dakota Ethanol	Wentworth	90	22.50	2.19
Ringneck Energy	Onida	80	21.00	1.93
POET Biorefining	Big Stone	79	20.85	1.91
POET Biorefining	Mitchell	68	19.20	1.62
Redfield Energy	Redfield	60	18.00	1.42
POET Biorefining	Hudson	56	17.40	1.31
POET Biorefining	Groton	53	16.95	1.24
Glacial Lakes Energy	Aberdeen	50	16.50	1.16
Glacial Lakes Energy	Huron	40	15.00	0.90
Red River Energy	Rosholt	35	14.25	0.77
POET Biorefining	Scotland	12	10.80	0.18
Total		**1,293**	**337.95**	**31.27**

Using the ethanol capacity and CO_2 emissions data provided for each ethanol plant in SD, the total capital and O&M cost are found to be $337.95 million and $31.27

million per year, respectively. For calculation purposes, the entire CCS process is modeled over the span of 20 years with an assumed 2-year construction period. The base case captures 3.89 million $MtCO_2$ per year from all 16 ethanol plants. Over 20 years, 77.8 million $MtCO_2$ would be prevented from entering the atmosphere. As described in the Literature Review, most recent data published by the EIA reports the annual energy-related CO_2 emissions in the state from 1970 to 2020. To project future energy-related emissions in the absence of CCS, data between years 2000 and 2020 are evaluated and a linear trendline is found. During the same operational period as the supposed project (2024-2043), SD would have emitted approximately 332.18 million MT of energy-related CO_2 in the absence of CCS. With CCS included in the state's ethanol facilities, this 77.8 million $MtCO_2$ saved would be equivalent to a 23% reduction in total energy-related CO_2 emissions for the state.

To validate the capture costs found in this study, a comparison can be made to those of the previous studies described in the Literature Review. The smaller scaled CO_2-EOR project in Nebraska and Kansas most closely matches the features of the SD model, with a combination of 15 ethanol plants and a CO_2 capture amount of 4.3 million MTY; therefore, explicit comparisons can be made. The larger scaled upper Midwest project is also displayed, though in the case of capture costs comparison, the smaller scaled model is more useful. It should be noted again that similar to the project modeled in this study, both of the case studies consist of a 2-year construction period and a 20-year operation period. Table 20 displays the key capture-related features of each project.

Table 20. Comparison of base case capital and O&M costs of ethanol CO_2 capture

	Base Case	Nebraska and Kansas	Largescale Midwest
Number of Ethanol Plants	16	15	34
CO_2 Captured (Million MTY)	3.89	4.30	9.85
Capital ($Million)	338	364	809
O&M ($Million/yr)	31	37	85

The approach taken by this analysis closely followed the methodology performed in the two case studies for the evaluation of capture costs. A distinction of the base case analysis is that each ethanol plant was analyzed individually rather than as a combined quantity like in the other cases. This resulted in a higher capital cost and a lower O&M cost relative to the case studies due to the nature of the equations described in Section 3.1.1. Nonetheless, as can be seen by the comparison table, the capture costs estimated in this study align with the overall trends of the two case studies. In the Nebraska and Kansas case, capture costs are slightly higher than the base case because of the greater CO_2 capture amount and plant capacity size. Because of these agreeing trends, the results found in this study are accepted.

Now that the capture results have been validated, further study on the economics of the capture process can be assessed. A key component to the overall viability of CCS is the cost per ton of CO_2 for each stage of the project (capture, transport, and storage). This value is commonly reported in literature and is useful in highlighting the most feasible scenario. The CO_2 cost per ton of capture is found using the total capital cost displayed in Table 20, and totaling the annual O&M cost over the operating period of the

project. For the base case, this leads to $625 million in total O&M costs (in real 2022$), not including financial escalation factors. Given the total CO_2 captured by the project over the 20-year period, 77.8 million MT, the estimated cost of captured CO_2 is $12.38/MT. As discussed in the Literature Review, the typical cost of CO_2 capture from ethanol fermentation is estimated to be around $14/Mt$CO_2$. It should be noted that the estimated cost per MtCO_2 for this study (and in the Literature Review) does not include benefits from the 45Q tax credit.

4.1.2 Transportation Results

The cost to transport CO_2 from the ethanol plants to the EOR units is determined using the NETL Transport Cost Model. This cost model requires the pipeline network to be analyzed in individual segments due to the varying length and tonnage of CO_2 transported between each point of capture. In this study, the transportation cost results draw conclusions about the entire pipeline network using data from the individual pipeline segments. A total of 16 segments are analyzed and the influence of each segment to the total cost of the transportation system is evaluated. Additionally, a correlation between certain physical characteristics of the pipeline and total investment cost is found. These influential pipeline properties include segment length, pipe nominal diameter, and number of booster pumps. Figure 23 – Figure 25 illustrate pipeline investment cost with respect to the specified pipeline properties of each segment. Also, the trendline that best fits each set of data along with the coefficient of determination (R^2 or R-squared) value is displayed in each figure.

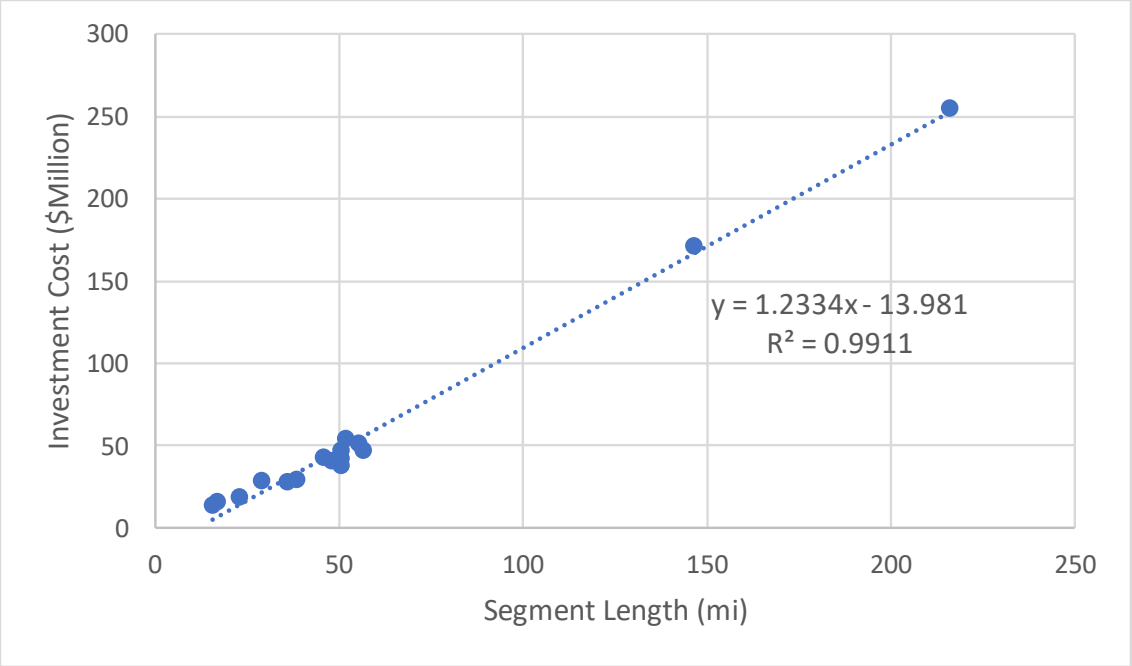

Figure 23. Pipeline segment investment cost per segment length

Figure 23 shows a strong linear relationship between pipeline investment cost and pipeline segment length. The figure also displays a high R-squared value of 0.99, indicating that the variation in pipeline investment cost can largely be explained by pipeline length. Likewise, from the plotted pipeline segment data, it can be concluded that longer pipelines will typically result in greater transportation costs. Therefore, shorter pipeline distances are recommended to enhance the economic feasibility of CCS operations. Because a large pipeline network is needed to deliver the captured CO_2 to the storage locations in SD, the economic feasibility of this CCS system is challenged.

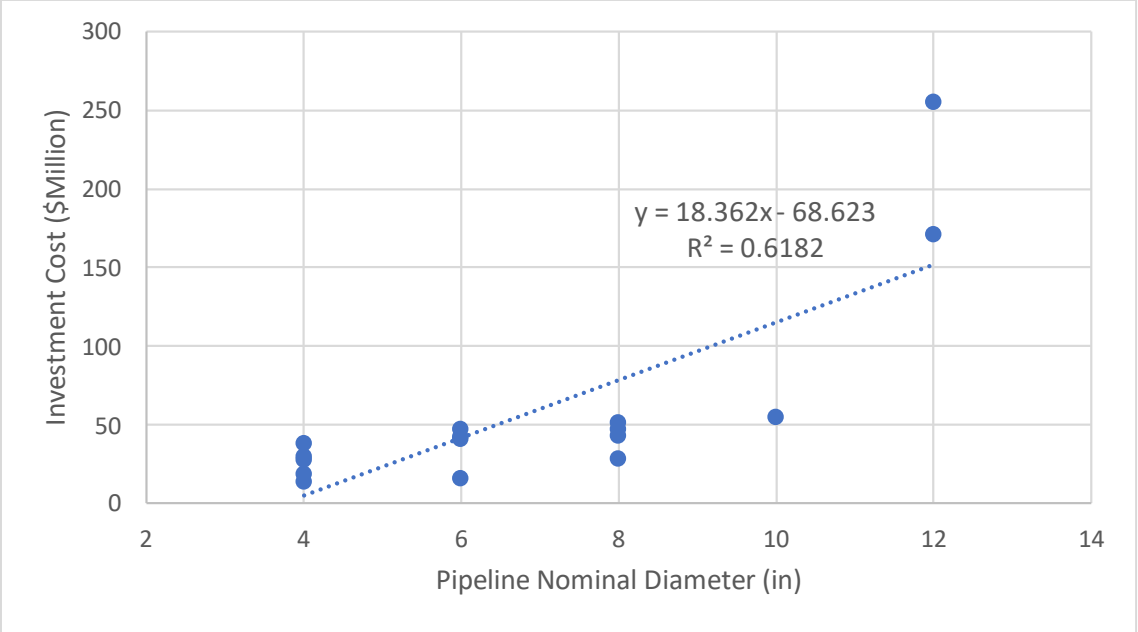

Figure 24. Pipeline segment investment cost per nominal diameter

Like the influence of pipeline length on the costs of the transportation system, a positive, linear relationship is found between pipeline investment cost and pipeline nominal diameter. Figure 24 shows that an increase in pipeline nominal diameter generally yields an increase in pipeline investment cost. Additionally, an R-squared value of 0.62 is displayed. Thus, while a linear relationship exists between the two variables, less of the variation in investment cost can be explained by pipeline nominal diameter than can be explained by pipeline length (0.99 > 0.62). Pipeline diameter is dependent on CO_2 flow rate meaning larger diameters are needed for greater amounts of transported CO_2 in a pipeline segment. So, although large-diameter pipelines are initially more cost-intensive, the overall transportation system is made more cost-effective by supplying more CO_2 and reducing the overall cost per MT through large-diameter segments.

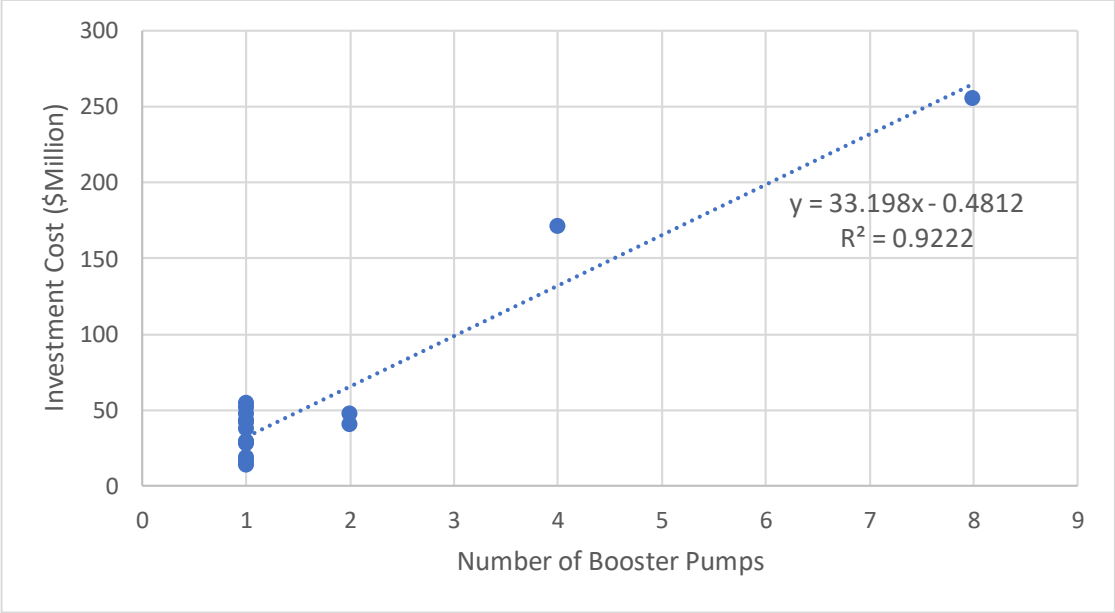

Figure 25. Pipeline segment investment cost per number of booster pumps

The investment cost of the transportation network is found to be affected by the number of booster pumps required throughout each pipeline segment. Similar to the trends of the previously described pipeline properties, a positive, linear relationship is shown in Figure 25 as well as an R-squared value of 0.92. It can be seen that an increase in number of booster pumps produce an increase in transportation investment cost. The number of booster pumps required throughout a pipeline segment largely corresponds to the amount of CO_2 transported throughout a pipeline segment. Areas with low flow over a longer length will require more booster pumps to push the CO_2 through the pipeline; thus, an increase in overall investment cost is traditionally experienced. Once the transportation costs of each segment have been determined, the results are combined to obtain the overall costs of the transportation system. Transportation capital and O&M costs are separated into different categories to highlight the primary contributors to overall costs. Table 21 summarizes this information for the base case.

Table 21. Base case transportation capital and O&M costs by category

Capital Costs ($Million)	
Materials	145
Labor	522
ROW-Damages	54
Miscellaneous	150
CO_2 Surge Tanks	25
Pipeline Control System	2
Booster pumps	24
Total	**922**
O&M Costs ($Million/yr)	
Pipeline O&M	10
Pipeline related equipment and pumps O&M	2
Electricity costs for pumps	7
Total	**19**

For this modeled system, the total transportation capital costs are estimated to be $922 million, and the annual O&M costs are estimated to be $19 million per year. As can be directly seen, labor constitutes the majority of total transportation capital costs. This can be mostly attributed to the extent of the pipeline network and amount of service required for production. Likewise, the primary component to transportation O&M costs is annual pipeline O&M also largely due to the total length of the pipeline. Because numerous pumps are needed to maintain CO_2 pressure from capture sources to oil fields,

the electricity costs for these booster pumps are also a significant variable in O&M costs. Ultimately, the distance required to transport the annual amount of CO_2 for EOR poses a serious impediment to the viability of the CCS system.

Currently, 3.89 million MtCO_2 is supplied by the 929-mile pipeline network. Relative to the location of capture sources, the storage site is on the opposite side of the state. Thus, feeder lines are needed to connect many of the capture sources to the trunk of the pipeline which then delivers the congregated CO_2 to the storage site. Ethanol facilities near the end of feeder lines, and farthest away from the trunk, generally transport smaller annual volumes of CO_2. By analyzing the transport cost of CO_2 in each segment, the influence of low CO_2 flow rates on the overall financial feasibility of the pipeline network can be addressed. Figure 26 shows this impact of varying CO_2 flow rates on total segment transport cost.

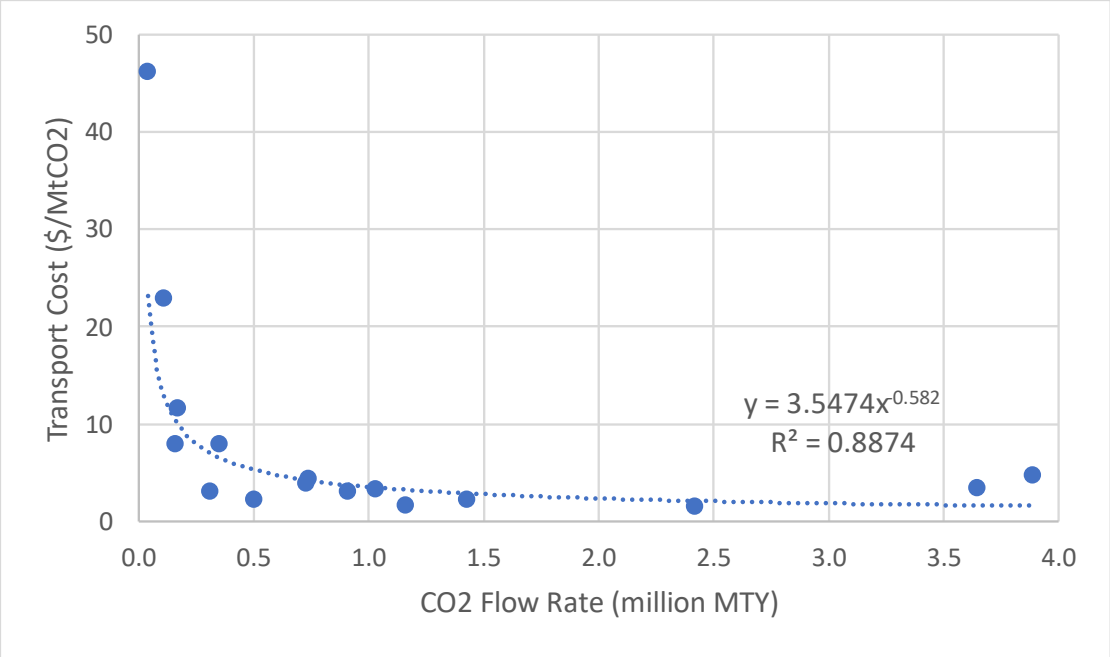

Figure 26. Transport cost corresponding to segment CO_2 flow rate

CO_2 transportation costs are notably dependent on the amount of CO_2 delivered in a pipeline. As seen in the figure, transport costs throughout the segments vary from nearly \$50/MtCO_2 to just over \$1/MtCO_2, with more variation occurring at low flow rates. Likewise, increasing CO_2 flow rates are correlated with decreasing CO_2 transportation costs. For instance, the segments in this model with higher transport costs are also the segments that supply lesser amounts of annual CO_2. Scotland, Rosholt, and Hudson represent the three highest CO_2 transportation costs of the pipeline network at an estimated \$46, \$23, and \$12 per MT. Taking an average of the CO_2 transport costs produced for each segment, the estimated overall transport cost of CO_2 for the pipeline network is \$8/MtCO_2. Accordingly, the financial feasibility of the pipeline network can be enhanced by selecting capture facilities that yield higher amounts of CO_2. Even further, minimizing total pipeline length (Figure 23) in combination with maximizing CO_2 capture rates will create the most cost-effective transportation option and could be

the key to large-scale CCS deployment in SD. It should be noted that the capture and transportation systems may be operated separately. If this is the case, the owner of the transportation system determines how to allocate CO_2 transport costs among the capture facilities; however, for this study, the specific cost of each segment is represented by the ratio of CO_2 supplied in the segment to the total amount delivered to the storage site. Furthermore, to validate the transportation costs determined by this analysis, corresponding results from the case studies described in the Literature Review are presented.

Table 22. Comparison of base case capital and O&M costs of CO_2 transportation

	Base Case	**Kansas and Nebraska**	**Largescale Midwest**
Number of Ethanol Plants	16	15	32
Pipeline Length (mi)	929	737	1,546
Capital ($Million)	922	642	1,857
O&M ($Million/yr)	19	16	47

Table 22 compares capital and O&M transportation costs evaluated from the different pipeline networks. Both case studies derived transportation costs using the same NETL cost model presented in this study. Again, both case studies are modeled as 20-year operational projects with 2-year construction periods, which is the same for the base case. Compared to the Kanas and Nebraska case, the base case consists of one more ethanol plant, yet the total pipeline network is increased by nearly 200 miles. An increase in pipeline length to this extent, along with the slight decrease in CO_2 capture rate, justifies the $280 million in capital costs for the base case, based on the discussions

provided in this analysis. Likewise, O&M costs for the base case are $3 million more per year than the Nebraska and Kansas case. Given the pipeline characteristics of the base case, and the fact that total transportation costs are found to be between the presented high and low case studies, the cost results determined in this study are accepted.

Ultimately, transportation expenses combined with capture expenses will help determine how economically viable it is to implement CCS within SD's ethanol industry. The lower the overall cost of CO_2 per MT transported and captured, the higher the applicable amount of economic benefits to the CCS system. As described in the Literature Review, the oil industry has a desire to purchase CO_2 for oil production; therefore, revenues from the sale of CO_2 to oil operators can counteract high capture and transportation costs. Hence, the more feasible a CCS operation is, the greater the impact SD can have to overall reductions in CO_2 emissions both statewide and nationwide. The quantity of benefits provided through oil production and tax credits will be discussed in the discussion of storage results. Data used to produce the transportation costs discussed in this section are presented in the Appendix.

4.1.3 Storage Results

The base case scenario involved utilizing EOR for the geological storage of CO_2. Geological storage with EOR is a prime option as it permanently stores CO_2 that would have entered the atmosphere as well as provides revenue through additional oil production. Harding County has multiple EOR units already in place, but none that utilize CO_2 as an injectant. Currently, 13 EOR units are established in SD and can be readily modified for CO_2 injection. However, as established in the Methodology, less than five years is estimated to be available for CO_2 storage. When including all the oil fields in

Harding County, over 16 years of storage becomes available. Therefore, for this analysis, 16 years will be analyzed first to determine the financial state of the CCS system at that point in time. Then, additional storage options will be assessed for the remaining four years of the project. To analyze the cost of CO_2 storage, each oil field is analyzed separately and then totaled to produce a value that represents the combined storage system. An oil price of $90/bbl is used in calculations for the base case. A summary of CO_2-EOR costs using the ARI and Dahowski et al publication is displayed in Table 23.

Table 23. CO_2-EOR costs in 2022 dollars

Capital Costs ($Million)	
Well drilling and completion cost	570.6
Conversion cost	1.6
Workover cost	3.3
CO_2 recycling plant investment	92.0
Total	**667.5**
O&M Costs ($Million/yr)	
Well O&M cost (including well workovers)	2.3
CO_2 recycling O&M cost	14.7
Lifting cost	66.5
General and administrative cost	13.8
Total	**97.3**

A substantial factor in storage costs is the drilling and completion of new wells for CO_2 injection. In this study, new wells are likely needed because the added oil fields

are not currently ready for EOR operations. For evaluation purposes, five new wells are assumed to be added initially, though the actual number of new wells needed at the selected fields is unknown. Another large contributor to storage capital costs is the construction of a CO_2 recycling plant. High CO_2 recycling costs are largely due to the capture and re-injection requirements of CO_2 that has broken through to the production wells. As described in the Methodology, the ARI cost model evaluates conversion and workover capital costs for each oil field based on reservoir depth, which is taken at an average 8,500 ft, therefore, generating the same cost result per oil field. Likewise, each EOR unit has equal annual well O&M, lifting, and general and administrative costs as estimated using the cost model. Combining the capital costs of all EOR units in Harding County, the total value for the base case model is $667.5 million. Similarly, the total O&M costs for the base case is $97.3 million per year. Future studies would need to be done to determine on-site reservoir properties and correspondingly evaluate the flow of CO_2 within the Harding County oil fields. Since the primary focus of this study is on the cost-effectiveness of capturing CO_2 from the state's ethanol facilities, only key aspects of the costs associated with CO_2 storage are needed in this assessment.

To determine the net storage cost of the system, the total amount of CO_2 stored needs to be estimated. Because the base case assumes a 10% OOIP recovery rate, approximately 158 MMbbl of oil is produced over the 16-year EOR storage operation. Additionally, it should be noted that approximately 0.32 MT of purchased CO_2 is injected and stored to produce one barrel of oil [130]. Therefore, over the lifetime of the EOR operation, approximately 50.44 million $MtCO_2$ will be injected, and on average, 3.15 $MtCO_2$ will be stored per year. The net CO_2 storage cost can be reduced through the

additional revenue of oil production for the storage system. Assuming an oil price of $90/bbl, an additional $887 million is produced per year, generating about $14,186 million throughout the 16 years. Combining the total storage costs and the generated revenues from oil production, the overall net storage cost for the system is $16 per MT of stored CO_2. The 45Q tax credit is not included in the net storage cost because in terms of an operator's perspective, the credit would first go to the operators of the capture equipment. However, when analyzing the NPV of the entire CCS system, this value is then included. Table 24 displays the different revenue streams of the CCS system as a direct result of EOR operations.

Table 24. Revenue generated from oil production and CO_2 storage

	Total
CO_2 stored (Million MT)	**50**
EOR oil production (MMbbl)	**158**
Revenue from oil production ($Million)	**14,186**
Revenue from 45Q tax credit ($Million)	**1,439**

For the base case scenario, the total revenue generated from claimed 45Q tax credits, over the 12-year claim period, is $1,439 million. Hence, with the characteristics of the base case, significant revenue is provided to SD when using CO_2 for EOR operations. Not only does combining CO_2 with EOR offset initial costs of the project by generating additional revenue, but capturing CO_2 for this profitable operation also prevents increasing amounts of carbon from entering the atmosphere. Throughout the project's 16-year timespan, the amount of CO_2 that is stored to generate the revenues

displayed in Table 24 is just over 50 million MT. In order to assess the profitability of the CO_2-EOR system in SD despite the limit in total oil reservoir storage, the NPV is calculated. This variable takes into account the total CO_2 capture, transport, and storage expenses and revenues provided an assumed discount rate of 10% for the system. Table 25 summarizes the factors leading to the overall NPV of the CO_2-EOR system.

Table 25. Base case storage economics for CO_2-EOR

Capture capital ($Million)	338
Transport capital ($Million)	922
Storage capital ($Million)	667
Total capital ($Million)	**1,927**
Capture O&M ($Million/yr)	32
Transport O&M ($Million/yr)	19
Storage O&M ($Million/yr)	97
Total O&M ($Million/yr)	**147**
Revenue from oil ($Million)	14,186
Revenue from 45Q tax credit ($Million)	1,439
Discount rate (%)	10
16-year NPV ($Million)	**4,648**

A crucial measurement in this table is the system's positive NPV. The CO_2-EOR project is expected to gain $4,648 million in current value profit during the 16-year EOR operation. With the added benefits of incremental oil production and the value obtained through the 45Q tax credit, the overall CO_2-EOR system is expected to generate a net

profit. Ultimately, this positive NPV ensures that the project has the means to be a financially feasible option in terms of utilizing CO_2-EOR. Moreover, after the 16-year EOR operation is finished, alternate storage options would be considered. One option for further storage would be to find additional oil fields for continual EOR storage. Because the Harding County oil fields are adjacent to the oil fields in the southwest corner of North Dakota, minimal pipeline distance would be required to extend the CCS pipeline network. Another option could be to supply to the captured CO_2 to a consumer industry for use in commercial applications such as food and beverage production and greenhouses. Storage in the state's saline formation is also an option, but further study would need to be done to quantify the overall costs and benefits of any alternative storage option.

4.2 Sensitivity Analyses

Modifications were made to the base case scenario and sensitivity analyses were performed to determine the effect of certain variables on the overall CCS system. The parameters adjusted were the price of oil and the oil recovery rate of the EOR units. By varying these parameters, a more cost-effective system can be produced, providing a greater opportunity for SD to both economically benefit from EOR operations and widely contribute to the reduction in CO_2 emissions.

4.2.1 Oil Price Sensitivity Results

Because the price of oil is known to fluctuate over time, it is difficult to accurately predict what the conditions will be for a future period. For this study, the base case assumed an oil price of $90/bbl, which closely matches the trends in prices to date; however, to understand the impact of these fluctuations to the modeled CCS operation,

the price of oil is taken to vary from a low case of $30/bbl to a high case of $90/bbl. Changing the price of oil will directly influence the amount of revenue generated from oil production, which is a major economic benefit provided from storing CO_2 in oil fields. Table 26 highlights the changes in the economics of the system when compared to the base case. Figure 27 correspondingly displays overall changes in the profitability of the CCS system with varying oil prices.

Table 26. Economic summary of EOR revenue and NPV with varying oil price

	Base Case	**Scenario A**	**Scenario B**
Oil price ($/bbl)	90	30	120
Revenue from oil ($Million/yr)	887	296	1,182
NPV ($Million)	4,648	24	6,961

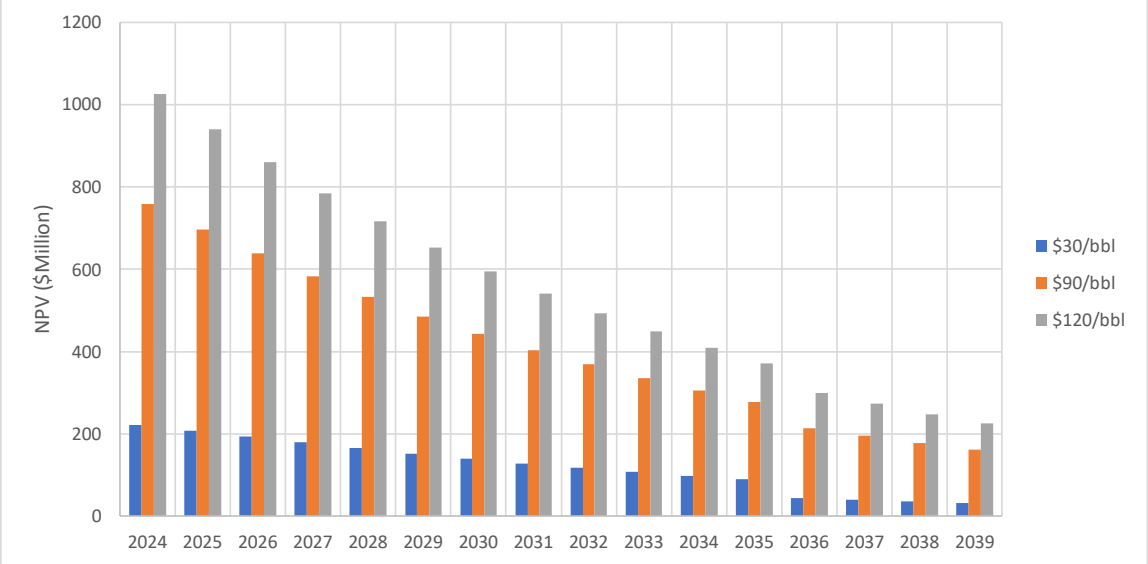

Figure 27. CO_2-EOR project NPV with varying oil price

The sensitivity study details that EOR revenue from additional oil production is very sensitive to changes in oil price. Overall, fluctuations in oil price can lead to large

changes in the NPV of CO_2-EOR projects. Like with all oil production operations, oil price is going to play an important role in the profits made from a system. For the modeled system, it can be seen that if oil prices decrease to $30/bbl, the NPV of the project would likely become negative if more years of storage are needed. Therefore, the results of this study show that oil prices at $90/bbl and above would generate significant streams of revenue that could offset high costs of the CCS network. It can also be established that the NPV results for each scenario, during the 16-year storage model, are positive values meaning the CO_2-EOR systems are expected to provide revenue to the operators. This indication makes establishing a CO_2-EOR operation in Harding County, SD an economically feasible option.

4.2.2 Oil Recovery Rate Sensitivity Results

The amount of OOIP able to be recovered by a CO_2-EOR is largely determined by the reservoir characteristics. Because reservoir properties are often not readily available, analytical or empirical models are mainly used. These models rely on a lot of assumptions regarding similar characteristics of regional reservoirs; however, without real on-site data, performance parameters are highly variable. By varying the overall oil recovery rate of the CO_2-EOR project, the effect on cost and revenue factors are measured. A summary of the estimated economics for each case in response to varying oil recovery rates is shown in Table 27.

Table 27. Economic summary of a CO_2-EOR project for varying oil recovery rates

	Base Case	**Scenario A**	**Scenario B**
%OOIP recovery	10	5	15
EOR oil (MMbbl)	158	79	236
Revenue from oil ($Million/yr)	887	443	1,330
Cumulative 45Q revenue ($Million)	1,439	720	2,159
NPV ($Million)	4,648	1,097	8,200

The measured parameters listed in Table 27 all vary to different degrees with respect to oil recovery rates. Overall, the combined sensitivity of EOR oil production and the two revenue streams can significantly affect the overall profitability of the CO_2-EOR project. Similar to the previous oil price sensitivity study, the NPV is also compared with the variations in oil recovery rates to determine if an expected profit to the CO_2-EOR operation can be provided. Figure 28 shows the variability of NPV with changes to oil recovery rates.

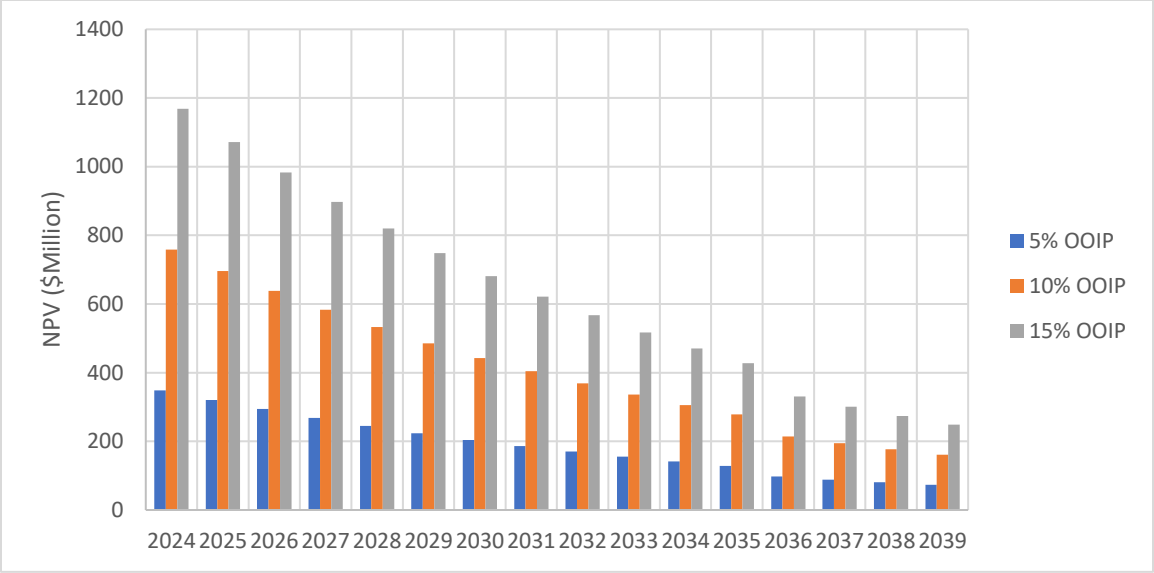

Figure 28. CO_2-EOR project NPV with varying oil recovery rates

NPV is highly sensitive to changes in oil recovery rates. From Figure 28, the NPV associated with a 15% OOIP recovery rate produces over double the amount of profit that would be seen by a 5% OOIP recovery rate. Contrast to changes in oil price, both revenue streams from CO_2 storage and oil production are affected by changes in oil recovery rates. For this study, OOIP recovery rates of 10% or higher are recommended to provide an economically feasible option. The NPV of 5% OOIP recovered or less is approaching negative values as the storage locations near end-of-life.

Combining the results of varying oil price and oil recovery rates, this study would not yield ideal benefits if under oil prices of $30/bbl or under 5% OOIP recovered. Yet, given the average properties presented in this study, a CO_2-EOR project for the duration of 16 years would provide generous amounts of revenue to the system. Likewise, all analyzed scenarios do produce positive NPV's therefore can be seen as a viable option in terms of CO_2 storage and economic benefits.

5 CONCLUSIONS AND FUTURE WORK

5.1 Conclusions

Carbon capture and storage technology has been used for roughly half a century and is reported to be a key factor in mitigating global CO_2 emissions; however, the high costs of CO_2 capture, compression, and transportation has significantly limited its wide-spread deployment. Because of the nearly pure stream of CO_2 that is emitted during fermentation, ethanol plants are prime candidates for reducing these high costs of implementation. Nonetheless, large-scale deployment and general research on the technology at ethanol facilities is scarce, hindering its capability to reduce global CO_2 emissions. South Dakota is a top ethanol producer in the US, creating opportunity for the state to bridge the gap between the reported high costs and wide-spread deployment. The purpose of this thesis was to evaluate this opportunity and determine the feasibility of CCS technology at the ethanol plants in SD.

Results show that when paired with the economic benefits from both EOR and the Section 45Q Tax Credit, establishing carbon capture technology at ethanol facilities in SD can be economically feasible. The base case yields an overall capture cost of \$12.39/$MtCO_2$, which is comparable to case studies and research presented in this study. Performed sensitivity studies show the most financially feasible scenario involves high oil prices (\$90/bbl and above) and high oil recovery rates (10% OOIP recovery and above) as these variables largely influence the expected profit of the CCS system. Along with the financial benefits provided to the state, the CCS system successfully stores 50.44 million $MtCO_2$ underground in the state's oil reservoirs. This is equivalent to nearly 11 million gasoline-powered vehicles driven for one year and the equivalent amount of

carbon sequestered by nearly 60 million acres of US forests in one year. Over the 16 year long storage period with EOR, total 50.44 million $MtCO_2$ that would have been released into the atmosphere by SD's ethanol facilities are captured, put to beneficial use with EOR, and stored in the state's oil fields.

5.2 Future Work

To ensure the accuracy of these results, future work could include performing reservoir simulations to better understand the internal flow of CO_2 and obtain oil production values based on the actual characteristics of the Harding County EOR units. Because access to reservoir simulation software was not available, this methodology could not be used, and general estimates had to be made. Also, site screening of the oil fields was not performed as that was outside of the scope of the study. Therefore, ensuring the oil fields in Harding County can sustain CO_2 over the 30-year duration of the EOR project would be recommended.

Because SD only has enough geological storage in the Harding County oil fields for approximately 16 years, more research needs to be performed into alternative storage options. The assessed CCS system captured CO_2 from the state's ethanol facilities for 20 years which leaves four years unaccounted for in terms of geological storage. This study assumed appropriate alternative methods would be applied and estimated the NPV according to the 16 years of storage in the oil fields. However, a more accurate depiction of the overall economics for a 20-year operational CCS system could be understood with a more in-depth analysis to alternative storage options.

6 APPENDIX

Table 28. SD ethanol plants annual production capacity and corn usage

Ethanol Plant	**Location**	**Ethanol Capacity (MMGY) [104]**	**Corn Usage (MMBUY)**
NuGen Energy	Marion	150	55.6
Valero Renewable Fuels	Aurora	140	51.9
Glacial Lakes Energy	Mina	140	51.9
Glacial Lakes Energy	Watertown	130	48.1
POET Biorefining	Chancellor	110	40.7
Dakota Ethanol	Wentworth	90	33.3
Ringneck Energy	Onida	80	29.6
POET Biorefining	Big Stone	79	29.3
POET Biorefining	Mitchell	68	25.2
Redfield Energy	Redfield	60	22.2
POET Biorefining	Hudson	56	20.7
POET Biorefining	Groton	53	19.6
Glacial Lakes Energy	Aberdeen	50	18.5
Glacial Lakes Energy	Huron	40	14.8
Red River Energy	Rosholt	35	13.0
POET Biorefining	Scotland	12	4.4
Total		**1,293**	**478.9**

$$\frac{lb\ CO_2}{gal\ Ethanol} = \rho_{ethanol} * \left(\frac{molecular\ wt\ CO_2}{molecular\ wt\ Ethanol}\right)$$

$$6.58\frac{lb\ Eth}{gal\ Eth} * \frac{44.01\frac{g\ CO_2}{mol} * \frac{0.002205\ lb}{g}}{46.07\frac{g\ Eth}{mol} * \frac{0.002205\ lb}{g}} = 6.29\frac{lb\ CO_2}{gal\ Eth} \quad (13)$$

$$\sim A\ pound\ conversion\ is\ added\ to\ emphasize\ units\ are \frac{lb\ CO_2}{gal\ Eth}$$

Table 29. E_{oil} at varying HCPV values for six cases presented in Peck and others [116]

	E_{oil} at HCPV (Mscf/STB OOIP)					
Case	**0.5**	**1.0**	**1.5**	**2.0**	**2.5**	**3.0**
1	0.44	0.60	0.72	0.81	0.88	0.94
2	0.57	0.78	0.91	1.00	1.07	1.13
3	0.34	0.45	0.53	0.58	0.61	0.64
4	0.46	0.59	0.65	0.69	0.71	0.72
5	0.32	0.38	0.41	0.42	0.43	0.44
6	0.21	0.25	0.26	0.26	0.27	0.27

Table 30. E_{oil} as a function of reservoir depth and thickness

	E_{oil} at Reservoir Thickness (ft)					
Depth (ft)	**4.5**	**25**	**45.5**	**66**	**137.5**	**209**
4000	0.85	0.94	1.04	1.13	0.89	0.64
5000	0.85	0.89	0.92	0.96	0.75	0.55
6000	0.85	0.83	0.81	0.79	0.62	0.46
7000	0.86	0.78	0.69	0.61	0.49	0.36
8000	0.86	0.72	0.58	0.44	0.36	0.27
9000	0.86	0.67	0.47	0.27	0.22	0.18

Table 31. CO_2 storage resource approximation data

EOR units	**OOIP (Million STB)**	E_{oil}	ρ_{CO_2}	G_{CO_2} **(Million MT)**
South Buffalo	113.67	0.78	0.05	4.63
Buffalo	54.11	0.78	0.05	2.20
West Buffalo	41.52	0.78	0.05	1.69
Central Buffalo	24.83	0.78	0.05	1.01
East Harding Springs	45.09	0.78	0.05	1.84
West Buffalo 'b'	41.95	0.78	0.05	1.71
Pete's Creek	50.23	0.78	0.05	2.04
North Buffalo	12.73	0.78	0.05	0.52
SD-State Line	16.74	0.78	0.05	0.68
Travers Ranch	6.66	0.78	0.05	0.27

Crooked Creek	13.33	0.78	0.05	0.54
Clarkson Ranch	7.56	0.78	0.05	0.31
Eagles Nest	6.76	0.78	0.05	0.28
Additional Oil Fields				
Buffalo	722.45	0.78	0.05	29.40
Table Mountain	138.81	0.78	0.05	5.65
Yellow Hair	118.35	0.78	0.05	4.82
Border	103.75	0.78	0.05	4.22
East Harding Springs	98.21	0.78	0.05	4.00
Pete's Creek	83.69	0.78	0.05	3.41
Bull Creek	65.73	0.78	0.05	2.68
South Medicine Pole Hills	55.90	0.78	0.05	2.27
Jones Creek	55.04	0.78	0.05	2.24
State Line	43.17	0.78	0.05	1.76
Corey Butte	34.23	0.78	0.05	1.39
Travers Ranch	33.96	0.78	0.05	1.38
Clarkson Ranch	16.32	0.78	0.05	0.66
Harding Springs	6.64	0.78	0.05	0.27
Total				**64.15**

Table 32. Individual pipeline segment transportation cost data

Segment	Segment length (mi)	CO_2 flow rate (Million MTY)	Transport cost ($/Mt$CO_2$)	Total capital ($Million)	Total O&M (Million/yr)
1	38	0.17	11.64	29	0.51
2	17	0.50	2.25	16	0.33
3	52	2.42	1.54	54	1.01
4	146	3.65	3.43	171	3.96
5	216	3.89	4.76	255	5.77
6	36	0.04	46.18	28	0.47
7	50	0.11	22.85	38	0.63
8	50	0.35	7.90	42	0.67
9	56	0.74	4.42	47	0.92
10	29	1.16	1.71	28	0.57
11	50	1.43	2.24	47	0.84
12	23	0.16	7.93	18	0.34
13	16	0.31	3.12	14	0.29
14	48	0.73	3.91	41	0.82
15	46	0.91	3.13	43	0.71
16	55	1.03	3.29	51	0.83
Total				**922**	**18.68**

Table 33. All Harding County oil fields capital costs

Oil Fields	**Capital Costs ($)**			
EOR units	**Well drilling and completion**	**Conversion**	**Workover**	**CO_2 recycling plant**
South Buffalo	21,132,763	57,415	122,230	32,808,727
Buffalo	21,132,763	57,415	122,230	18,295,222
West Buffalo	21,132,763	57,415	122,230	8,860,060
Central Buffalo	21,132,763	57,415	122,230	6,921,302
East Harding Springs	21,132,763	57,415	122,230	5,876,465
West Buffalo 'b'	21,132,763	57,415	122,230	5,790,180
Pete's Creek	21,132,763	57,415	122,230	4,428,645
North Buffalo	21,132,763	57,415	122,230	3,868,559
SD-State Line	21,132,763	57,415	122,230	3,089,995
Travers Ranch	21,132,763	57,415	122,230	1,509,966
Crooked Creek	21,132,763	57,415	122,230	262,006
Clarkson Ranch	21,132,763	57,415	122,230	250,667
Eagles Nest	21,132,763	57,415	122,230	75,606
Additional Oil Fields				
Buffalo	21,132,763	57,415	122,230	22,253,236
Table Mountain	21,132,763	57,415	122,230	8,155,331
Yellow Hair	21,132,763	57,415	122,230	6,921,692
Border	21,132,763	57,415	122,230	6,041,194
East Harding Springs	21,132,763	57,415	122,230	4,065,902

Pete's Creek	21,132,763	57,415	122,230	3,610,120
Bull Creek	21,132,763	57,415	122,230	3,748,132
South Medicine Pole Hills	21,132,763	57,415	122,230	3,154,855
Jones Creek	21,132,763	57,415	122,230	3,103,061
State Line	21,132,763	57,415	122,230	1,535,451
Corey Butte	21,132,763	57,415	122,230	1,775,998
Travers Ranch	21,132,763	57,415	122,230	1,415,456
Clarkson Ranch	21,132,763	57,415	122,230	698,514
Harding Springs	21,132,763	57,415	122,230	183,763
Total	**570,584,607**	**1,550,205**	**3,300,210**	**92,037,400**
			Total	**667,472,422**

Table 34. All Harding County oil fields O&M costs

	Annual O&M ($/yr)			
EOR units	**Annual O&M cost**	**CO_2 recycling O&M cost**	**Lifting cost**	**G&A**
South Buffalo	86,291	1,447,258	2,462,902	509,839
Buffalo	86,291	807,038	2,462,902	509,839
West Buffalo	86,291	390,835	2,462,902	509,839
Central Buffalo	86,291	305,312	2,462,902	509,839
East Harding Springs	86,291	259,222	2,462,902	509,839
West Buffalo 'b'	86,291	255,416	2,462,902	509,839
Pete's Creek	86,291	195,356	2,462,902	509,839
North Buffalo	86,291	170,650	2,462,902	509,839
SD-State Line	86,291	136,306	2,462,902	509,839
Travers Ranch	86,291	66,608	2,462,902	509,839
Crooked Creek	86,291	11,558	2,462,902	509,839
Clarkson Ranch	86,291	11,057	2,462,902	509,839
Eagles Nest	86,291	3,335	2,462,902	509,839
Additional oil fields				
Buffalo	86,291	3,560,518	2,462,902	509,839
Table Mountain	86,291	1,304,853	2,462,902	509,839
Yellow Hair	86,291	1,107,471	2,462,902	509,839
Border	86,291	966,591	2,462,902	509,839
East Harding Springs	86,291	650,544	2,462,902	509,839

Pete's Creek	86,291	577,619	2,462,902	509,839
Bull Creek	86,291	599,701	2,462,902	509,839
South Medicine Pole Hills	86,291	504,777	2,462,902	509,839
Jones Creek	86,291	496,490	2,462,902	509,839
State Line	86,291	245,672	2,462,902	509,839
Corey Butte	86,291	284,160	2,462,902	509,839
Travers Ranch	86,291	226,473	2,462,902	509,839
Clarkson Ranch	86,291	111,762	2,462,902	509,839
Harding Springs	86,291	29,402	2,462,902	509,839
Total	**2,329,857**	**14,725,984**	**66,498,349**	**13,765,641**
			Total	**97,319,831**

Table 35. All Harding County oil fields produced revenue per year

	Oil Revenue		
EOR units	**Total EOR oil production (bbl)**	**Annual production (bbl/yr)**	**Revenue ($/yr)**
South Buffalo	11,366,725	710,420	63,937,829
Buffalo	5,411,002	338,188	30,436,887
West Buffalo	4,151,845	259,490	23,354,126
Central Buffalo	2,482,915	155,182	13,966,399
East Harding Springs	4,509,403	281,838	25,365,393
West Buffalo 'b'	4,194,985	262,187	23,596,792
Pete's Creek	5,023,231	313,952	28,255,676
North Buffalo	1,273,267	79,579	7,162,126
SD-State Line	1,674,355	104,647	9,418,246
Travers Ranch	665,981	41,624	3,746,143
Crooked Creek	1,333,004	83,313	7,498,148
Clarkson Ranch	756,459	47,279	4,255,084
Eagles Nest	676,224	42,264	3,803,759
Additional oil fields			
Buffalo	43,364,543	2,710,284	243,925,556
Table Mountain	13,880,712	867,545	78,079,007
Yellow Hair	11,835,298	739,706	66,573,552
Border	10,375,403	648,463	58,361,643
East Harding Springs	4,635,484	289,718	26,074,600

Pete's Creek	3,345,792	209,112	18,820,081
Bull Creek	6,573,431	410,839	36,975,548
South Medicine Pole Hills	5,589,758	349,360	31,442,390
Jones Creek	5,503,882	343,993	30,959,336
State Line	2,642,875	165,180	14,866,170
Corey Butte	2,090,333	130,646	11,758,120
Travers Ranch	2,730,031	170,627	15,356,426
Clarkson Ranch	875,188	54,699	4,922,932
Harding Springs	663,589	41,474	3,732,686
Total	**157,625,717**	**9,851,607**	**886,644,656**

7 REFERENCES

[1] U.S. Energy Information Administration, 2021, *Electric Power Annual*, Table 3.1.A, from https://www.eia.gov/tools/faqs/faq.php?id=427&t=3

[2] U.S. Energy Information Administration, 2021, *Monthly Energy Review*, Table 1.3 and 10.1, April 2021, preliminary data, from https://www.eia.gov/energyexplained/us-energy-facts/

[3] U.S. Energy Information Administration, 2021, *Monthly Energy Review*, from https://www.eia.gov/todayinenergy/detail.php?id=48596

[4] IPCC, 2019, "Global Warming of 1.5°C", from https://www.ipcc.ch/sr15/faq/faq-chapter-1/.

[5] United Nations, *Treaty Series*, vol. 3156, C.N.63.2016.TREATIES-XXVII.7.d of 16 February 2016 (Opening for signature) and C.N.92.2016.TREATIES-XXVII.7.d of 17 March 2016 (Issuance of Certified True Copies)

[6] EPA, 2022, "Basics of Climate Change," from https://www.epa.gov/climatechange-science/basics-climate-change.

[7] Hodnebrog, O., Shine, K., and Wallington, T., 2020, Halocarbons: What Are They and Why Are They Important? *EOS, 101,* https://doi.org/10.1029/2020EO149045.

[8] National Geographic Society, 2019, "The Carbon Cycle," from https://www.nationalgeographic.org/encyclopedia/carbon-cycle.

[9] NOAA, 2021, "Carbon Cycle" from https://www.noaa.gov/education/resource-collections/climate/carbon-cycle.

[10] University of California, Davis, 2020, "How Carbon Neutral is Different than Climate Neutral," from https://clear.ucdavis.edu/explainers/carbon-neutral-versus-climate-neutral.

[11] The Climate Pledge, 2021, "Net-Zero Carbon by 2040," from https://www.theclimatepledge.com/us/en.

[12] Riebeek, H. and Simmon, R., 2011, "The Carbon Cycle," from https://earthobservatory.nasa.gov/features/CarbonCycle.

[13] EPA, 2022, "Inventory of U.S. Greenhouse Gas Emissions and Sinks: 1990-2020," U.S. Environmental Protection Agency, EPA 430-R-22-003

[14] IPCC, 2014, *Climate Change 2014: Synthesis Report. Contribution of Working Groups I, II and III to the Fifth Assessment Report of the Intergovernmental Panel on Climate Change*, Core Writing Team, R.K. Pachauri and L.A. Meyer (eds.), Geneva, Switzerland.

[15] IPCC, 2022, *Climate Change 2022: Mitigation of Climate Change. Contribution of Working Group III to the Sixth Assessment Report of the Intergovernmental Panel on Climate Change*. P.R. Shukla, J. Skea, R. Slade, A. Al Khourdajie, R. van Diemen et. al. (eds.), Cambridge University Press, Cambridge, UK and New York, NY.

[16] IEA, 2021, "About CCUS," IEA Report, Paris, France.

[17] EPA, 2022, "Greenhouse Gas Equivalencies Calculator," from https://www.epa.gov/energy/greenhouse-gas-equivalencies-calculator

[18] IEA, 2022, "Carbon Capture, Utilization and Storage," from https://www.iea.org/fuels-and-technologies/carbon-capture-utilisation-and-storage

[19] Global CCS Institute, 2020, "Carbon Capture and Storage: Challenges, enablers and opportunities for deployment," from https://www.globalccsinstitute.com/news-media/insights/carbon-capture-and-storage-challenges-enablers-and-opportunities-for-deployment/

[20] Fowler, S., Roush, R., and Wise, J., 2013, *Concepts of Biology*, OpenStax, Houston, TX. Chap. 20.

[21] Rye, C., Wise, R., Jurukovski, V., DeSaix, J., Choi, J., and Avissar, Y., 2016, *Biology*, OpenStax, Houston, TX. Chap. 6-7.

[22] Wilkin, D. and Brainerd, J., 2016, *CK-12 Biology Advanced Concepts*, CK-12 Foundation, Chap. 18.9.

[23] EPA, 2021, "Understanding the Science of Ocean and Coastal Acidification," from https://www.epa.gov/ocean-acidification/understanding-science-ocean-and-coastal-acidification

[24] Butler, J. and Montzka, S., 2021, "The NOAA Annual Greenhouse Gas Index (AGGI)," NOAA Global Monitoring Laboratory, Boulder, CO.

[25] IPCC, 2007, *Climate Change 2007: The Physical Science Basis, Contribution of Working Group I to the Fourth Assessment Report of the Intergovernmental Panel on Climate Change*, Solomon, S., D. Qin, M. Manning, Z. Chen, M. Marquis, et. al. (eds.), Cambridge University Press, Cambridge, UK and New York, NY, Chap. 1.

[26] EIA, 2021, "Energy and the Environment Explained," from https://www.eia.gov/energyexplained/energy-and-the-environment/greenhouse-gases-and-the-climate.php.

[27] Stancil, J., 2019, "The Power of One Tree – The Very Air We Breathe," US Department of Agriculture, from https://www.usda.gov/media/blog.

[28] International Union for Conservation of Nature (IUCN), 2021, "Forests and Climate Change," IUCN Issues Briefs, Gland, Switzerland.

[29] FAO, 2020, Global Forest Resources Assessment 2020: Main report. Rome.

[30] Goldewijk, K., Beusen, A., van Drecht, G., and de Vos, M., 2010, "The HYDE 3.1 spatially explicit database of human-induced global land-use change over the past 12,000 years," *Glob. Ecol. and Biogeogr*., **20**, pp. 73-86.

[31] PRB, "2020 World Population Data Sheet," PRB, Washington, DC.

[32] Cai, Q., Yan, X., Li, Y. et al., 2018, "Global patterns of human and livestock respiration," *Sci Rep*, **8**:9278.

[33] Roser, M. and Ritchie, H., 2021, "Forests and Deforestation," from https://ourworldindata.org/forest-area.

[34] Hoover, K. and Riddle, A., 2020, "Forest Carbon Primer," R46312, Congressional Research Service (CRS), Library of Congress, Washington, DC.

[35] Cassia, R., Nocioni, M., Correa-Aragunde, N., and Lamattina, L., 2018, "Climate Change and the Impact of Greenhouse Gasses: CO_2 and NO, Friends and Foes of Plant Oxidative Stress," *Frontiers in Plant Sci*., **9**:273.

[36] Wenzel T., 2021, *Molecular and Atomic Spectroscopy*, Bates College, Lewiston, ME, Chap. 4.

[37] Olbrycht, R., Kaluza, M., Wittchen, W., Borecki, M., Wiecek, B., and Mey, G., 2016, "Gas Identification and Estimation of its Concentration in a Tube Using Hyperspectral Thermography Approach," *2016 Quantitative InfraRed Thermography Conference*, Canada, pp. 605-610.

[38] IPCC, 2021, *Climate Change 2021: The Physical Science Basis. Contribution of Working Group I to the Sixth Assessment Report of the Intergovernmental Panel on Climate Change*, Masson-Delmotte, V., P. Zhai, A. Pirani, S.L. Connors, C. Péan, et. al. (eds.), Cambridge University Press, Cambridge, UK, and New York, NY. Chap. 7.

[39] Sherwood, S., Dixit, V., and Salomez, C., 2018, "The Global Warming Potential of Near-Surface Emitted Water Vapor," *Environ. Res. Lett.*, **13**(10), 104006.

[40] Liang, S. and Wang, J., 2020, *Advanced Remote Sensing*, 2nd ed., Academic Press, Chap. 4.

[41] The Royal Society, 2008, "Climate Change Controversies: A Simple Guide," Registered Charity No 207043, London, UK.

[42] IEA, 2021, "Greenhouse Gas Emissions from Energy Data Explorer," IEA, Paris.

[43] NOAA National Centers for Environmental Information, 2021, "State of the Climate: Monthly Global Climate Report for Annual 2020," from https://www.ncei.noaa.gov/access/monitoring/monthly-report/global/202013.

[44] Energy Information Administration, 2021, “Biofuels Explained,” from https://www.eia.gov/energyexplained/biofuels/ethanol.php

[45] Cruz, C., Souza, G., and Cortez, L., 2014, *Future Energy: Improved, Sustainable and Clean Options for Our Planet,* 2nd ed., Elsevier, London, UK, Chap. 11.

[46] Renewable Fuels Association (RFA), n.d., “How is Ethanol Made?” from https://ethanolrfa.org/

[47] US Department of Agriculture, 2022, “2021 State Agriculture Overview” from https://www.nass.usda.gov/Statistics_by_State/South_Dakota/index.php

[48] EIA, 2022, “South Dakota State Energy Profile,” from https://www.eia.gov/state/print.php?sid=SD.

[49] Xu, Y., Isom, L., and Hanna, M., 2010, “Adding value to carbon dioxide from ethanol fermentations,” *Bioresource Technology*, **101(**2010), pp. 3311-3319.

[50] Rosentrater, K., Kalscheuer, K., Garcia, A., and Wright, C., 2008, “The South Dakota Fuel Ethanol Industry,” *Fact Sheets*, Paper 144.

[51] RFA, 2022, “Annual Industry Outlook,” from https://ethanolrfa.org/resources/annual-industry-outlook.

[52] RFA, 2022, *Zeroing in on New Opportunities: 2022 Ethanol Industry Outlook,* Washington, DC.

[53] EIA, 2022, State Energy Data Systems, Table P4. Primary Energy Production Estimates in Physical Units, Ranked by State, 2020.

[54] EIA, 2022, State Energy Data Systems, Table F25. Fuel Ethanol Consumption Estimates, 2020.

[55] EIA, 2022, State Energy Data Systems, Table C3. Primary Energy Consumption Estimates, 2020.

[56] IEA, 2022, “Global Energy Review: CO_2 Emissions in 2021,” IEA, Paris.

[57] U.S. Census Bureau, 2021, “Population,” from https://www.census.gov/quickfacts/SD.

[58] Chontanawat, J., 2019, “Relationship between energy consumption, CO_2 emission and economic growth in ASEAN: Cointegration and causality model,” *ICEER 2019, 22-25 July*, University of Aveiro, Portugal, Energy Reports, **6**, pp. 660-665.

[59] Shaari, M., Karim, Z., and Abidin, N., 2020, “The Effects of Energy Consumption and National Output on CO_2 Emissions: New Evidence from OIC Countries Using a Panel ARDL Analysis,” *Sustainability*, 12**(8)**, 3312.

[60] EIA, 2022, State Energy Data Systems, Table C11. Total Energy Consumption Estimates by End-Use Sector, Ranked by State, 2020.

[61] Mosier, N. and Ileleji, K., 2020, "How Fuel Ethanol is Made from Corn," *Bioenergy: Biomass to Biofuels and Waste to Energy*, 2nd ed., Elsevier, pp. 539-544.

[62] EIA, 2022, "Table A3. Approximate Heat Content of Petroleum Consumption and Fuel Ethanol," *Monthly Energy Review*, U.S. Energy Information Administration, Washington DC.

[63] EPA, 2009, "Mandatory Reporting of Greenhouse Gases," Rules and Regulations, 74 FR 56259, *Federal Register*, **74**(209), pp. 56260-56519.

[64] EIA, 2022, "Table A2. Approximate Heat Content of Petroleum Production, Imports, and Exports," *Monthly Energy Review*, U.S. Energy Information Administration, Washington DC.

[65] EIA, 2019, State Energy Data System, Rankings: Total Energy Consumed per Capita, 2019.

[66] EIA, 2020, State Energy Data System, South Dakota Energy Consumption by End-Use Sector, 2020.

[67] EIA, 2019, State Energy Data System, Table C14. Total Energy Consumption Estimates per Capita by End-Use Sector, Ranked by State, 2019.

[68] EPA, 2018, "Green Vehicle Guide," from https://www.epa.gov/greenvehicles

[69] EIA, 2019, State Energy Data System, Rankings: Total Carbon Dioxide Emissions, 2019, Excel file.

[70] EIA, 2022, State Energy Data System, Energy-Related CO_2 Emission Data Tables, Table 4. Per capita energy-related carbon dioxide emissions by state, Excel file.

[71] EIA, 2022, State Energy Data System, Energy-Related CO_2 Emission Data Tables, Table 3. State energy-related carbon dioxide emissions by sector, Excel file.

[72] Lewandrowski, J., Rosenfeld, J., Pape, D., Hendrickson, T., Jaglo, K., and Moffroid, K., 2018, "The greenhouse gas benefits of corn ethanol – assessing recent evidence," *Biofuels*, **11**(3), pp. 361-375.

[73] Center for Climate and Energy Solutions, 2021, "Carbon Capture," from https://www.c2es.org/content/carbon-capture/

[74] Fennell, P., Florin, N., Napp, T., and Hills, T., 2012, "CCS from industrial sources," *Sustainable Technologies, Systems and Policies*, **2012**(2).

[75] Leung, D., Caramanna, G., and Maroto-Valer, M., 2014, "An overview of current status of carbon dioxide capture and storage technologies," *Renewable and Sustainable Energy Reviews*, **39**(2014), pp. 426-443.

[76] Page, S., Williamson, A., and Mason, I., 2008, "Carbon capture and storage: Fundamental thermodynamics and current technology," *Energy Policy*, **37**(2009), pp. 3314-3324.

[77] Minchener, A., 2013, "Gasification based CCS challenges and opportunities for China," *Fuel*, **116**(15), pp. 904-909.

[78] de Coninck H., Mikunda T., Gielen D., Nussbaumer P., and Shchreck B., 2010, Carbon Capture and Storage in Industrial Applications, Technology Synthesis Report. United Nations Industrial Development Organization, Vienna, Austria.

[79] IEAGHG, 2013, "Information Sheets for CCS," 2013/16, Cheltenham, United Kingdom.

[80] Global CCS Institute, 2021, "Facilities Database," from https://CO_2re.co/FacilityData.

[81] Sanchez, D., Johnson, N., McCoy, S., Turner, P., and Mach, K., 2018, "Near-term deployment of carbon capture and sequestration from biorefineries in the United States," Proceedings of the National Academy of Sciences of the USA, **115**(42), pp. 4875-4880.

[82] Bains, P., Psarras, P., and Wilcox, J., 2017, "CO_2 capture from the industry sector," *Progress in Energy and Combustion Science*, **63**(2017), pp. 146-172.

[83] IPCC, 2005, *IPCC Special Report on Carbon Dioxide Capture and Storage. Prepared by Working Group III of the Intergovernmental Panel on Climate Change*, Cambridge University Press, Cambridge, UK and New York, NY, Chap. 4.

[84] Mohammadi, M., Hourfar, F., Elkamel, A., and Leonenko, Y., 2019, "Economic Optimization Design of CO_2 Pipeline Transportation with Booster Stations," *Ind. Eng. Chem. Res.*, **58**, pp. 16730-16742.

[85] Peletiri, S., Rahmanian, N., and Mujtaba, I., 2018, "CO_2 Pipeline Design: A Review," *Energies*, **11**(9), 2184.

[86] Jones, A. and Lawson, A., 2021, "Carbon Capture and Sequestration (CCS) in the United States," R44902, Congressional Research Service (CRS), Library of Congress, Washington, DC.

[87] Edwards, R. and Celia, M., 2018, "Infrastructure to enable deployment of carbon capture, utilization, and storage in the United States," *Proceedings of the National Academy of Sciences of the USA*, **115**(38), pp. E8815-E8824.

[88] Abramson, E., McFarlane, D, and Brown, J., 2020, "Transport Infrastructure for Carbon Capture and Storage," White Paper on Regional Infrastructure for Midcentury Decarbonization, Great Plains Institute (GPI) and Regional Carbon Capture Deployment Initiative.

[89] Cao, C., Liu, H., Hou, Z., Mehmood, F., Liao, J., and Feng, W., 2020, "A Review of CO_2 Storage in View of Safety and Cost-Effectiveness," *Energies*, **13**(3), 600.

[90] IPCC, 2005, *IPCC Special Report on Carbon Dioxide Capture and Storage. Prepared by Working Group III of the Intergovernmental Panel on Climate Change*, Cambridge University Press, Cambridge, UK and New York, NY, Chap. 5.

[91] Fujioka, M., Yamaguchi, S., and Nako, M., 2010, "CO_2-ECBM Field Tests in the Ishikari Coal Basin of Japan," *Int Journal of Coal Geology*, **82**(3-4), pp. 287-298.

[92] Kearns, D., Liu, H., and Consoli, C., 2021, "Technology Readiness and Costs of CCS," Global CCS Institute, Melbourne, Australia.

[93] Hannis, S., Lu J., Chadwick, A., Hovorka, S., Kirk, K., Romanak, K., and Pearce, J., 2017, "CO_2 Storage in Depleted or Depleting Oil and Gas Fields: What can We Learn from Existing Projects?" *Energy Procedia*, **14**, pp. 5680-5690.

[94] IEA, 2015, "Storing CO_2 through Enhanced Oil Recovery," IEA Report, Paris, France.

[95] Carpenter, S. and Koperna, G., 2014, "Development of the first internationally accepted standard for geologic storage of carbon dioxide utilizing Enhanced Oil Recovery (EOR) under the International Standards Organization (ISO) Technical Committee TC-265," *Energy Procedia*, **63**, pp. 6717–6729.

[96] Yu, W. and Sepehrnoori, K., 2018, *Shale Gas and Tight Oil Reservoir Simulation*, Gulf Professional Publishing, Cambridge, MA, Chap. 8.

[97] Olabode, O., Isehunwa, S., Orodu, O., and Ake, D., 2021, "Optimizing Productivity in Oil Rims: Simulation Studies on Horizontal Well Placement Under Simultaneous Oil and Gas Production," *J Petrol Explor Prod Technol*, **11**, pp. 385-397.

[98] Zhou, X., Alotaibi, F., Kokal, S., Alhashboul, A., and Al-Qahtani, J., 2017, "A New Approach of Pressure Profile and Oil Recovery during Dual and Single Carbonate Core Flooding by Seawater and CO_2 Injection Process at Reservoir Conditions," *SPE/IATMI Asia Pacific Oil & Gas Conference and Exhibition*, Jakarta, Indonesia, SPE-186381-MS.

[99] Advanced Resources International, Inc. and Melzer Consulting, 2010, "Optimization of CO_2 storage in CO_2 enhanced oil recovery projects," Department of Energy & Climate Change (DECC), Office of Carbon Capture & Storage.

[100] Jia, B., Tsau, J-S., and Barati, R., 2019, "A Review of the Current Progress of CO_2 Injection EOR and Carbon Storage in Shale Oil Reservoirs," *Fuel*, **236**, pp. 404-427.

[101] Xu, L., Ye, W., Chen, Y., Chen, B., and Cui, Y., 2018, "A New Approach for Determination of Gas Breakthrough in Saturated Materials with Low Permeability," *Engineering Geology*, **241**, pp. 121-131.

[102] Hao, M., Liao, S., Yu, G., Lei, X., and Tang, Y., 2020, "Performance Optimization of CO_2 Huff-n-Puff for Multifractured Horizontal Wells in Tight oil Reservoirs," *Geofluids*, **2020**, Article ID 8840384, 13 pages.

[103] Hoffman, T. and Reichhardt, D., 2020, "Recovery Mechanisms for Cyclic (Huff-n-Puff) Gas Injection in Unconventional Reservoirs: A Quantitative Evaluation Using Numerical Simulation," *Energies*, **13**(18), 4944.

[104] RFA, n.d., "Ethanol Biorefinery Locations," from https://ethanolrfa.org/.

[105] Dubois, M, White, S., and Carr, T., 2002, "Co-generation, Ethanol Production and CO_2 Enhanced Oil Recovery: A Model for Environmentally and Economically Sound Linked Energy Systems," *Proceedings 2002 AAPG Annual Meeting*, Houston, TX, p. A46.

[106] Leroux, K., 2017, "Integrated carbon capture and storage for North Dakota ethanol production," Final Report, DOE Project # DE-F0024233.

[107] McPherson, B., 2010, "Integrated Mid-Continent Carbon Capture, Sequestration and Enhanced Oil Recovery Project," Final Report, DOE Project # DE-FE0001942.

[108] GPI, 2017, "Capturing and Utilizing CO_2 from Ethanol: Adding Economic Value and Jobs to Rural Economies and Communities While Reducing Emissions," White paper prepared by the State CO_2-EOR Deployment Work Group.

[109] Morgan, D., Grant, T., and Remson, D., 2022, "FECM/NETL CO_2 Transport Cost Model (2022)," NETL, DOE/NETL-2022/3243. https://netl.doe.gov/energy-analysis/search?search=CO_2TransportCostModel.

[110] Dubois, M., McFarlane, D., and Bidgoli, T., 2017, "CO_2 Pipeline Cost Analysis Utilizing a Modified FE/NETL CO_2 Transport Cost Model Tool," Poster presentation, *Carbon Storage and Oil and Natural Gas Technologies Review Meeting*, Pittsburgh, PA.

[111] Morgan, D., Guinan, A., and Sheriff, A., 2022, "FECM/NETL CO_2 Transport Cost Model (2022): Description and User's Manual," NETL, DOE/NETL-2022/3218, Pittsburgh, PA.

[112] Parker, N., 2004, "Using Natural Gas Transmission Pipeline Costs to Estimate Hydrogen Pipeline Costs," UCD-ITS-RR-04-35, Institute of Transportation Studies, University of California, Davis, CA.

[113] Goodman, A., Hakala, A., Bromhal, G., Deel, D., Rodosta, T., Frailey, S., Small, M., Allen, D., Romanov, V., Fazio, J., Huerta, N., McIntyre, D., Kutchko, B., and Guthrie, G., 2011, "U.S. DOE Methodology for the Development of Geologic Storage Potential for Carbon Dioxide at the National and Regional Scale," *Int J Greenh Gas Control*, **5**(2011), pp. 952-965.

[114] SD Department of Agriculture and Natural Resources (DANR), n.d., “Oil & Gas Map-Based Data Source,” Geological Survey Program, Vermillion, SD.

[115] Sun, S. and Zhang, T., 2020, *Reservoir Simulations: Machine Learning and Modeling*, Gulf Professional Publishing, Cambridge, MA, Chap. 1.

[116] Peck, W., Azzolina, N., Ge, J., Bosshart, N., Burton-Kelly, M., Gorecki, C., Gorz, A., Ayash, S., Nakles, D., and Melzer, S., 2018, "Quantifying CO_2 Storage Efficiency Factors in Hydrocarbon Reservoirs: A Detailed Look at CO_2 Enhanced Oil Recovery," *Int J Greenhouse Gas Control*, **69**, pp. 41-51.

[117] Sippel, M., Luff, K., Hendricks, M., and Eby, D., 1998, "Reservoir Characterization of the Ordovician Red River Formation in Southwest Williston Basin Bowman Co., ND and Harding Co. SD," DE98000487, National Petroleum Technology Office, Tulsa, OK.

[118] SD DANR, n.d., “Issued Board Orders: orders applicable to enhanced recovery units (alphabetical by unit),” Excel file.

[119] Nesheim, T., 2017, “Oil and Gas Potential of the Red River Formation, Southwestern North Dakota,” Department of Mineral Resources, Bismark, ND.

[120] National Energy Technology Laboratory, 2017, “FE/NETL CO_2 OnShore Saline Storage Cost Model,” DOE/NETL-2017/1669, Version 3, US Department of Energy, https://www.netl.doe.gov/research/energy-analysis/search-publications/vuedetails?id=2403

[121] Internal Revenue Service (IRS), Treasury, 2021, “Credit for Carbon Oxide Sequestration,” Rules and Regulations, 86 FR 4728, *Federal Register*, **86**(10), pp. 4728-4773.

[122] Jones, A. and Sherlock, M., 2021, “The Tax Credit for Carbon Sequestration (Section 45Q),” IF11455, Congressional Research Service (CRS), Library of Congress, Washington, DC.

[123] Coppinger, B., 2020, “2020 Section 43 Inflation Adjustment,” Notice 2020-31, IRS, Washington, DC.

[124] McCoy, S., 2008, “The Economics of CO_2 Transport by Pipeline and Storage in Saline Aquifers and Oil Reservoirs,” Ph.D. thesis, Department of Engineering & Public Policy, Carnegie Mellon University.

[125] SD DANR, n.d., “Oil & Gas in South Dakota: production and injection data,” Data/Reports, Excel.

[126] EIA, 2022, “Domestic Crude Oil First Purchase Prices by Area,” from https://www.eia.gov/petroleum/data.php.

[127] Advanced Resources International, 2006, "Basin Oriented Strategies for CO_2 Enhanced Oil Recovery: Williston Basin," DOE, Office of Fossil Energy and Office of Oil and Natural Gas.

[128] Dahowski, R., Davidson, C., Li, X., and Wei, N., 2012, "A \$70/tCO_2greenhouse gas mitigation backstop for China's industrial and electric power sectors: Insights from a comprehensive CCS cost curve," *Int J Greenh Gas Control*, **11**, pp. 73-85.

[129] Wei, N., Li, X., Dahowski, R., Davidson, C., Liu, S., and Zha, Y., 2015, "Economic Evaluation on CO_2-EOR of Onshore Oil Fields in China," *Int J Greenh Gas Control*, **37**, pp. 170-181.

[130] Ferguson, R., Nichols, C., Leeuwen, T., and Kuuskraa V., 2009, "Storing CO_2 with Enhanced Oil Recovery," *Energy Procedia*, **1**(1), pp. 1989-1996.